

Extension of the Isobaric Nucleon Model for Pion Production in Pion-Nucleon, Nucleon-Nucleon, and Antinucleon-Nucleon Interactions*

R. M. STERNHEIMER AND S. J. LINDENBAUM
Brookhaven National Laboratory, Upton, New York

(Received February 28, 1961)

The isobaric nucleon model of pion production in nucleon-nucleon and pion-nucleon collisions has been extended to include the effect of the higher resonances in the isotopic spin $T=\frac{1}{2}$ state of the pion-nucleon system, in addition to the effect of the well-known low-energy $T=\frac{3}{2}$ resonance which has been previously investigated. The higher $T=\frac{1}{2}$ resonances are centered at incident pion energies of 600 and 880 Mev, and thus correspond to isobar masses $m_1=1.51$ and 1.68 Bev, respectively, as compared to $m_1=1.23$ Bev for the $T=\frac{3}{2}$ resonance. For the inelastic pion-nucleon interactions, calculations of the various pion and recoil nucleon energy spectra have been carried out for incident pion energies $T_{\pi,\text{inc}}=1.0, 1.4$, and 2.0 Bev. We have considered both single and double pion production by the incident pion, corresponding to two-pion and three-pion final states, respectively. General equations for the center-of-mass energy spectra of the final-state pions and nucleons have been obtained for all single and double pion production reactions from both π^-p and π^+p collisions. The results of the present extended isobar model at $T_{\pi,\text{inc}}=1.0$ Bev are in reasonable agreement with the combined data from three experiments on π^-p interactions in the region

of 1.0 Bev incident energy. The Q value distributions for pion-nucleon and pion-pion pairs have been calculated for single pion production at $T_{\pi,\text{inc}}=1.0$ Bev. The present extension of the isobar model can also be used to treat up to four-pion final states in $\pi-N$ interactions, and up to eight-pion final states in $N-N$ interactions.

For pion production in nucleon-nucleon collisions, we have obtained the branching ratios for all pion production reactions which involve the isobaric states N_1^* , N_{2a}^* , and N_{2b}^* , corresponding to the $T=\frac{3}{2}$ and $T=\frac{1}{2}$ resonances. General equations for the energy spectra of the final-state pions and nucleons have been derived for all single- and double-pion production reactions from both $p-p$ and $n-p$ collisions. Calculations of the various pion and nucleon energy spectra have been carried out for incident nucleon energies of 2.3 and 3.0 Bev. For the processes of pion production in antinucleon-nucleon interactions which do not result in annihilation, it has been assumed that an anti-isobar \bar{N}_α^* can be produced, which is the antiparticle of the isobar N_α^* . Specific results have been obtained for both single and double pion production in $\bar{p}-p$, $\bar{p}-n$, and $\bar{n}-p$ collisions.

I. INTRODUCTION

IN previous papers,¹⁻³ we have proposed an isobaric nucleon model of pion production in nucleon-nucleon ($N-N$) and pion-nucleon ($\pi-N$) collisions. In this model, it is assumed that in the primary ($N-N$ or $\pi-N$) interaction the nucleon is excited to an isobaric state N_α^* which subsequently decays into a nucleon and one or several pions. In the previous calculations, we have considered only the isobaric state N_1^* corresponding to the well-known pion-nucleon resonance with isotopic spin $T=\frac{3}{2}$ and angular momentum $J=\frac{3}{2}$ at an incident pion energy $T_\pi=180$ Mev. The isobar N_1^* is assumed to decay into a nucleon and a pion. Thus, for $\pi-N$ collisions, we have given a treatment of production of one additional pion (i.e., two pions in the final state); for $N-N$ collisions, we have considered both single pion and double pion production. This isobar model involving the state N_1^* only has been able to give reasonable agreement with most of the dominant features of a number of experiments on inelastic $N-N$ and $\pi-N$ interactions.⁴⁻¹³

* Work performed under the auspices of the U. S. Atomic Energy Commission.

¹ S. J. Lindenbaum and R. M. Sternheimer, Phys. Rev. **105**, 1874 (1957); this paper will be referred to as I. Earlier references are also summarized in this paper. S. J. Lindenbaum and R. M. Sternheimer, *ibid.* **106**, 1107 (1957).

² R. M. Sternheimer and S. J. Lindenbaum, Phys. Rev. **109**, 1723 (1958). This paper will be referred to as II.

³ S. J. Lindenbaum and R. M. Sternheimer, Phys. Rev. Letters **5**, 24 (1960). See also *Proceedings of the 1960 Annual International Conference on High-Energy Physics at Rochester* (Interscience Publishers, Inc., New York, 1960), p. 205.

⁴ S. J. Lindenbaum and L. C. L. Yuan, Phys. Rev. **93**, 1431 (1954), and **103**, 404 (1956).

⁵ W. B. Fowler, R. P. Shutt, A. M. Thorndike, and W. L. Whittemore, Phys. Rev. **95**, 1026 (1954).

It has been recently shown that the cross section for π^-p scattering [$\sigma(\pi^-p)$] has two maxima in the region of $T_\pi=500-1000$ Mev pion energy.¹⁴⁻¹⁹ These two maxima, which are centered at $T_\pi=600$ and 880 Mev, correspond to peaks in the cross section $\sigma_{\frac{1}{2}}$ for interactions in the isotopic spin $T=\frac{1}{2}$ state of the pion-nucleon system. It seems reasonable to assume that these two additional peaks correspond to resonances in a

⁶ T. W. Morris, E. C. Fowler, and J. D. Garrison, Phys. Rev. **103**, 1472 (1956); W. B. Fowler, R. P. Shutt, A. M. Thorndike, and W. L. Whittemore, *ibid.* **103**, 1479 (1956); M. M. Block *et al.*, *ibid.* **103**, 1484 (1956); W. B. Fowler *et al.*, *ibid.* **103**, 1489 (1956).

⁷ R. Cester, T. F. Hoang, and A. Kernan, Phys. Rev. **103**, 1443 (1956); I. S. Hughes, P. V. March, H. Muirhead, and W. O. Lock, Phil. Mag. **2**, 215 (1957).

⁸ W. A. Wallenmeyer, Phys. Rev. **105**, 1058 (1957).

⁹ A. P. Batson, B. B. Culwick, J. G. Hill, and L. Riddiford, Proc. Roy. Soc. (London) **A251**, 218 (1959).

¹⁰ G. B. Chadwick, G. B. Collins, C. E. Swartz, A. Roberts, S. DeBenedetti, N. C. Hien, and P. J. Duke, Phys. Rev. Letters **4**, 611 (1960).

¹¹ L. M. Eisberg, W. B. Fowler, R. M. Lea, W. D. Shephard, R. P. Shutt, A. M. Thorndike, and W. L. Whittemore, Phys. Rev. **97**, 797 (1955).

¹² W. D. Walker, F. Hushfar, and W. D. Shephard, Phys. Rev. **104**, 526 (1956).

¹³ W. D. Walker and J. Crussard, Phys. Rev. **98**, 1416 (1955).

¹⁴ R. L. Cool, O. Piccioni, and D. Clark, Phys. Rev. **103**, 1082 (1956).

¹⁵ J. W. DeWire, H. E. Jackson, and R. Littauer, Phys. Rev. **110**, 1208 (1958); M. Heinberg, W. M. McClelland, F. Turkot, W. M. Woodward, R. R. Wilson, and D. M. Zipoy, *ibid.* **110**, 1211 (1958); R. R. Wilson, *ibid.* **110**, 1212 (1958).

¹⁶ F. P. Dixon and R. L. Walker, Phys. Rev. Letters **1**, 142 and 458 (1958); J. I. Vette, Phys. Rev. **111**, 622 (1958).

¹⁷ H. C. Burrowes, D. O. Caldwell, D. H. Frisch, D. A. Hill, D. M. Ritson, R. A. Schluter, and M. A. Wahlig, Phys. Rev. Letters **2**, 119 (1959).

¹⁸ J. C. Brisson, J. Detoeuf, P. Falk-Vairant, L. Van Rossum, G. Valladas, and L. C. L. Yuan, Phys. Rev. Letters **3**, 561 (1959).

¹⁹ T. J. Devlin, B. C. Barish, W. N. Hess, V. Perez-Mendez, and J. Solomon, Phys. Rev. Letters **4**, 242 (1960).

particular angular momentum state with $T=\frac{1}{2}$, or possibly in several overlapping states. In this case, we can consider the resonant states as additional isobaric states of the nucleon, which will be denoted by N_{2a}^* and N_{2b}^* for the $T_\pi=600$ and 880 Mev resonances, respectively. The isobar masses m_I which correspond to these pion kinetic energies are: $m_I=1.51$ and 1.68 Bev, respectively, as compared to a mass $m_I=1.225$ Bev pertaining to the N_1^* isobar (center of the $T=J=\frac{3}{2}$ resonance at $T_\pi=180$ Mev).

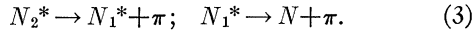
As a natural extension of our previous isobar model, which quite generally formulated the possibility of other higher-energy isobaric nucleon levels, we assume that the pion production can proceed via the $T=\frac{1}{2}$ isobars N_{2a}^* and N_{2b}^* , in addition to the previously considered processes via the $T=\frac{3}{2}$ isobar N_1^* . We will consider together the two states N_{2a}^* and N_{2b}^* , and we will refer to the group of the higher energy $T=\frac{1}{2}$ states as N_2^* . The probability $P_{\frac{1}{2}}(m_I)dm_I$ for exciting the isobar N_2^* in the mass range between m_I and m_I+dm_I is obtained from an expression similar to that used in I for the formation of the N_1^* isobar:

$$P_{\frac{1}{2}}(m_I)dm_I = C\sigma_{\frac{1}{2}}(m_I)Fdm_I, \quad (1)$$

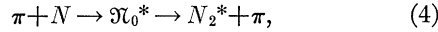
where C is a constant, $\sigma_{\frac{1}{2}}(m_I)$ is the total interaction cross section for the pion-nucleon system in the $T=\frac{1}{2}$ state, and F is the appropriate two-body phase space factor for N_2^* and the other (recoil) particle in the final state (e.g., N_2^*+N or $N_2^*+\pi$).

It appears reasonable to assume that transitions between any two isobaric states can occur by emission of a single pion, and that transitions which involve the simultaneous emission of two or more pions have a small probability.

It will therefore be assumed that the isobar N_2^* can decay either directly into a nucleon and a pion, or into N_1^* and a pion (provided that the latter transition is energetically possible). Thus we have the reactions:



In reaction (3), two pions are produced from the decay of N_2^* , whereas in reaction (2) only one pion is emitted. Thus for $\pi-N$ interactions, in which N_2^* is produced, we have the reaction:



where \mathfrak{N}_0^* is the initial compound state of the pion-nucleon system, which for π^-+p will obviously be a mixture of isotopic spin $T=\frac{1}{2}$ and $T=\frac{3}{2}$ states. For reaction (4), we have the possibility of both two-pion and three-pion final states, corresponding to production of one or two additional pions, respectively.²⁰

²⁰ As will be discussed below [after Eq. (27)], four-pion final states which can be obtained by considering the additional transition $N_{2b}^* \rightarrow N_{2a}^* + \pi$, will be neglected in the present treatment.

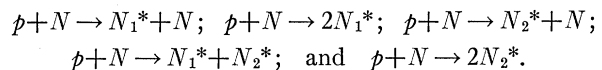
In Sec. II of the present paper, we obtain the general equations for pion production in pion-nucleon collisions via the isobaric states N_1^* and N_2^* . In particular, we obtain the partial cross sections for all possible two-pion and three-pion final states for π^-+p and π^++p interactions. Moreover, the expressions for the momentum spectra of the final-state pions will be given in terms of certain basic spectra $J_{\pi,i}$.

The procedure of the calculation of the pion spectra $J_{\pi,i}$ and the recoil nucleon spectra $I_{N,i}^{(\pi)}$ is given in Sec. III. Calculations have been carried out for incident pion kinetic energies $T_{\pi,\text{inc}}=1.0, 1.4$, and 2.0 Bev.

In Sec. IV, we give a comparison of the present extended isobar model with the results of three recent experiments on inelastic π^-+p interactions at $T_{\pi,\text{inc}} \cong 1.0$ Bev. It will be shown that reasonable agreement can be obtained with the dominant features of the experimental results for the reactions leading to both the two-pion and three-pion final states.

In Sec. V, we give the expressions for the Q -value distributions of the various types of pion-nucleon pairs which arise in pion production in pion-nucleon interactions. The expressions for the probability distributions $P(Q)$ are given in terms of certain basic distributions $P_{\pi N, \alpha}^{(\eta)}(Q)$. In particular, $P_{\pi N, 1}^{(a)}(Q)$ is the Q -value distribution for a nucleon and pion originating from the N_1^* isobar. Thus $P_{\pi N, 1}^{(a)}$ is essentially given by $\sigma_{\frac{1}{2}}(m_1)F$, where $\sigma_{\frac{1}{2}}$ is the $T=\frac{3}{2}$ cross section for the $\pi-N$ system, and F is the two-body phase space factor for an isobar of mass m_1 and the recoil pion. Similarly, $P_{\pi N, 2}^{(a)}(Q)$ denotes the Q -value distribution for the pion-nucleon pair originating from the decay of the N_2^* isobar. $P_{\pi N, 2}^{(a)}$ is essentially given by $\sigma_{\frac{1}{2}}(m_2)F$.

In Sec. VI, we obtain the branching ratios for the various final states for pion production in nucleon-nucleon collisions, specifically $p-p$ and $n-p$ collisions. For $n-p$ collisions, the branching ratios involve, in some cases, the phase angle φ_0 between the matrix elements for production in the isotopic spin $T=1$ and $T=0$ states. The basic reactions for which branching ratios have been obtained are the following:

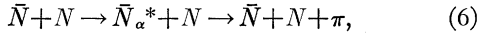
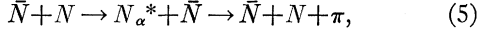


In Sec. VII, we give the expressions for the energy spectra of pions and nucleons from inelastic $p-p$ and $n-p$ interactions leading to single and double pion production. These spectra are given in terms of certain basic spectra (such as $I_{\pi,i}^{(A)}$ and $I_{N,i}^{(A)}$) which are analogous to the spectra $J_{\pi,i}$ and $I_{N,i}^{(\pi)}$ pertaining to pion-nucleon interactions.

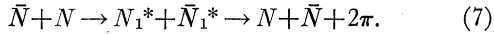
In Sec. VIII, we obtain the basic pion and nucleon energy spectra for the reaction: $N+N \rightarrow N_2^* + N$ at the incident nucleon kinetic energies $T_{N,\text{inc}}=2.3$ and 3.0 Bev. In addition, the energy spectra of the pions and nucleons from the reaction $N+N \rightarrow N_1^* + N_2^*$ have been evaluated for $T_{N,\text{inc}}=3.0$ Bev. The resulting

energy spectra are presented in several figures, together with the spectra arising from the reactions: $N+N \rightarrow N_1^*+N$ and $N+N \rightarrow 2N_1^*$, which have been previously obtained in I. In connection with the choice of the energies $T_{N,\text{inc}}=2.3$ and 3.0 Bev, it should be noted that the effective thresholds for the reactions $N+N \rightarrow N_2^*+N$ and $N+N \rightarrow N_1^*+N_2^*$ are $T_{N,\text{inc}} \sim 1.6$ and ~ 2.6 Bev, respectively. For this reason, calculations for $N+N \rightarrow N_1^*+N_2^*$ were not carried out at 2.3 Bev, but only at 3.0 Bev. The threshold values given above correspond to formation of the isobars N_1^* and N_2^* with mass values exceeding somewhat (by ~ 80 Mev) the mass pertaining to the peak of the cross section σ_1 ($m_1=1.23$ Bev) and the first maximum of σ_2 ($m_2=1.51$ Bev). Specifically, we used: $m(N_1^*)=1.3$ Bev, $m(N_2^*)=1.6$ Bev.

In Sec. IX, we consider the process of pion production in antinucleon-nucleon collisions which do not result in annihilation. Specifically, we have carried out calculations for $\bar{p}-p$, $\bar{p}-n$, and $\bar{n}-p$ interactions. For single-pion production, the basic reactions are as follows:



where \bar{N}_α^* denotes an anti-isobar, i.e., the antiparticle of the isobar N_α^* . We note that reactions (5) and (6) have equal cross sections from charge conjugation invariance. For double-pion production, the following reaction has been considered:



We have obtained the branching ratios for the various possible one-pion and two-pion final states arising from reactions (5)–(7). In addition, expressions for the energy spectra of the pions and nucleons have been derived, together with the expressions for the Q -value distributions for the pion-nucleon and pion-antinucleon pairs. The energy spectrum of the nucleons from the single-pion production reactions can be expressed in terms of the functions $I_{N,1}$ and $I_{N,2}$ which have been introduced and calculated in I for the case of nucleon-nucleon interactions. For the double-pion production reaction (7), the nucleon spectrum is given by the distribution $I_{N,q}$ obtained in I. Similarly, the pion spectrum for reactions (5) and (6) is given by $I_{\pi,s}$ of reference 1, while the pion spectrum for reaction (7) is given by the function $I_{\pi,d}$ which has also been obtained in reference 1. For single-pion production, the Q -value distribution $P(Q)$ is found to be a linear combination of the functions $\bar{P}_1(Q)$ and $\bar{P}_2(Q)$ which have been introduced in I for the case of nucleon-nucleon collisions.

In Sec. X, we outline a procedure for the evaluation of certain basic cross sections for pion-nucleon interactions, $\sigma_{2T,\alpha}$, from experimental data on the cross sections for the various single- and double-pion production reactions from $\pi^- - p$ and $\pi^- - p$ collisions. The

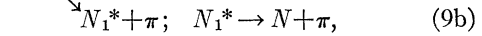
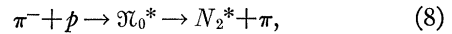
cross sections $\sigma_{2T,\alpha}$ are defined in Sec. II and enter into the expressions for the energy spectra of the final-state pions which are given in this section.

In Sec. XI, a procedure is described for the calculation of the basic cross sections for nucleon-nucleon interactions, $\sigma_1, \sigma_2, \dots, \sigma_6$, from experimental values of the cross sections for the various pion production reactions from $p-p$ and $n-p$ collisions. The discussion of Sec. XI is very similar to that of Sec. X, except that it pertains to nucleon-nucleon rather than pion-nucleon interactions. The cross sections $\sigma_1-\sigma_6$ enter into the equations for the pion and nucleon energy spectra from $p-p$ and $n-p$ collisions, which are obtained in Sec. VII.

II. GENERAL EQUATIONS FOR PION PRODUCTION IN PION-NUCLEON COLLISIONS

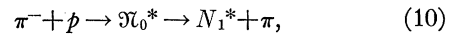
We will now proceed to derive the general equations for the energy spectra and branching ratios for the pion production in pion-nucleon collisions via the reaction $\pi+N \rightarrow N_2^*+\pi$. The cross sections and energy distributions which are thus obtained from the N_2^* processes must be added to the corresponding cross sections and energy distributions arising from the N_1^* processes: $\pi+N \rightarrow N_1^*+\pi$, which have been previously obtained in II. The approximation in which these cross sections can be simply added is that the N_1^* and N_2^* isobars are considered as different particles (having appreciably different masses, and also different isotopic spin and different decay modes). Therefore, it is necessarily assumed that the lifetime of N_1^* and N_2^* is sufficiently long so that the decay takes place outside the range of interaction of the decay products, and interference effects due to a possible short lifetime are neglected.

We shall first consider pion production in $\pi^- - p$ collisions. The basic reactions involved are as follows:



where \mathfrak{N}_0^* is the initial compound state of the $\pi-N$ system, which subsequently decays into $N_2^*+\pi$.

The pion production which proceeds directly via N_1^* involves the following reactions:



In analogy to Eq. (21) of II, the partial cross sections and energy spectra of the final reaction products from (8)–(9b) are determined by:

$$|\Psi_{\pi^- - p}^{(2)(\text{final})}|^2 = |\Psi_{\pi^- - p}^{(2)}(T=\frac{1}{2})|^2 - \rho_2^{\frac{1}{2}} \exp(i\varphi_2) \Psi_{\pi^- - p}^{(2)}(T=\frac{3}{2})|^2, \quad (12)$$

where the superscript (2) indicates that the production goes via N_2^* ; $\Psi_{\pi^-p}^{(2)}(T=\frac{1}{2})$ and $\Psi_{\pi^-p}^{(2)}(T=\frac{3}{2})$ are the wave functions for the final state consisting of N_2^* and a recoil pion, with total isotopic spin $T=\frac{1}{2}$ and $T=\frac{3}{2}$, respectively, and with z component $T_z=-\frac{1}{2}$ in each case; $\rho_2 \equiv \sigma_{32}/(2\sigma_{12})$, where σ_{32} is the inelastic cross section pertaining to N_2^* for the $\pi-N$ system in the $T=\frac{3}{2}$ state, and σ_{12} is the corresponding cross section in the $T=\frac{1}{2}$ state; φ_2 is the phase difference between the matrix elements for production of $N_2^*+\pi$ in the $T=\frac{3}{2}$ and $T=\frac{1}{2}$ states.

The wave functions

$$\Psi_{\pi^-p}^{(2)}(T=\frac{1}{2}) \quad \text{and} \quad \Psi_{\pi^-p}^{(2)}(T=\frac{3}{2})$$

are given by

$$\Psi_{\pi^-p}^{(2)}(T=\frac{1}{2}) = -(\frac{2}{3})^{\frac{1}{2}}\lambda_{\frac{1}{2}}\xi_{-1} + (\frac{1}{3})^{\frac{1}{2}}\lambda_{-\frac{1}{2}}\xi_0, \quad (13)$$

$$\Psi_{\pi^-p}^{(2)}(T=\frac{3}{2}) = (\frac{1}{3})^{\frac{1}{2}}\lambda_{\frac{1}{2}}\xi_{-1} + (\frac{2}{3})^{\frac{1}{2}}\lambda_{-\frac{1}{2}}\xi_0, \quad (14)$$

where λ_{Tz} is the wave function for the N_2^* isobar with z component of isotopic spin $T_z (= \frac{1}{2} \text{ or } -\frac{1}{2})$, and ξ_{Tz} is the wave function of the recoil pion in reaction (8).

From Eqs. (12)–(14), one obtains

$$|\Psi_{\pi^-p}^{(2)(\text{final})}|^2 = A\lambda_{\frac{1}{2}}^2\xi_{-1}^2 + B\lambda_{-\frac{1}{2}}^2\xi_0^2, \quad (15)$$

where the constants A , B , and b are defined by

$$A \equiv \frac{2}{3} + \frac{1}{3}\rho_2 + b, \quad (16)$$

$$B \equiv \frac{1}{3} + \frac{2}{3}\rho_2 - b, \quad (17)$$

$$b \equiv (2\sqrt{2}/3)\rho_2^{\frac{1}{2}} \cos\varphi_2. \quad (18)$$

For the direct decay of N_2^* into a nucleon and a pion [reaction (9a)], $\lambda_{\frac{1}{2}}$ and $\lambda_{-\frac{1}{2}}$ are equivalent to the following:

$$\lambda_{\frac{1}{2}} = -(\frac{1}{3})^{\frac{1}{2}}\zeta_0\kappa_{\frac{1}{2}} + (\frac{2}{3})^{\frac{1}{2}}\zeta_1\kappa_{-\frac{1}{2}}, \quad (19)$$

$$\lambda_{-\frac{1}{2}} = -(\frac{2}{3})^{\frac{1}{2}}\zeta_{-1}\kappa_{\frac{1}{2}} + (\frac{1}{3})^{\frac{1}{2}}\zeta_0\kappa_{-\frac{1}{2}}, \quad (20)$$

where ζ_{Tz} and κ_{Tz} are the wave functions of the decay pion and the final nucleon, respectively. On the other hand, for the decay of N_2^* into N_1^* and a pion [Eq. (9b)], $\lambda_{\frac{1}{2}}$ and $\lambda_{-\frac{1}{2}}$ become

$$\lambda_{\frac{1}{2}} = (\frac{1}{6})^{\frac{1}{2}}\psi_{-\frac{1}{2}} - (\frac{1}{3})^{\frac{1}{2}}\psi_{\frac{1}{2}}\nu_0 + (\frac{1}{2})^{\frac{1}{2}}\psi_{\frac{3}{2}}\nu_{-1}, \quad (21)$$

$$\lambda_{-\frac{1}{2}} = (\frac{1}{2})^{\frac{1}{2}}\psi_{-\frac{1}{2}}\nu_1 - (\frac{1}{3})^{\frac{1}{2}}\psi_{-\frac{1}{2}}\nu_0 + (\frac{1}{6})^{\frac{1}{2}}\psi_{\frac{1}{2}}\nu_{-1}, \quad (22)$$

where ψ_{Tz} is the wave function of the N_1^* isobar, and ν_{Tz} is the wave function of the pion emitted in the transition $N_2^* \rightarrow N_1^* + \pi$. In this process, N_1^* decays subsequently into $N + \pi$, and the appropriate charge ratios are obtained from the following equations:

$$\psi_{\frac{1}{2}} = \mu_1\chi_{\frac{1}{2}}, \quad (23)$$

$$\psi_{\frac{3}{2}} = (\frac{2}{3})^{\frac{1}{2}}\mu_2\chi_{\frac{1}{2}} + (\frac{1}{3})^{\frac{1}{2}}\mu_1\chi_{-\frac{1}{2}}, \quad (24)$$

$$\psi_{-\frac{1}{2}} = (\frac{1}{3})^{\frac{1}{2}}\mu_{-1}\chi_{\frac{1}{2}} + (\frac{2}{3})^{\frac{1}{2}}\mu_0\chi_{-\frac{1}{2}}, \quad (25)$$

$$\psi_{-\frac{3}{2}} = \mu_{-1}\chi_{-\frac{1}{2}}, \quad (26)$$

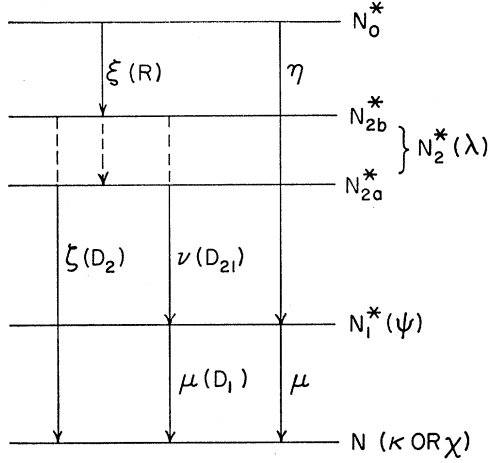


FIG. 1. Schematic diagram showing isobaric states of nucleon (N_0^* , N_{2a}^* , N_{2b}^*) and initial state for pion-nucleon collisions (N_0^*). The diagram indicates the notation employed for the wave functions of the particles involved, and for the various types of pions [see Eq. (27)].

where μ_{Tz} and χ_{Tz} are the wave functions of the decay pion and nucleon, respectively, for the process

$$N_1^* \rightarrow N + \pi.$$

Figure 1 shows schematically the notation used for the various types of pions and the recoil nucleon. The transition marked η corresponds to the recoil pion in the previously studied process (10) and (11) which goes directly via N_1^* [see Eq. (15) of II]. The notations (R), (D_2), (D_{21}), and (D_1) will be explained below.

From Eqs. (15) and (19)–(26), we can now obtain the equation for the intensities of the various types of final pions and reactions:

$$\begin{aligned} & |\Psi_{\pi^-p}^{(2)(\text{final})}|^2 \\ &= AP_s[\frac{1}{3}(R-D_2^0p_2) + \frac{2}{3}(R-D_2^-p_2)] \\ &+ BP_s[\frac{2}{3}(R^0D_2^-p_2) + \frac{1}{3}(R^0D_2^0n_2)] \\ &+ AP_d[(1/18)(R-D_{21}^+D_1^-p_1) + \frac{1}{9}(R-D_{21}^+D_1^0n_1) \\ &+ (2/9)(R-D_{21}^0D_1^0p_1) + \frac{1}{9}(R-D_{21}^0D_1^+n_1) \\ &+ \frac{1}{2}(R-D_{21}^-D_1^+p_1)] + BP_d[\frac{1}{2}(R^0D_{21}^+D_1^-n_1) \\ &+ \frac{1}{9}(R^0D_{21}^0D_1^-p_1) + (2/9)(R^0D_{21}^0D_1^0n_1) \\ &+ \frac{1}{9}(R^0D_{21}^-D_1^0p_1) + (1/18)(R^0D_{21}^-D_1^+n_1)], \end{aligned} \quad (27)$$

where P_s is the relative probability that N_2^* decays into $N + \pi$ [Eq. (9a)], giving rise to single pion production, while P_d is the relative probability for the decay $N_2^* \rightarrow N_1^* + \pi$ (double pion production). Obviously, $P_s + P_d = 1$. The value of P_d must be determined from the requirement that the calculated double-pion cross section should agree with the observed cross section for double-pion production at the energy considered. In Eq. (27), $R^{\pm,0}$ denotes the recoil pion in Eq. (8); $D_2^{\pm,0}$ denotes the decay pion from $N_2^* \rightarrow N + \pi$; p_2 or n_2 denotes a proton or neutron which originates from the decay of N_2^* ; $D_{21}^{\pm,0}$ denotes the decay pion from $N_2^* \rightarrow N_1^* + \pi$; $D_1^{\pm,0}$ denotes the decay pion

from $N_1^* \rightarrow N + \pi$, and p_1 or n_1 is the corresponding nucleon. The charge state of the pion is indicated in each case as a superscript. We note that $R^{\pm,0}$ corresponds to pions with wave function $\xi_{1,0,-1}$. D_2 corresponds to pions with wave function ζ ; similarly, D_{21} corresponds to ν , and D_1 corresponds to μ . The nucleons p_2 and n_2 have the wave function κ , while the nucleons p_1 and n_1 have the wave function χ . These relationships are indicated in Fig. 1.

We note that in the preceding discussion we have not included the effect of a possible transition between the states N_{2b}^* and N_{2a}^* with emission of a pion: $N_{2b}^* \rightarrow N_{2a}^* + \pi$. The main reason for neglecting this contribution is that for the centers of the corresponding resonances, the isobar mass difference is $\Delta m_I = 1.68 - 1.51 = 0.17$ Bev, which is only 30 Mev in excess of the pion mass. Thus, the phase space factor for the decay $N_{2b}^* \rightarrow N_{2a}^* + \pi$ will be very small compared to the phase space for the competing modes of decay; $N_{2b}^* \rightarrow N + \pi$ and $N_{2b}^* \rightarrow N_1^* + \pi$ [see Eqs. (82) and (83)]. However, it may be remarked that if we consider the transition from an isobaric state on the high-energy side of the center of the N_{2b}^* resonance to a state on the low-energy side of the N_{2a}^* resonance, the decay $N_{2b}^* \rightarrow N_{2a}^* + \pi$ will not be quite as improbable as for the example considered above, on account of the larger isobar mass difference Δm_I . In this connection, we note that for an incident π^- energy $T_{\pi,\text{inc}}$ in the range from ~ 0.8 to 1.0 Bev, the isotopic spin $T = \frac{1}{2}$ part of the $\pi^- - p$ interaction will probably proceed mainly via the N_{2b}^* state, which is centered at $T_{\pi,\text{inc}} = 880$ Mev. In this case, the initial compound state of the $\pi - N$ system, \mathfrak{N}_0^* , will have a large component of N_{2b}^* . Thus the transition $\mathfrak{N}_0^* \rightarrow N_2^* + \pi$ of reaction (8) will have a contribution from the decay $N_{2b}^* \rightarrow N_{2a}^* + \pi$. In the present extended isobar model, this contribution is automatically included as a part of the pion spectrum $J_{\pi,3}$.

The possible reactions for $\pi^- - p$ interactions will be labeled by (I), (II), and (III) for the two-pion final states (single-pion production), and by (A)-(D) for the three-pion final states (double-pion production). The possible reactions are as follows:

$$\pi^- + p \rightarrow n + \pi^+ + \pi^-, \quad (\text{I})$$

$$\pi^- + p \rightarrow p + \pi^- + \pi^0, \quad (\text{II})$$

$$\pi^- + p \rightarrow n + 2\pi^0, \quad (\text{III})$$

$$\pi^- + p \rightarrow p + \pi^+ + 2\pi^-, \quad (\text{A})$$

$$\pi^- + p \rightarrow p + \pi^- + 2\pi^0, \quad (\text{B})$$

$$\pi^- + p \rightarrow n + \pi^+ + \pi^0 + \pi^-, \quad (\text{C})$$

$$\pi^- + p \rightarrow n + 3\pi^0. \quad (\text{D})$$

We note that among the reactions leading to 3 pions in the final state, (A) leads to formation of 4-prong events, while (B) and (C) lead to formation of 2-prong events.

From Eq. (27) of the present paper, and from the results of II, one obtains the following expressions for the total cross sections for both N_1^* and N_2^* processes, for the various reactions. The total cross sections will be denoted by $\sigma^{(\text{I})}, \sigma^{(\text{II})}, \dots \sigma^{(\text{D})}$, where the superscript indicates the reaction considered. We find:

$$\sigma^{(\text{I})} = \frac{2}{3} \sigma_{11} \left(\frac{5}{9} + \frac{26}{45} \rho_1 + \frac{7}{9} a \right) + \frac{4}{9} \sigma_{12,s}, \quad (28)$$

$$\sigma^{(\text{II})} = \frac{2}{3} \sigma_{11} \left(\frac{2}{9} + \frac{17}{45} \rho_1 - \frac{5}{9} a \right) + \frac{2}{9} \sigma_{12,s} (A + 2B), \quad (29)$$

$$\sigma^{(\text{III})} = \frac{2}{3} \sigma_{11} \left(\frac{2}{9} + \frac{2}{45} \rho_1 - \frac{2}{9} a \right) + \frac{2}{9} \sigma_{12,s} B, \quad (30)$$

$$\sigma^{(\text{A})} = (10/27) A \sigma_{12,d}, \quad (31)$$

$$\sigma^{(\text{B})} = (4/27) \sigma_{12,d} (1 + \rho_2), \quad (32)$$

$$\sigma^{(\text{C})} = (2/27) \sigma_{12,d} (2A + 5B), \quad (33)$$

$$\sigma^{(\text{D})} = (4/27) \sigma_{12,d} B, \quad (34)$$

where σ_{11} denotes the cross section for producing $N_1^* + \pi$ [Eq. (10)] in the state of total isotopic spin $T = \frac{1}{2}$; $\sigma_{12,s}$ and $\sigma_{12,d}$ are the parts of the cross section σ_{12} which pertain to single-pion production and double-pion production, respectively. σ_{12} has been defined above [after Eq. (12)] as the cross section for producing $N_2^* + \pi$ in the state of total isotopic spin $T = \frac{1}{2}$. In general, we use the notation $\sigma_{2T,\alpha}$ for the cross section for producing $N_\alpha + \pi$ ($\alpha = 1$ or 2) in the state of total isotopic spin T . In Eqs. (28)-(30), ρ_1 is defined as: $\rho_1 \equiv \sigma_{31}/(2\sigma_{11})$, i.e., ρ_1 is the same as the ratio ρ used in II. The constant a is defined in the same manner as in II:

$$a \equiv (2/5^{\frac{1}{2}}) \rho_1^{\frac{1}{2}} \cos \varphi_1, \quad (34a)$$

where φ_1 is the phase angle between the matrix elements for production of $N_1^* + \pi$ in the $T = \frac{1}{2}$ and $T = \frac{3}{2}$ states. Thus φ_1 is the same as the angle φ defined in II [see Eqs. (20), (21), and (27) of II].

The differential cross sections as a function of center-of-mass momentum \bar{p}_π for the pions from the reactions (I)-(III) are given by:

$$\begin{aligned} \left(\frac{d\sigma}{d\bar{p}_\pi} \right)^{(\text{I})} (\pi^-) = & \frac{2}{3} \left[\left(\frac{1}{2} + \frac{2}{5} \rho_1 + a \right) J_{\pi,1} \right. \\ & \left. + \left(\frac{1}{18} + \frac{8}{45} \rho_1 - \frac{2}{9} a \right) J_{\pi,2} \right] \\ & + \frac{4}{9} \sigma_{12,s} A J_{\pi,3}, \quad (35) \end{aligned}$$

$$\begin{aligned} \left(\frac{d\sigma}{d\bar{p}_\pi} \right)^{(I)} (\pi^+) = & \frac{2}{3} \sigma_{11} \left[\left(\frac{1}{18} + \frac{8}{45} \rho_1 - \frac{2}{9} a \right) J_{\pi,1} \right. \\ & \left. + \left(\frac{1}{2} + \frac{2}{5} \rho_1 + a \right) J_{\pi,2} \right] \\ & + \frac{4}{9} \sigma_{12,s} A J_{\pi,4}, \quad (36) \end{aligned}$$

$$\begin{aligned} \left(\frac{d\sigma}{d\bar{p}_\pi} \right)^{(II)} (\pi^-) = & \frac{2}{3} \sigma_{11} \left[\left(\frac{1}{9} + \frac{1}{45} \rho_1 - \frac{1}{9} a \right) J_{\pi,1} \right. \\ & \left. + \left(\frac{1}{9} + \frac{16}{45} \rho_1 - \frac{4}{9} a \right) J_{\pi,2} \right] \\ & + \frac{2}{9} \sigma_{12,s} (A J_{\pi,3} + 2 B J_{\pi,4}), \quad (37) \end{aligned}$$

$$\begin{aligned} \left(\frac{d\sigma}{d\bar{p}_\pi} \right)^{(II)} (\pi^0) = & \frac{2}{3} \sigma_{11} \left[\left(\frac{1}{9} + \frac{16}{45} \rho_1 - \frac{4}{9} a \right) J_{\pi,1} \right. \\ & \left. + \left(\frac{1}{9} + \frac{1}{45} \rho_1 - \frac{1}{9} a \right) J_{\pi,2} \right] \\ & + \frac{2}{9} \sigma_{12,s} (2 B J_{\pi,3} + A J_{\pi,4}), \quad (38) \end{aligned}$$

$$\begin{aligned} \left(\frac{d\sigma}{d\bar{p}_\pi} \right)^{(III)} (\pi^0) = & \frac{2}{3} \sigma_{11} \left(\frac{2}{9} + \frac{2}{45} \rho_1 - \frac{2}{9} a \right) (J_{\pi,1} + J_{\pi,2}) \\ & + \frac{2}{9} \sigma_{12,s} B (J_{\pi,3} + J_{\pi,4}). \quad (39) \end{aligned}$$

Here $J_{\pi,1}$ and $J_{\pi,2}$ are the center-of-mass (c.m.) momentum spectra for the N_1^* processes previously considered in II. Thus $J_{\pi,1}$ pertains to the decay pion from reaction (11); $J_{\pi,2}$ denotes the c.m. spectrum of the recoil pion from (10). Similarly, for the N_2^* reactions, $J_{\pi,3}$ denotes the spectrum of the recoil pion from (8), while $J_{\pi,4}$ is the spectrum of the decay pion from (9a). All of the spectra $J_{\pi,i}$ are normalized to unity, i.e.,

$$\int_0^{\bar{p}_{\pi,\max}} J_{\pi,i} d\bar{p}_\pi = 1, \quad (40)$$

where $\bar{p}_{\pi,\max}$ is the maximum possible value of \bar{p}_π .

The spectra (35)–(38) are normalized to the corresponding total cross sections $\sigma^{(I)}$ and $\sigma^{(II)}$ [Eqs. (28) and (29)]. The spectrum (39) for the π^0 mesons from reaction (III) has been normalized to twice the cross section $\sigma^{(III)}$ [Eq. (30)] since there are two π^0 's originating from the reaction. For the three-pion events, for which $d\sigma/d\bar{p}_\pi$ is given below, a similar normalization

has been used, i.e., for the π^- from reaction (A) and the π^0 from reaction (B), the expressions for $d\sigma/d\bar{p}_\pi$ are normalized to $2\sigma^{(A)}$ and $2\sigma^{(B)}$, respectively, while $d\sigma/d\bar{p}_\pi$ for the π^0 from reaction (D) is normalized to $3\sigma^{(D)}$.

The pion momentum spectra from reactions (A)–(D) are given by:

$$\left(\frac{d\sigma}{d\bar{p}_\pi} \right)^{(A)} (\pi^+) = \frac{10}{27} A \sigma_{12,d} (0.1 J_{\pi,5} + 0.9 J_{\pi,6}), \quad (41)$$

$$\left(\frac{d\sigma}{d\bar{p}_\pi} \right)^{(A)} (\pi^-) = \frac{10}{27} A \sigma_{12,d} (J_{\pi,3} + 0.9 J_{\pi,5} + 0.1 J_{\pi,6}), \quad (42)$$

$$\left(\frac{d\sigma}{d\bar{p}_\pi} \right)^{(B)} (\pi^0) = \frac{8}{27} \sigma_{12,d} [A J_{\pi,3} + 0.5 B (J_{\pi,5} + J_{\pi,6})], \quad (43)$$

$$\begin{aligned} \left(\frac{d\sigma}{d\bar{p}_\pi} \right)^{(B)} (\pi^-) = & \frac{1}{27} \sigma_{12,d} [2 B J_{\pi,3} \\ & + (2A+B)(J_{\pi,5} + J_{\pi,6})], \quad (44) \end{aligned}$$

$$\begin{aligned} \left(\frac{d\sigma}{d\bar{p}_\pi} \right)^{(C)} (\pi^+) = & \frac{1}{27} \sigma_{12,d} [(2A+9B) J_{\pi,5} \\ & + (2A+B) J_{\pi,6}], \quad (45) \end{aligned}$$

$$\left(\frac{d\sigma}{d\bar{p}_\pi} \right)^{(C)} (\pi^0) = \frac{2}{27} \sigma_{12,d} [5 B J_{\pi,3} + A (J_{\pi,5} + J_{\pi,6})], \quad (46)$$

$$\left(\frac{d\sigma}{d\bar{p}_\pi} \right)^{(C)} (\pi^-) = \frac{1}{27} \sigma_{12,d} [4 A J_{\pi,3} + B (J_{\pi,5} + 9 J_{\pi,6})], \quad (47)$$

$$\left(\frac{d\sigma}{d\bar{p}_\pi} \right)^{(D)} (\pi^0) = \frac{4}{27} \sigma_{12,d} B (J_{\pi,3} + J_{\pi,5} + J_{\pi,6}). \quad (48)$$

Here, as in Eqs. (35)–(39), the parenthesis $(\pi^{\pm,0})$ after $(d\sigma/d\bar{p}_\pi)$ indicates the pion considered for which the momentum spectrum is given. In Eqs. (41)–(48), $J_{\pi,5}$ denotes the c.m. momentum spectrum of the pion emitted in the decay $N_2^* \rightarrow N_1^* + \pi$, while $J_{\pi,6}$ is the spectrum of the pion emitted in the subsequent decay of N_1^* [Eq. (9b)].

We shall now consider the pion production in $\pi^+ - p$ collisions. In this case, the wave function for the final state $\Psi_{\pi^+ - p}^{(2)(final)}$ is given by:

$$\Psi_{\pi^+ - p}^{(2)(final)} = \xi_1 \lambda_{\frac{1}{2}}. \quad (49)$$

From Eqs. (19), (21), and (23)–(25), one obtains:

$$\begin{aligned} & |\Psi_{\pi^+ - p}^{(2)(final)}|^2 \\ & = P_s [\frac{1}{3} (R^+ D_2^0 p_2) + \frac{2}{3} (R^+ D_2^+ n_2)] \\ & \quad + P_d [(1/18) (R^+ D_{21}^+ D_1^- p_1) + \frac{1}{9} (R^+ D_{21}^+ D_1^0 n_1) \\ & \quad + (2/9) (R^+ D_{21}^0 D_1^0 p_1) + \frac{1}{9} (R^+ D_{21}^0 D_1^+ n_1) \\ & \quad + \frac{1}{2} (R^+ D_{21}^- D_1^+ p_1)]. \quad (50) \end{aligned}$$

For the $\pi^+ - p$ interactions, the two-pion final states will be labelled (IV) and (V), while the three-pion final

states will be labelled (E), (F), and (G). The possible reactions are as follows:

$$\pi^+ + p \rightarrow p + \pi^+ + \pi^0, \quad (\text{IV})$$

$$\pi^+ + p \rightarrow n + 2\pi^+, \quad (\text{V})$$

$$\pi^+ + p \rightarrow p + 2\pi^+ + \pi^-, \quad (\text{E})$$

$$\pi^+ + p \rightarrow p + \pi^+ + 2\pi^0, \quad (\text{F})$$

$$\pi^+ + p \rightarrow n + 2\pi^+ + \pi^0. \quad (\text{G})$$

The total cross sections for these reactions are given by

$$\sigma^{(\text{IV})} = (13/15)\sigma_{31} + \frac{1}{3}\sigma_{32,s} \quad (51)$$

$$\sigma^{(\text{V})} = (2/15)\sigma_{31} + \frac{2}{3}\sigma_{32,s}, \quad (52)$$

$$\sigma^{(\text{E})} = (5/9)\sigma_{32,d}, \quad (53)$$

$$\sigma^{(\text{F})} = \sigma^{(\text{G})} = (2/9)\sigma_{32,d}. \quad (54)$$

The following expressions for the c.m. momentum spectra are normalized to $n_\pi\sigma$, where n_π is the number of pions of the charge state considered, and σ is the total cross section as given by Eqs. (51)–(54). This normalization is similar to that used above for the spectra from $\pi^- - p$ interactions.

From Eq. (50), one obtains

$$\left(\frac{d\sigma}{d\bar{p}_\pi} \right)^{(\text{IV})} (\pi^+) = \sigma_{31} \left(\frac{3}{5} J_{\pi,1} + \frac{4}{15} J_{\pi,2} \right) + \frac{1}{3} \sigma_{32,s} J_{\pi,3}, \quad (55)$$

$$\left(\frac{d\sigma}{d\bar{p}_\pi} \right)^{(\text{IV})} (\pi^0) = \sigma_{31} \left(\frac{4}{15} J_{\pi,1} + \frac{3}{5} J_{\pi,2} \right) + \frac{1}{3} \sigma_{32,s} J_{\pi,4}, \quad (56)$$

$$\begin{aligned} \left(\frac{d\sigma}{d\bar{p}_\pi} \right)^{(\text{V})} (\pi^+) &= \frac{2}{15} \sigma_{31} (J_{\pi,1} + J_{\pi,2}) \\ &\quad + \frac{2}{3} \sigma_{32,s} (J_{\pi,3} + J_{\pi,4}), \end{aligned} \quad (57)$$

$$\left(\frac{d\sigma}{d\bar{p}_\pi} \right)^{(\text{E})} (\pi^+) = \sigma_{32,d} \left(\frac{5}{9} J_{\pi,3} + \frac{1}{18} J_{\pi,5} + \frac{1}{2} J_{\pi,6} \right), \quad (58)$$

$$\left(\frac{d\sigma}{d\bar{p}_\pi} \right)^{(\text{E})} (\pi^-) = \sigma_{32,d} \left(\frac{1}{2} J_{\pi,5} + \frac{1}{18} J_{\pi,6} \right), \quad (59)$$

$$\left(\frac{d\sigma}{d\bar{p}_\pi} \right)^{(\text{F})} (\pi^+) = \frac{2}{9} \sigma_{32,d} J_{\pi,3}, \quad (60)$$

$$\left(\frac{d\sigma}{d\bar{p}_\pi} \right)^{(\text{F})} (\pi^0) = \frac{2}{9} \sigma_{32,d} (J_{\pi,5} + J_{\pi,6}), \quad (61)$$

$$\left(\frac{d\sigma}{d\bar{p}_\pi} \right)^{(\text{G})} (\pi^+) = \sigma_{32,d} \left[\frac{2}{9} J_{\pi,3} + \frac{1}{9} (J_{\pi,5} + J_{\pi,6}) \right], \quad (62)$$

$$\left(\frac{d\sigma}{d\bar{p}_\pi} \right)^{(\text{G})} (\pi^0) = \frac{1}{9} \sigma_{32,d} (J_{\pi,5} + J_{\pi,6}), \quad (63)$$

where $\sigma_{32,s}$ and $\sigma_{32,d}$ are parts of σ_{32} which pertain to

single-pion production and double-pion production, respectively.

In connection with the total cross sections of Eqs. (28)–(34), we note that for the two-pion final states, we obtain

$$\begin{aligned} \sigma^{(\text{I})} + \sigma^{(\text{II})} + \sigma^{(\text{III})} &= \frac{2}{3}\sigma_{11}(1+\rho_1) + \frac{2}{3}\sigma_{12,s}(1+\rho_2) \\ &= \frac{2}{3}\sigma_{11} + \frac{1}{3}\sigma_{31} + \frac{2}{3}\sigma_{12,s} + \frac{1}{3}\sigma_{32,s}. \end{aligned} \quad (64)$$

This result was to be expected, since the cross section for any process (via N_1^* or N_2^*) arising from $\pi^- - p$ interactions is equal to $[\frac{2}{3}\sigma(T=\frac{1}{2}) + \frac{1}{3}\sigma(T=\frac{3}{2})]$, where $\sigma(T=\frac{1}{2})$ and $\sigma(T=\frac{3}{2})$ are the corresponding cross sections for the $T=\frac{1}{2}$ and $T=\frac{3}{2}$ isotopic spin states.

Similarly, for the three-pion final states, we have

$$\begin{aligned} \sigma^{(\text{A})} + \sigma^{(\text{B})} + \sigma^{(\text{C})} + \sigma^{(\text{D})} &= \frac{2}{3}\sigma_{12,d}(1+\rho_2) \\ &= \frac{2}{3}\sigma_{12,d} + \frac{1}{3}\sigma_{32,d}. \end{aligned} \quad (65)$$

From Eqs. (51)–(54), one obtains for $\pi^- - p$ interactions:

$$\sigma^{(\text{IV})} + \sigma^{(\text{V})} = \sigma_{31} + \sigma_{32,s}, \quad (66)$$

$$\sigma^{(\text{E})} + \sigma^{(\text{F})} + \sigma^{(\text{G})} = \sigma_{32,d}. \quad (67)$$

In connection with the inelastic $\pi^- - p$ interactions discussed in II, we have defined the ratio R of the cross sections for reactions (I) and (II): $R \equiv \sigma^{(\text{II})}/\sigma^{(\text{I})}$. With the inclusion of the N_2^* processes, one obtains from Eqs. (28) and (29):

$$\begin{aligned} R &= \frac{\sigma^{(\text{II})}}{\sigma^{(\text{I})}} = \frac{\sigma(p + \pi^- + \pi^0)}{\sigma(n + \pi^+ + \pi^-)} \\ &= \frac{10 + 17\rho_1 - 25a + 15\tau(A + 2B)}{25 + 26\rho_1 + 35a + 30\tau A}, \end{aligned} \quad (68)$$

where the constant τ is defined by

$$\tau \equiv \sigma_{12,s}/\sigma_{11}. \quad (69)$$

For $\sigma_{12,s}=0$ ($\tau=0$), Eq. (68) reduces to Eq. (37) of II, as is expected. For $\sigma_{11}=0$ ($\tau=\infty$), corresponding to the presence of N_2^* processes only, the expression for R becomes

$$R(\tau=\infty) = \frac{1}{2} + B/A. \quad (70)$$

It may be noted that the ratio R depends on the five parameters ρ_1 , φ_1 , ρ_2 , φ_2 , and τ , so that R will be most useful in determining any of these constants, when it is combined with information from other sources. One such possibility is the measurement of $\sigma^{(\text{III})}$, and hence the determination of the ratio $S \equiv \sigma^{(\text{III})}/\sigma^{(\text{I})}$ [see Eq. (30)]. If it is assumed that the N_2^* processes are negligible, so that $\tau \sim 0$, then R depends only on ρ_1 and φ_1 , as has been discussed in II. Information on the constants ρ_2 , φ_2 , and τ can be obtained from a measurement of the partial cross sections for the three-pion events [Eqs. (31)–(34)].

In II, we have introduced the ratio ξ of the intensity of fast π^+ to slow π^+ mesons from the reaction (I) [see

Eq. (42) of II]. The intensity of fast π^+ was taken as the coefficient of $J_{\pi,2}$ in Eq. (36) ($J_{\pi,2}$ =spectrum of recoil pions), while the intensity of slow π^+ was assumed to be given by the coefficient of $J_{\pi,1}$ (decay pions). With the inclusion of N_2^* reactions, we have in addition a term proportional to $J_{\pi,4}$ (decay pions from $N_2^* \rightarrow N + \pi$). As will be shown below, the $J_{\pi,4}$ spectrum consists predominantly of fast pions, so that the coefficient of $J_{\pi,4}$ can be combined with that of $J_{\pi,2}$ in Eq. (36), in order to obtain the ratio ξ including the N_2^* processes. We thus find

$$\xi = (45 + 36\rho_1 + 90a + 60\tau A) / (5 + 16\rho_1 - 20a). \quad (71)$$

Of course, for $\tau=0$, Eq. (71) reduces to Eq. (42) of II. The shape of the π^+ spectrum from reaction (I), which determines the experimental value of ξ , can thus be used as an additional restriction on the parameters ρ_i , φ_i , and τ , besides the values of R and S defined above.

For the $\pi^+ - p$ interactions, the situation is very much simpler, since one is dealing with a pure $T=\frac{3}{2}$ state, so that the parameters ρ_i and φ_i do not enter. We will define the ratio U of the single-pion production reactions, as follows:

$$U \equiv \frac{\sigma^{(IV)}}{\sigma^{(V)}} = \frac{\sigma(p + \pi^+ + \pi^0)}{\sigma(n + \pi^+ + \pi^+)} = \frac{13 + 5\eta}{2 + 10\eta}, \quad (72)$$

where the constant η is defined by

$$\eta \equiv \sigma_{32,s} / \sigma_{31}. \quad (73)$$

Equation (72) shows that a measurement of U enables one to determine directly the ratio η , which gives the relative strength of the N_2^* processes (leading to single-pion production) and the N_1^* reactions. We note that for $\sigma_{32,s}=0$ ($\eta=0$), we have $U=6.5$, as was pointed out in II [Eq. (36)]. On the other hand, for $\sigma_{31}=0$ ($\eta=\infty$; absence of N_1^* reactions), we would obtain $U=0.5$. For other values of η , the present isobar model predicts that the value of U should be intermediate between the extreme values of 0.5 and 6.5. From Eq. (72), we obtain the following expression for η in terms of U :

$$\eta = (13 - 2U) / (10U - 5). \quad (74)$$

III. CALCULATION OF THE PION SPECTRA $J_{\pi,i}$ AND THE NUCLEON SPECTRA $I_{N,i}^{(\pi)}$ FROM PION-NUCLEON INTERACTIONS

In this section, we will describe the procedure of the calculation of the pion spectra $J_{\pi,i}$ and the recoil nucleon spectra $I_{N,i}^{(\pi)}$. Calculations were carried out for incident pion energies $T_{\pi,\text{inc}}=1.0, 1.4$, and 2.0 Bev.

The procedure of the calculation of $J_{\pi,1}$ and $J_{\pi,2}$ has been described in II. These spectra pertain to the decay pion and the recoil pion, respectively, from the

reactions via N_1^* [Eqs. (10) and (11)].²¹ The spectra $J_{\pi,3}$ and $J_{\pi,4}$ which pertain to the N_2^* reactions (8) and (9a) are obtained in essentially the same manner as $J_{\pi,1}$ and $J_{\pi,2}$. Thus $J_{\pi,3}$ represents the spectrum of the recoil pions from reaction (8). $J_{\pi,4}$ is given by

$$J_{\pi,4}(\bar{T}_\pi) = K_3 \sigma_{\frac{1}{2}}(m_2) \bar{v}_\pi (dm_2/d\bar{T}_\pi) F, \quad (75)$$

where K_3 is a normalization factor; $\sigma_{\frac{1}{2}}(m_2)$ is the total $T=\frac{1}{2}$ pion-nucleon scattering cross section at the incident pion energy which corresponds to an energy $m_2 c^2$ in the center-of-mass system of the pion and nucleon (rest system of the isobar); m_2 is the mass of the isobar N_2^* for which the recoil pion has the energy \bar{T}_π in the center-of-mass system of reaction (8); F is the two-body phase space factor for the recoil pion and N_2^* , for the appropriate total energy \bar{E} in the c.m. system of reaction (8):

$$F = \bar{p}_\pi \bar{E}_\pi \bar{E}_{N_2} / \bar{E}, \quad (76)$$

where \bar{E}_π and \bar{E}_{N_2} are the center-of-mass total energies of the pion and N_2^* , respectively; \bar{p}_π is the c.m. momentum of either particle; and $\bar{E} = \bar{E}_\pi + \bar{E}_{N_2}$.

We note that for $\sigma_{\frac{1}{2}}$ we use the total $T=\frac{1}{2}$ cross section for all values of m_2 which are kinematically possible. Thus, at an incident energy $T_{\pi,\text{inc}}=1.0$ Bev, for which $\bar{E}=1.743$ Bev, the range of m_2 extends from $m_{2,\min}=m_N+m_\pi=1.078$ Bev up to $m_{2,\max}=\bar{E}-m_\pi=1.603$ Bev, and therefore includes the lower maximum of the $T=\frac{1}{2}$ cross section, which is centered at $m_2=1.51$ Bev. The choice of the lower limit for m_2 will be discussed in more detail below.

In order to obtain the values of $\sigma_{\frac{1}{2}}$ used in the calculations, we employed the experimental values of $\sigma(\pi^- - p)$ and $\sigma(\pi^+ - p)$ determined by Brisson *et al.*¹⁸ and Devlin *et al.*¹⁹

In the calculations pertaining to Eq. (75), the range of m_2 was divided into equal intervals of 25 Mev. The j th interval, centered at mass $m_2=m_{2j}$, gives rise to a step function of value $g_{j,3}$:

$$g_{j,3} \equiv K_3 \sigma_{\frac{1}{2}}(m_{2j}) F_j \bar{v}_{\pi,j} / (\bar{T}_{\pi^{(j+)}} - \bar{T}_{\pi^{(j-)}}), \quad (77)$$

which represents $J_{\pi,3}$ in the interval from $\bar{T}_{\pi^{(j-)}}$ to $\bar{T}_{\pi^{(j+)}}$. Here $\bar{T}_{\pi^{(j\pm)}}$ is given by

$$\bar{T}_{\pi^{(j\pm)}} = \frac{1}{2} [\bar{T}_{\pi^{(j)}} + \bar{T}_{\pi^{(j\pm1)}}, \quad (78)$$

where $\bar{T}_{\pi^{(j)}}$ is the value of the recoil pion energy \bar{T}_π which pertains to the isobar N_2^* with mass m_{2j} . In Eq. (77), $\sigma_{\frac{1}{2}}(m_{2j})$, F_j , and $\bar{v}_{\pi,j}$ are the values of $\sigma_{\frac{1}{2}}$, F , and \bar{v}_π pertaining to m_{2j} [see Eqs. (7) and (8) of II].

The spectrum $J_{\pi,4}$ represents the c.m. momentum distribution of the pions from the decay of N_2^* [Eq.

²¹ We note that a derivation of the factor $\sigma_{\frac{1}{2}}(m_l)F$ in the expression for the probability $P_{\frac{1}{2}}(m_l)$ for the formation of the $T=\frac{3}{2}$ isobar N_1^* with mass m_l has also been given by S. Bergia, F. Bonsignori, and A. Stanghellini, Nuovo cimento **16**, 1073 (1960). They find that interference effects due to the finite lifetime of the isobar are small except at lower energies than are considered here.

(9a)]. $J_{\pi,4}$ is given by

$$\begin{aligned} \frac{J_{\pi,4}(\bar{T}_\pi)}{\bar{v}_\pi} &\equiv I_{\pi,4}(\bar{T}_\pi) \\ &= K_4 \int_{m_2,\min}^{m_2,\max} \sigma_{\frac{1}{2}}(m_2) F G_\pi [1 - \epsilon(m_2)] dm_2, \end{aligned} \quad (79)$$

where K_4 is a normalization factor, $m_{2,\min} = m_N + m_\pi = 1.078$ Bev, $m_{2,\max} = \bar{E} - m_\pi$, and F is the appropriate two-body phase space factor; $I_{\pi,4}$ is the corresponding c.m. energy distribution of the pions. The factor $[1 - \epsilon(m_2)]$ in the integrand of (79) takes into account the possibility that N_2^* may decay into $N_1^* + \pi$, rather than $N + \pi$. Thus, $\epsilon(m_2)$ is defined as the probability of the decay $N_2^* \rightarrow N_1^* + \pi$ for an isobar N_2^* of mass m_2 . The method of determination of $\epsilon(m_2)$ will be described below. In Eq. (79), G_π is a step function of value:

$$G_\pi = 1/(\bar{T}_{\pi,\max} - \bar{T}_{\pi,\min}) \quad \text{for } \bar{T}_{\pi,\min} < \bar{T}_\pi < \bar{T}_{\pi,\max}, \quad (80)$$

$$G_\pi = 0 \quad \text{for } \bar{T}_\pi < \bar{T}_{\pi,\min} \text{ and } \bar{T}_\pi > \bar{T}_{\pi,\max}, \quad (80a)$$

where $\bar{T}_{\pi,\min}$ and $\bar{T}_{\pi,\max}$ are the minimum and maximum values of the c.m. energy of the decay pion from the isobar N_2^* with mass m_2 . In Eqs. (80) and (80a), it has been assumed that the isobar N_2^* decays isotropically in its rest system. For simplicity, this assumption will be made throughout this paper for both N_1^* and N_2^* decays (see footnote 19 of I).

In analogy to Eq. (5) of II, the spectrum $I_{\pi,4}$ is obtained by adding the step functions $g_{j,4}$ defined by

$$\begin{aligned} g_{j,4} &\equiv \frac{K_4 \sigma_{\frac{1}{2}}(m_{2,j}) F [1 - \epsilon(m_{2,j})]}{\bar{T}_{\pi,\max}^{(j)} - \bar{T}_{\pi,\min}^{(j)}} \\ &\quad \text{for } \bar{T}_{\pi,\min}^{(j)} < \bar{T}_\pi < \bar{T}_{\pi,\max}^{(j)}, \end{aligned} \quad (81)$$

$$g_{j,4} = 0, \quad \text{for } \bar{T}_\pi < \bar{T}_{\pi,\min}^{(j)} \text{ and } \bar{T}_\pi > \bar{T}_{\pi,\max}^{(j)}, \quad (81a)$$

where F_j , $\bar{T}_{\pi,\max}^{(j)}$, and $\bar{T}_{\pi,\min}^{(j)}$ are the values of F , $\bar{T}_{\pi,\max}$, and $\bar{T}_{\pi,\min}$ pertaining to $m_{2,j}$.

The probability $\epsilon(m_2)$ which enters into Eq. (79) is determined in the following manner. For a definite mass $m_1^{(\alpha)}$ of the isobar N_1^* we can obtain the phase space for the decay of N_2^* (with mass m_2) into N_1^* . This phase space will be denoted by $F_d(N_2^* \rightarrow N_1^{(\alpha)*})$, and is given by

$$F_d(N_2^* \rightarrow N_1^{(\alpha)*}) = p_\pi^{(\alpha)*} E_{N_1^{(\alpha)*}} / m_2, \quad (82)$$

where $p_\pi^{(\alpha)*} = p_{N_1^{(\alpha)*}}$ is the momentum of the pion (or N_1^*) in the rest system of N_2^* ; $E_\pi^{(\alpha)*}$ and $E_{N_1^{(\alpha)*}}$ are the total energies of the pion and of N_1^* in this system. We have: $m_2 = E_\pi^{(\alpha)*} + E_{N_1^{(\alpha)*}}$.

In similarity to (82), we can obtain the phase space factor $F_d(N_2^* \rightarrow N)$ for the decay $N_2^* \rightarrow N + \pi$. We have

$$F_d(N_2^* \rightarrow N) = p_\pi^{(N)*} E_\pi^{(N)*} E_N^{(N)*} / m_2, \quad (83)$$

where $p_\pi^{(N)*} = p_N^{(N)*}$ is the momentum of the pion (or

nucleon) in the rest system of N_2^* ; $E_\pi^{(N)*}$ and $E_N^{(N)*}$ are the total energies of the pion and nucleon in this rest system.

We assume that the two alternate modes of decay ($m_2 > m_1^{(\alpha)} + m_\pi$) proceed in proportion to their respective phase factors F_d . Thus the probability ϵ is obtained from

$$\epsilon(m_2) = \frac{F_d(N_2^* \rightarrow N_1^{(\alpha)*})}{F_d(N_2^* \rightarrow N) + F_d(N_2^* \rightarrow N_1^{(\alpha)*})}. \quad (84)$$

As indicated, ϵ is only a function of the mass m_2 of the isobar N_2^* (for a fixed choice of $m_1^{(\alpha)}$). Representative values of $\epsilon(m_2)$ for $m_1^{(\alpha)} = 1.225$ Bev are as follows: $\epsilon(1.365 \text{ Bev}) = 0$; $\epsilon(1.40) = 0.120$; $\epsilon(1.50) = 0.246$; $\epsilon(1.60) = 0.312$; $\epsilon(1.80) = 0.381$; $\epsilon(2.00) = 0.419$.

The average of $\epsilon(m_2)$ over the mass distribution of N_2^* is given by

$$\langle \epsilon(m_2) \rangle = \frac{\int_{m_2,\min}^{m_2,\max} \sigma_{\frac{1}{2}}(m_2) F \epsilon(m_2) dm_2}{\int_{m_2,\min}^{m_2,\max} \sigma_{\frac{1}{2}}(m_2) F dm_2}, \quad (85)$$

where $m_{2,\min} = m_N + m_\pi = 1.078$ Bev, and $m_{2,\max} = \bar{E} - m_\pi$. If one uses $m_1^{(\alpha)} = 1.225$ Bev for the calculation of $\epsilon(m_2)$, one obtains the following values of $\langle \epsilon(m_2) \rangle$ from Eq. (85): $\langle \epsilon(m_2) \rangle = 0.111$ at $T_{\pi,\text{inc}} = 1.0$ Bev, 0.192 at 1.4 Bev, and 0.247 at 2.0 Bev.

In obtaining the values of $\epsilon(m_2)$ used in the calculation of the spectrum $J_{\pi,4}$, we have assumed for simplicity that the isobar N_1^* has the fixed mass $m_1^{(\alpha)} = 1.225$ Bev, corresponding to the center of the $T=J=\frac{3}{2}$ resonance. The resulting error in $J_{\pi,4}$ which is introduced by this simplification is expected to be quite small, since $J_{\pi,4}$ involves the difference $1 - \epsilon(m_2)$, and the effective values of $\epsilon(m_2)$ are only of order 0.1–0.2. On the other hand, as will be discussed below, for the spectra $J_{\pi,5}$ and $J_{\pi,6}$ pertaining to the three-pion final states, which involve $\epsilon^{(\alpha)}(m_2)$ directly [rather than $(1 - \epsilon)$], we have used an appropriate average of the spectra $J_{\pi,5}^{(\alpha)}$ and $J_{\pi,6}^{(\alpha)}$ obtained for three mass values $m_1^{(\alpha)}$ of the isobar N_1^* .

In connection with the pion spectrum $J_{\pi,4}$, we note that the preceding calculation is based on Eq. (80), which gives the decay pion spectrum for the isobar N_2^* with fixed mass m_2 , irrespective of the angle of the decay pion with respect to the direction of motion of N_2^* . Thus, if the cross section for isobar production is not isotropic in the c.m. system, $J_{\pi,4}$ must be interpreted as the momentum spectrum integrated over all angles $\hat{\theta}_\pi$ of the pion with respect to the incident direction (i.e., $J_{\pi,4} \propto d\sigma/d\hat{p}_\pi$). In the special case that the isobar production is isotropic, this restriction is not necessary, and $J_{\pi,4}$ is then proportional to the differential cross section $d^2\sigma/d\hat{p}_\pi d\Omega_\pi$ at all angles $\hat{\theta}_\pi$. The same remark applies for all of the other decay spectra obtained in this paper (e.g., $J_{\pi,1}$, $J_{\pi,5}$, and $J_{\pi,6}$ for

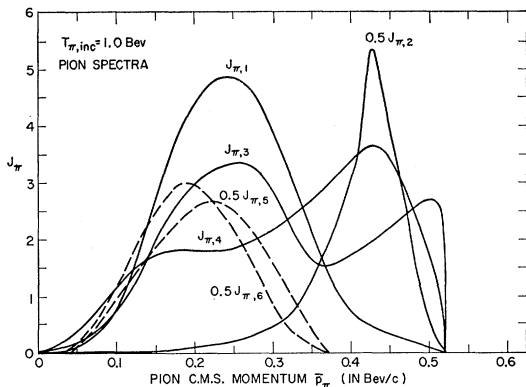


FIG. 2. Center-of-mass momentum spectra of pions from pion-nucleon interactions at an incident pion energy $T_{\pi,\text{inc}}=1.0$ Bev. The spectra $J_{\pi,3}$ and $J_{\pi,4}$ were calculated by including the contribution of the low-energy $T=\frac{1}{2}$ cross section.

$\pi-N$ interactions). The possibility of other than isotropic distributions for the isobar production cross section has been considered in I.

The spectrum $J_{\pi,5}$ gives the momentum distribution of the decay pions from $N_2^* \rightarrow N_1^* + \pi$. For the purpose of the present calculation, it was assumed that the mass distribution of N_1^* [which is given by the scattering cross section $\sigma(\pi^+ - p)$] can be effectively replaced by three mass values $m_1^{(\alpha)}$, with $m_1^{(1)}=1.15$ Bev (weight $w=0.25$), $m_1^{(2)}=1.225$ Bev ($w=0.5$), and $m_1^{(3)}=1.30$ Bev ($w=0.25$). The value $m_1^{(2)}=1.225$ Bev corresponds to the center of the $T=\frac{3}{2}$ resonance (incident pion energy $T_\pi=180$ Mev). In view of the narrowness of the mass distribution of N_1^* , it is believed that no appreciable error is introduced by the present procedure involving the $m_1^{(\alpha)}$.

For each $m_1^{(\alpha)}$, the calculation proceeds in the same manner as for $J_{\pi,4}$ except that the maximum and minimum pion energies $\bar{T}_{\pi,\text{max}}^{(\alpha)}$ and $\bar{T}_{\pi,\text{min}}^{(\alpha)}$ now depend on $m_1^{(\alpha)}$. We have

$$\begin{aligned}\bar{T}_{\pi,\text{max}}^{(\alpha)} &= \bar{\gamma}_2 [E_\pi^{(\alpha)*} + \bar{v}_2 p_\pi^{(\alpha)*}] - m_\pi, \\ \bar{T}_{\pi,\text{min}}^{(\alpha)} &= \bar{\gamma}_2 [E_\pi^{(\alpha)*} - \bar{v}_2 p_\pi^{(\alpha)*}] - m_\pi,\end{aligned}\quad (86)$$

where \bar{v}_2 is the velocity of N_2^* in the c.m. system of reaction (8); $\bar{\gamma}_2 \equiv (1 - \bar{v}_2^2)^{-\frac{1}{2}}$; $E_\pi^{(\alpha)*}$ and $p_\pi^{(\alpha)*}$ are the total energy and momentum of the pion (in the rest system of N_2^*) for the decay $N_2^* \rightarrow N_1^* + \pi$, where N_1^* has mass $m_1^{(\alpha)}$.

It should be noted that instead of the factor $[1 - \epsilon(m_2)]$ which appears in Eq. (79) for $J_{\pi,4}$, the integrand for the spectrum $J_{\pi,5}$ contains the factor $\epsilon^{(\alpha)}(m_2)$, since $J_{\pi,5}$ pertains to the decay $N_2^* \rightarrow N_1^* + \pi$ for which the probability is $\epsilon^{(\alpha)}(m_2)$. Thus the integrand of $J_{\pi,5}$ is given by: $\sigma_{\frac{1}{2}}(m_2) F G_\pi^{(\alpha)} \epsilon^{(\alpha)}(m_2)$, where $G_\pi^{(\alpha)}$ is obtained by means of $\bar{T}_{\pi,\text{max}}^{(\alpha)}$ and $\bar{T}_{\pi,\text{min}}^{(\alpha)}$ as given by Eq. (86). We have obtained for each $J_{\pi,5}^{(\alpha)}$ ($\alpha=1, 2, 3$) the appropriate probability $\epsilon^{(\alpha)}(m_2)$, calculated by assuming a mass $m_1^{(\alpha)}$ ($=1.15, 1.225$, or 1.30 Bev) for the isobar N_1^* .

For each $m_1^{(\alpha)}$, one thus obtains a spectrum $J_{\pi,6}^{(\alpha)}$.

The final spectrum $J_{\pi,5}$ is given by

$$J_{\pi,5} = 0.25 J_{\pi,5}^{(1)} + 0.50 J_{\pi,5}^{(2)} + 0.25 J_{\pi,5}^{(3)}. \quad (87)$$

The spectrum $J_{\pi,6}$ pertains to the decay pions from $N_1^* \rightarrow N + \pi$, which follow the decay $N_2^* \rightarrow N_1^* + \pi$. Here again the same three values of $m_1^{(\alpha)}$ were used, and a spectrum $J_{\pi,6}^{(\alpha)}$ was calculated for each $m_1^{(\alpha)}$. In order to obtain $J_{\pi,6}^{(\alpha)}$, we note that for a given value of m_{2j} , and a given $m_1^{(\alpha)}$, the isobar N_1^* will have a uniform distribution of energies between the values $\bar{T}_{1,\text{min}}^{(\alpha)}$ and $\bar{T}_{1,\text{max}}^{(\alpha)}$, where

$$\begin{aligned}\bar{T}_{1,\text{max}}^{(\alpha)} &= \bar{\gamma}_2 [E_1^{(\alpha)*} + \bar{v}_2 p_1^{(\alpha)*}] - m_1^{(\alpha)}, \\ \bar{T}_{1,\text{min}}^{(\alpha)} &= \bar{\gamma}_2 [E_1^{(\alpha)*} - \bar{v}_2 p_1^{(\alpha)*}] - m_1^{(\alpha)}.\end{aligned}\quad (88)$$

Here $E_1^{(\alpha)*}$ and $p_1^{(\alpha)*}$ are the total energy and momentum of N_1^* (in the rest system of N_2^*) for the decay $N_2^* \rightarrow N_1^* + \pi$. For each value of \bar{T}_1 , one has in turn a step function giving the c.m. energy distribution of the final decay pion from $N_1^* \rightarrow N + \pi$. In the present calculation, five such rectangles were added for each value of m_{2j} and $m_1^{(\alpha)}$. These rectangles pertain to isobars N_1^* with the following kinetic energies:

$$\bar{T}_{1,1}^{(\alpha)} = \bar{T}_{1,\text{max}}^{(\alpha)}, \quad (\text{weight } w=0.125); \quad (89a)$$

$$\bar{T}_{1,2}^{(\alpha)} = \frac{3}{4} \bar{T}_{1,\text{max}}^{(\alpha)} + \frac{1}{4} \bar{T}_{1,\text{min}}^{(\alpha)}, \quad (w=0.25); \quad (89b)$$

$$\bar{T}_{1,3}^{(\alpha)} = \frac{1}{2} (\bar{T}_{1,\text{max}}^{(\alpha)} + \bar{T}_{1,\text{min}}^{(\alpha)}), \quad (w=0.25); \quad (89c)$$

$$\bar{T}_{1,4}^{(\alpha)} = \frac{1}{4} \bar{T}_{1,\text{min}}^{(\alpha)} + \frac{3}{4} \bar{T}_{1,\text{max}}^{(\alpha)}, \quad (w=0.25); \quad (89d)$$

$$\bar{T}_{1,5}^{(\alpha)} = \bar{T}_{1,\text{min}}^{(\alpha)}, \quad (w=0.125). \quad (89e)$$

This procedure gives the contribution to $J_{\pi,6}^{(\alpha)}$ from a single m_{2j} . The weighting factor for the different m_{2j} values is given by $\sigma_{\frac{1}{2}}(m_{2j}) F \epsilon^{(\alpha)}(m_{2j})$. By adding the partial spectra due to all possible m_{2j} values, one obtains $J_{\pi,6}^{(\alpha)}$. Finally $J_{\pi,6}$ is given by

$$J_{\pi,6} = 0.25 J_{\pi,6}^{(1)} + 0.50 J_{\pi,6}^{(2)} + 0.25 J_{\pi,6}^{(3)}. \quad (90)$$

The spectra $J_{\pi,5}$ and $J_{\pi,6}$ were normalized to 1, in the same manner as $J_{\pi,1} - J_{\pi,4}$.

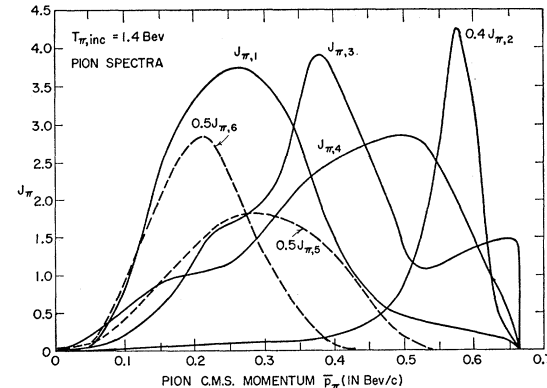


FIG. 3. Center-of-mass momentum spectra of pions from pion-nucleon interactions at an incident pion energy $T_{\pi,\text{inc}}=1.4$ Bev. The spectra $J_{\pi,3}$ and $J_{\pi,4}$ were calculated by including the contribution of the low-energy $T=\frac{1}{2}$ cross section.

In order to summarize the notation used for the $J_{\pi,i}$, we may refer to Fig. 1. Thus, the spectrum $J_{\pi,1}$ corresponds to the transition μ following η ; $J_{\pi,2}$ corresponds to η . Similarly, $J_{\pi,3}$ is the spectrum for the transition $\xi(R)$; $J_{\pi,4}$ corresponds to $\zeta(D_2)$; $J_{\pi,5}$ corresponds to $\nu(D_{21})$; and $J_{\pi,6}$ is the spectrum due to the transition $\mu(D_1)$ following $\nu(D_{21})$.

The pion spectra $J_{\pi,i}$ obtained from the present calculations for $T_{\pi,\text{inc}}=1.0, 1.4, and 2.0 Bev are shown in Figs. 2–4, respectively. It should be noted that both for the spectra $J_{\pi,1}$ and $J_{\pi,2}$ which involve the cross section $\sigma_{\frac{1}{2}}$, and for the spectra $J_{\pi,3}-J_{\pi,6}$ which involve $\sigma_{\frac{3}{2}}$, it was assumed that all isobar masses m_I which are kinematically possible will contribute to the pion production. Thus, the minimum mass $m_{I,\text{min}}$ equals $m_N+m_\pi=1.078$ Bev, while the maximum mass $m_{I,\text{max}}$ is given by: $\bar{E}-m_\pi$, where \bar{E} is the total energy in the c.m. system. Thus, $m_{I,\text{max}}=1.603, 1.806$, and 2.077 Bev for $T_{\pi,\text{inc}}=1.0, 1.4$, and 2.0 Bev, respectively.$

In the work of II, we have used a cutoff $M_b \equiv m_N+m_\pi+0.5$ Bev = 1.578 Bev for the maximum isobar mass $m_{I,\text{max}}$ which was used in connection with $\sigma_{\frac{1}{2}}(m_1)$ for the calculation of the spectra $J_{\pi,1}$ and $J_{\pi,2}$ pertaining to the N_1^* reactions (10) and (11). The motivation for this procedure was that the N_1^* processes are believed to be mainly due to the effect of the $T=J=\frac{3}{2}$ resonance centered at $T_\pi=180$ Mev. The isobar mass $M_b=1.578$ Bev corresponds to an incident pion energy $T_\pi=710$ Mev. At energies above this value, and actually already in the region of $T_\pi \sim 500-700$ Mev, the experimental values of $\sigma_{\frac{1}{2}}$ are quite small, and are probably not due primarily to the tail of the $T=J=\frac{3}{2}$ resonance. Hence it was argued that the values of $m_I > M_b$ should not be included, since they do not represent the effect of the low-energy $T=J=\frac{3}{2}$ isobar. However, in the present extended isobar model, it seems more reasonable to include all mass values m_I which are kinematically possible. The cross section $\sigma_{\frac{1}{2}}(m_I)$ for mass values $m_I > M_b$ may represent the effect of unresolved isobaric levels centered at higher energies, and, in particular, the effect of the $T=\frac{3}{2}$ resonance maximum centered at a pion energy $T_\pi=1.35$ Bev ($m_I=1.92$ Bev). It should be pointed out that the present procedure of including all possible mass values m_I for the $T=\frac{3}{2}$ states is consistent with the procedure employed for the $T=\frac{1}{2}$ states in the calculation of the spectra $J_{\pi,3}-J_{\pi,6}$.

In connection with the lower limit $m_{I,\text{min}}=1.078$ Bev, which has been used here for the N_2^* processes (spectra $J_{\pi,3}-J_{\pi,6}$), we note that the $T=\frac{1}{2}$ cross section $\sigma_{\frac{1}{2}}$ is quite small and approximately constant for T_π below ~ 300 Mev ($\sigma_{\frac{1}{2}} \sim 7$ mb). In our previous work,³ we have neglected $\sigma_{\frac{1}{2}}$ for incident pion energies $T_\pi \lesssim 300$ Mev, i.e., for values of the isobar mass $m_I \lesssim 1.30$ Bev. Although the low-energy $T=\frac{1}{2}$ cross section is small, it has a rather pronounced effect on the resultant pion spectra at $T_{\pi,\text{inc}}=1.0$ Bev, as will be shown below. It should be pointed out that the treatment of the low-energy $T=\frac{1}{2}$ cross section is to some extent an open

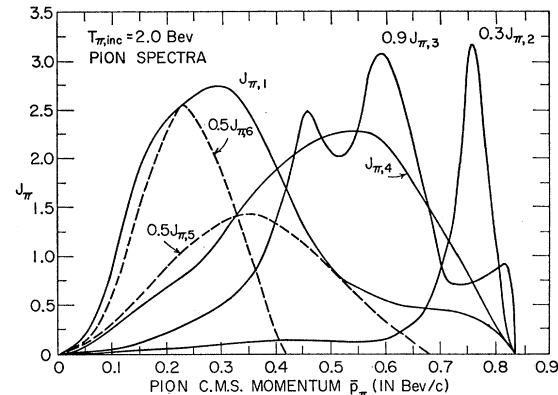


FIG. 4. Center-of-mass momentum spectra of pions from pion-nucleon interactions at an incident pion energy $T_{\pi,\text{inc}}=2.0$ Bev. The spectra $J_{\pi,3}$ and $J_{\pi,4}$ were calculated by including the contribution of the low-energy $T=\frac{1}{2}$ cross section.

question, and that the two possible procedures should be regarded as alternative possibilities. The present procedure of including the low-energy $\sigma_{\frac{1}{2}}$ is more consistent from the point of view of the extended isobar model, in which the $T=\frac{1}{2}$ and $T=\frac{3}{2}$ cross sections are treated on the same footing, i.e., the same (kinematical) limits for m_I are used for both $\sigma_{\frac{1}{2}}$ and $\sigma_{\frac{3}{2}}$. On the other hand, one can argue that the low-energy $\sigma_{\frac{1}{2}}$ corresponds predominantly to S -wave scattering, and therefore the inclusion of this cross section allows for low-energy S -wave pion production. In this connection, it is possible that some selection rule prevents the emission of pions in S states relative to the decay nucleon from the N_2^* isobar. In any case, the fact that the S -wave cross section $\sigma_{\frac{1}{2}}$ (~ 7 mb) is very small compared to the maximum of the cross section $\sigma_{\frac{3}{2}}$ (~ 200 mb), which corresponds essentially to a pure P state, indicates that the S -wave pion production will be very small compared to the P -wave production at low incident energies ($m_I \lesssim 1.3$ Bev).

For comparison with the results for the pion spectra obtained by the present procedure, we have shown in Figs. 5 and 6 the pion spectra for $T_{\pi,\text{inc}}=1.0$ and 1.4 Bev, which have been previously obtained³ by neglecting the low-energy $T=\frac{1}{2}$ cross section.

The spectra $J_{\pi,1}-J_{\pi,6}$ for $T_{\pi,\text{inc}}=1.0$ Bev are shown in Fig. 2. It is seen that the principal maximum of the recoil spectrum $J_{\pi,3}$ from the N_2^* processes approximately coincides with the maximum of the decay spectrum $J_{\pi,1}$ for the N_1^* reactions ($\bar{p}_\pi \approx 0.25$ Bev/c), and similarly, the maximum of $J_{\pi,4}$ occurs at about the same momentum (≈ 0.43 Bev/c) as the peak of $J_{\pi,2}$. However, it should be pointed out that this close agreement holds only for $T_{\pi,\text{inc}} \sim 1.0$ Bev. At appreciably higher incident energies, the maxima of the corresponding spectra will, in general, be separated. This will be shown below for $T_{\pi,\text{inc}}=1.4$ and 2.0 Bev.

The second maximum of the $J_{\pi,3}$ curve at $\bar{p}_\pi \sim 0.5$ Bev/c is a direct consequence of the inclusion of the

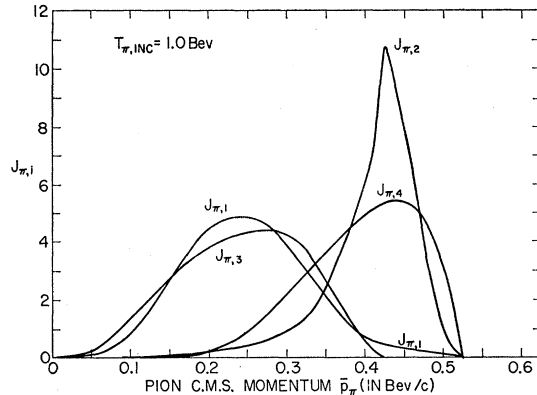


Fig. 5. Center-of-mass momentum spectra of pions from pion-nucleon interactions at an incident pion energy $T_{\pi,\text{inc}}=1.0$ Bev. The spectra $J_{\pi,3}$ and $J_{\pi,4}$ were obtained by neglecting the low-energy $T=\frac{1}{2}$ cross section.

low-energy $T=\frac{1}{2}$ cross section. This maximum arises from the increase of the phase space factor F with increasing momentum \bar{p}_π of the recoil pion, and the approximate constancy of σ_3 with energy (for $T_\pi \lesssim 300$ Mev). On the other hand, the principal maximum of $J_{\pi,3}$ (at 0.25 Bev/c) is essentially not affected by the inclusion of the low-energy σ_3 , as is shown by a comparison of Fig. 2 with Fig. 5. However, it may be noted that whereas the spectra $J_{\pi,1}-J_{\pi,4}$ of Fig. 2 all have the same maximum momentum $\bar{p}_{\pi,m}=0.52$ Bev/c, the spectrum $J_{\pi,3}$ of Fig. 5 has a lower value of $\bar{p}_{\pi,m}$ (0.42 Bev/c) than the other spectra for two pions in the final state ($J_{\pi,1}$, $J_{\pi,2}$, and $J_{\pi,4}$). The lower maximum recoil momentum $\bar{p}_{\pi,m}$ for $J_{\pi,3}$ of Fig. 5 is caused by the omission of the low-energy $T=\frac{1}{2}$ cross section.

In both Figs. 2 and 5, the maximum of the decay spectrum $J_{\pi,4}$ occurs at high momenta ($\bar{p}_\pi \approx 0.42$ Bev/c), as a result of the large difference of mass between the isobar N_{2a}^* and the nucleon ($m_I - m_N = 1.51 - 0.94 = 0.57$ Bev, where m_I is taken as the center of the $T_\pi=600$ Mev resonance). It should be noted that the present curve of $J_{\pi,4}$ (Fig. 2) has a relatively flat region near $\bar{p}_\pi=0.2$ Bev/c, whereas the spectrum $J_{\pi,4}$ of Fig. 5 drops rapidly to zero below 0.2 Bev/c. Thus the present procedure gives a considerably larger intensity of low-energy decay pions than that which would be obtained by neglecting the low-energy $T=\frac{1}{2}$ cross section. This change is directly attributable to the presence of isobars N_2^* having low mass values, which favors the emission of low-energy decay pions.

The spectra $J_{\pi,5}$ and $J_{\pi,6}$ of Fig. 2 are centered at relatively small momenta ($\bar{p}_\pi \sim 0.2$ Bev/c), and have a low value for the maximum momentum, $\bar{p}_{\pi,m}=0.37$ Bev/c. This behavior was to be expected, since these spectra correspond to production of two additional pions by the incident pion. It may be noted that the momentum distributions $J_{\pi,5}$ and $J_{\pi,6}$ are essentially unaffected by the low-energy $T=\frac{1}{2}$ cross section, since

the low mass values, $m_I \lesssim 1.3$ Bev, do not enter into the calculation of these spectra. [The minimum mass $m_{I,\min}$ is given by: $m_1^{(\alpha)} + m_\pi$, which is 1.29 Bev for $m_1^{(1)}=1.15$ Bev.]

Similar results have been obtained for $T_{\pi,\text{inc}}=1.4$ Bev (see Figs. 3 and 6). The spectra $J_{\pi,1}$ and $J_{\pi,2}$ obtained in the present work (Fig. 3) can be compared with those previously obtained in II for $T_{\pi,\text{inc}}=1.37$ Bev (Fig. 2 of II). The maxima of the spectra from the two calculations are in essential agreement, as would be expected. However, it may be noted that the present spectrum $J_{\pi,1}$ (Fig. 3) has a larger high-energy tail (from $\bar{p}_\pi \sim 0.5$ to $\bar{p}_{\pi,m}=0.66$ Bev/c) than the spectrum $J_{\pi,1}$ of II. This change is a direct consequence of the inclusion of $\sigma_3(m_1)$ for isobar masses up to $m_{I,\max}=1.806$ Bev in the present work, whereas a cutoff at $M_b=1.58$ Bev was used in the previous calculations, as discussed above. The presence of isobars with large mass favors the emission of high-energy decay pions. It is also seen from Fig. 3 that the present spectrum $J_{\pi,2}$ extends to zero energy, whereas the previous $J_{\pi,2}$ (Fig. 2 of II) had a cutoff at $\bar{p}_\pi \approx 290$ Mev/c. This cutoff was also due to the use of the upper limit $M_b=1.58$ Bev for the range of isobar masses m_I .

Concerning the curve of $J_{\pi,3}$ of Fig. 3, we note that the somewhat irregular shape of this spectrum (below 0.5 Bev/c) is directly caused by the presence of the two peaks in the $T=\frac{1}{2}$ cross section $\sigma_3(m_2)$. As shown by Eqs. (75) and (77), the recoil spectrum $J_{\pi,3}$ is proportional to $\sigma_3(m_2)F$. Thus the maximum of $J_{\pi,3}$ at $\bar{p}_\pi=0.38$ Bev/c corresponds to the formation of an isobar N_{2a}^* at the first (lower-energy) peak of the $T=\frac{1}{2}$ cross section, for which $m_2=1.51$ Bev. On the other hand, the region of $\bar{p}_\pi \approx 0.26$ Bev/c, where the slope of $J_{\pi,3}$ has a relative minimum, pertains to a recoil pion which is made together with an isobar N_{2b}^* at the second (higher-energy) peak of the $T=\frac{1}{2}$ cross section ($m_2=1.68$ Bev). The reason why in this region there is no additional maximum, but only a decrease of the slope of $J_{\pi,3}$, is that the phase space factor F decreases rapidly with increasing m_2 , and hence with decreasing momentum \bar{p}_π of the recoil pion. We note that $\bar{p}_\pi=0$ corresponds to an isobar with maximum possible mass m_2 , which is 1.806 Bev for $T_{\pi,\text{inc}}=1.4$ Bev ($\bar{E}=1.946$ Bev = $m_{2,\max} + m_\pi$). The decrease of $J_{\pi,3}$ on the high-energy side of the maximum at 0.38 Bev/c is due to the decrease of $\sigma_3(m_2)$ with decreasing m_2 , i.e., with increasing momentum \bar{p}_π . In Fig. 3, there is a second maximum of the $J_{\pi,3}$ curve at high momenta ($\bar{p}_\pi \sim 0.65$ Bev/c) which arises from the low-energy $T=\frac{1}{2}$ cross section. This maximum is qualitatively similar to the second maximum of $J_{\pi,3}$ for $T_{\pi,\text{inc}}=1.0$ Bev, which has been discussed above. However, Fig. 3 shows that the high-energy maximum of $J_{\pi,3}$ is considerably less pronounced at 1.4 Bev than at 1.0 Bev. This result arises from the fact that the range of isobar masses is appreciably larger at 1.4 Bev than at 1.0 Bev ($m_{I,\max}=1.806$ Bev, as compared to 1.603 Bev at $T_{\pi,\text{inc}}=1.0$ Bev), so that

the region $m_I \lesssim 1.3$ Bev which gives rise to the second maximum of $J_{\pi,3}$ is relatively less important.

The decay spectrum $J_{\pi,4}$ of Fig. 3 has the same general features as the corresponding spectrum $J_{\pi,4}$ at 1.0 Bev (Fig. 2). Thus there is a high-energy maximum at $\bar{p}_\pi = 0.5$ Bev/c, and an almost flat region near $\bar{p}_\pi = 0.2$ Bev/c, which arises from the low-mass $T = \frac{1}{2}$ isobars which are included in the present work. Similarly to the behavior of the high-energy maximum of $J_{\pi,3}$, the increase of the intensity of $J_{\pi,4}$ at $\bar{p}_\pi \sim 0.2$ Bev/c due to the low-energy σ_2 is also somewhat less important at 1.4 Bev than at 1.0 Bev. It may be noted that aside from the high-energy maximum of $J_{\pi,3}$ and the behavior of $J_{\pi,4}$ at low momenta, the main features of $J_{\pi,3}$ and $J_{\pi,4}$ are essentially the same for the two alternative procedures concerning the low-energy σ_2 (compare Figs. 3 and 6).

In connection with the approximate coincidence of the maxima of $J_{\pi,1}$ and $J_{\pi,3}$, and also of $J_{\pi,2}$ and $J_{\pi,4}$ at $T_{\pi,\text{inc}} = 1.0$ Bev, we note that at 1.4 Bev these maxima are separated by ~ 0.1 Bev/c. Thus the momentum \bar{p}_π^M at which the maximum occurs is 0.27 Bev/c for $J_{\pi,1}$, as compared to 0.38 Bev/c for $J_{\pi,3}$, and similarly, $\bar{p}_\pi^M = 0.57$ and 0.50 Bev/c for $J_{\pi,2}$ and $J_{\pi,4}$, respectively. At 2.0 Bev, the separation of the corresponding maxima is still larger. In fact, at this energy, the two principal maxima of the recoil spectrum $J_{\pi,3}$ lie in the region of the maximum of the decay spectrum $J_{\pi,4}$ (see Fig. 4). Thus $J_{\pi,3}$ and $J_{\pi,4}$ no longer correspond to "slow" pions and "fast" pions, respectively. The reason is that with increasing incident energy, the momentum \bar{p}_π^M of the maximum of the recoil spectrum $J_{\pi,3}$ increases rapidly (from 0.25 Bev/c at 1.0 Bev to 0.5 Bev/c at 2.0 Bev), whereas the momentum \bar{p}_π^M of the maximum of the decay spectrum $J_{\pi,4}$ increases much more slowly with $T_{\pi,\text{inc}}$, since it is determined primarily by the mass difference $m_I - m_N$.

The spectra $J_{\pi,5}$ and $J_{\pi,6}$ have their maxima at relatively low momenta, although the maximum of $J_{\pi,5}$ ($\bar{p}_\pi^M = 0.28$ Bev/c) occurs at a somewhat higher momentum than the maximum of $J_{\pi,6}$ ($\bar{p}_\pi^M = 0.21$ Bev/c). This feature becomes more noticeable at $T_{\pi,\text{inc}} = 2.0$ Bev (Fig. 4), where the maxima of $J_{\pi,5}$ and $J_{\pi,6}$ occur at 0.35 and 0.22 Bev/c, respectively. Thus, while the momentum \bar{p}_π^M for which the maximum of $J_{\pi,6}$ occurs is practically independent of the incident energy $T_{\pi,\text{inc}}$, the value of \bar{p}_π^M for $J_{\pi,5}$ increases approximately linearly with increasing $T_{\pi,\text{inc}}$ (from 0.22 Bev/c at 1.0 Bev to 0.35 Bev/c at 2.0 Bev).

Although the various effects which enter into the calculation of $J_{\pi,5}$ and $J_{\pi,6}$ are quite complicated, a reasonably simple explanation for the different behavior of $J_{\pi,5}$ and $J_{\pi,6}$ can be given. As $T_{\pi,\text{inc}}$ is increased, the total c.m. energy \bar{E} increases, which results directly in an increase of the kinetic energy of the isobar N_2^* produced in reaction (8), and an increase of the average $\langle m_2 \rangle$ of the mass distribution of N_2^* . Both effects will contribute to increase the average energy of the pion

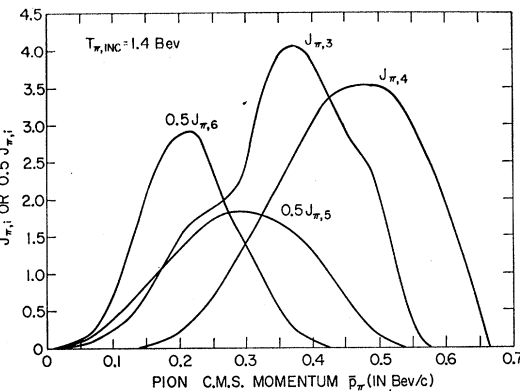


FIG. 6. Center-of-mass momentum spectra of pions from pion-nucleon interactions at an incident pion energy $T_{\pi,\text{inc}} = 1.4$ Bev. The spectra $J_{\pi,3}$ and $J_{\pi,4}$ were obtained by neglecting the low-energy $T = \frac{1}{2}$ cross section.

from the decay $N_2^* \rightarrow N_1^* + \pi$ [Eq. (9b)], whose momentum spectrum is $J_{\pi,5}$. This would explain the increase of \bar{p}_π^M for $J_{\pi,5}$ with increasing $T_{\pi,\text{inc}}$. On the other hand, the effective mass distribution of the isobar N_1^* is essentially independent of $T_{\pi,\text{inc}}$, so that one would not expect a variation of the spectrum of the decay pion from $N_1^* \rightarrow N + \pi$, except for the influence of the increase of the average velocity of N_1^* with increasing $T_{\pi,\text{inc}}$. The latter effect is probably rather small. In this connection, we note that the momentum \bar{p}_π^M of the maximum of the decay spectrum $J_{\pi,1}$ varies very slowly with incident energy (from 0.24 Bev/c at 1.0 Bev to 0.29 Bev/c at 2.0 Bev) even though the total energy \bar{E} in the c.m. system increases considerably (by 0.474 Bev between $T_{\pi,\text{inc}} = 1.0$ and 2.0 Bev).

The various pion spectra for $T_{\pi,\text{inc}} = 2.0$ Bev are shown in Fig. 4. Similarly to Figs. 2 and 3, these spectra were also obtained with the inclusion of the low-energy $T = \frac{1}{2}$ cross section. However, it is seen that the high-energy maximum of $J_{\pi,3}$ (at 0.82 Bev/c) which arises from this procedure is not very pronounced, thus continuing the trend already noted in going from 1.0 to 1.4 Bev. The reason is, of course, that the region of $m_I \lesssim 1.3$ Bev is quite unimportant compared to the total range of isobar masses, which extends up to $m_{I,\text{max}} = 2.077$ Bev. We note that $J_{\pi,3}$ has two prominent maxima at lower momenta (0.46 and 0.59 Bev/c), which correspond directly to the two resonant states N_{2a}^* and N_{2b}^* . It would obviously be of interest to confirm the existence of these maxima experimentally.

By comparing the maximum of $J_{\pi,2}$ for $T_{\pi,\text{inc}} = 2.0$ Bev with the corresponding maxima for $J_{\pi,2}$ for 1.0 and 1.4 Bev, it is seen that the maximum at 2.0 Bev is somewhat narrower than the maxima at the two lower energies. The widths at half maximum, as obtained from the curves of $J_{\pi,2}$, are as follows: 78 Mev/c at 1.0 Bev, 75 Mev/c at 1.4 Bev, and 64 Mev/c at 2.0 Bev. The narrowing which takes place in going from 1.4 to 2.0 Bev is probably mainly a kinematic effect, as will be shown in the following discussion.

For a narrow resonance, the width at half maximum, $\Delta\bar{p}_R$, for the momentum spectrum of the recoil particle is given by

$$\Delta\bar{p}_R = |\partial\bar{p}_R/\partial m_I| \Delta m_I, \quad (91)$$

where Δm_I is the width at half maximum for the cross section $\sigma(m_I)$, and \bar{p}_R is the c.m. momentum of the recoil particle (pion or nucleon). We obtain

$$\bar{p}_R^2 = D / (4\bar{E}^2), \quad (92)$$

where \bar{E} is the total energy in the c.m. system, and D is defined by

$$D \equiv [(\bar{E} + m_I)^2 - m_R^2][(\bar{E} - m_I)^2 - m_R^2]. \quad (93)$$

Equations (92) and (93) give

$$\bar{E}^2 \partial\bar{p}_R^2 / \partial m_I = \frac{1}{4} \partial D / \partial m_I = -m_I (\bar{E}^2 + m_R^2 - m_I^2). \quad (94)$$

We have

$$\partial\bar{p}_R / \partial m_I = (1/2\bar{p}_R) (\partial\bar{p}_R^2 / \partial m_I), \quad (95)$$

whence

$$\Delta\bar{p}_R = \left| \frac{\partial\bar{p}_R}{\partial m_I} \right| \Delta m_I = \frac{m_I}{2\bar{p}_R} \left[1 - \left(\frac{m_I^2 - m_R^2}{\bar{E}^2} \right) \right] \Delta m_I. \quad (96)$$

For sufficiently large \bar{E} , for which the variation of the square bracket with \bar{E} is small, the width $\Delta\bar{p}_R$ will therefore decrease approximately as $1/\bar{p}_R$ with increasing incident energy.

In the present case, for incident pions, we have $\Delta\sigma_{\pi} = 115$ Mev, $m_R = 0.140$ Bev, $m_I = 1.225$ Bev, $\bar{E} = 1.743, 1.946$, and 2.217 Bev for $T_{\pi,\text{inc}} = 1.0, 1.4$, and 2.0 Bev, respectively; $\bar{p}_{\pi} = 0.425, 0.570$, and 0.755 Bev/c at $1.0, 1.4$, and 2.0 Bev, respectively. From Eq. (96), one obtains $\Delta\bar{p}_{\pi} = 85, 75$, and 65 Mev/c for $1.0, 1.4$, and 2.0 Bev, respectively. These results are in satisfactory agreement with the widths obtained above from the curves of $J_{\pi,2}$, especially at 1.4 and 2.0 Bev.

In Fig. 4 for $T_{\pi,\text{inc}} = 2.0$ Bev, it may be noted that the spectrum $J_{\pi,1}$ has a sizable high-energy tail, extending from $\bar{p}_{\pi} \sim 0.5$ Bev/c to $\bar{p}_{\pi,\text{max}} = 0.83$ Bev/c. This part of the $J_{\pi,1}$ curve is due primarily to the decay of isobars N_1^* having a large mass, i.e., with m_I between ~ 1.5 Bev and $m_{I,\text{max}} = 2.077$ Bev. For the spectrum $J_{\pi,4}$, we note that there is only a weak indication of the low-energy shelf or flat region which was found at 1.0 and 1.4 Bev. Thus, there is a region of relatively small slope $dJ_{\pi,4}/d\bar{p}_{\pi}$ in the neighborhood of $\bar{p}_{\pi} = 0.2$ Bev/c (followed by a region with steeper slope, from $\bar{p}_{\pi} \approx 0.3$ to 0.4 Bev/c). It was already pointed out that for 1.4 Bev, the flat region is much less conspicuous than at 1.0 Bev. The result for 2.0 Bev is a continuation of this trend. Since the shelf found at 1.0 Bev arises from the low-energy $T = \frac{1}{2}$ cross section, one expects a much decreased effect at 2.0 Bev, since the region of $m_I \lesssim 1.3$ Bev becomes quite unimportant compared to the total range of possible isobar masses.

The spectra $J_{\pi,5}$ and $J_{\pi,6}$ of Fig. 4 were obtained with the assumption of a single mass value $m_1 = 1.225$ Bev for the isobar N_1^* . This assumption is not expected to lead to appreciable errors for $T_{\pi,\text{inc}} = 2.0$ Bev, since the maximum isobar mass $m_{I,\text{max}} = 2.077$ Bev is considerably larger than the threshold for the decay $N_2^* \rightarrow N_1^* + \pi$, which lies at $m_2 = 1.365$ Bev for $m_1 = 1.225$ Bev. Thus the effects of differences in the probability ϵ and the phase space factor F , which arise from the small spread of the effective masses of N_1^* , will be quite unimportant at 2.0 Bev. We note that for 1.0 and 1.4 Bev, the procedure involving the three mass values $m_1^{(\alpha)}$ was used in obtaining $J_{\pi,5}$ and $J_{\pi,6}$, as has been described above [Eqs. (87) and (90)].

We have also obtained the c.m. energy spectra of the nucleons from reactions (9a), (9b), and (11). These spectra will be denoted by $I_{N,i}^{(\pi)}$ ($i = 1, 2, 3$). Here the superscript (π) is used to distinguish these spectra, corresponding to incident pions from the spectra $I_{N,1}$, $I_{N,2}$, $I_{N,i}^{(A)}$, and $I_{N,i}^{(B)}$, which pertain to the recoil nucleons from nucleon-nucleon interactions (see Sec. VI). The notation for the $I_{N,i}^{(\pi)}$ is as follows: $I_{N,1}^{(\pi)}$ denotes the spectrum of the decay nucleon from the N_1^* reaction (11). Similarly, $I_{N,2}^{(\pi)}$ pertains to the nucleon from reaction (9a), which is emitted in the direct decay: $N_2^* \rightarrow N + \pi$. The spectrum $I_{N,3}^{(\pi)}$ pertains to the nucleon from reaction (9b), in which N_2^* decays by emission of two pions.

The calculation of $I_{N,1}^{(\pi)}$ and $I_{N,2}^{(\pi)}$ is entirely analogous to the calculation of the pion decay spectra $J_{\pi,1}$ and $J_{\pi,4}$. Thus $I_{N,2}^{(\pi)}$ is obtained from an equation similar to (79), except that G_{π} is replaced by the corresponding function G_N for the energy distribution of the decay nucleon. The step functions of the type of $g_{j,4}$ are obtained from Eq. (81), in which the denominator $\bar{T}_{\pi,\text{max}}^{(j)} - \bar{T}_{\pi,\text{min}}^{(j)}$ must be replaced by $\bar{T}_{N,\text{max}}^{(j)} - \bar{T}_{N,\text{min}}^{(j)}$.

The spectrum $I_{N,1}^{(\pi)}$ pertaining to the N_1^* processes is obtained in a similar manner from Eqs. (79) and (81), by replacing the factor $\sigma_{\frac{1}{2}}(m_2)[1 - \epsilon(m_2)]$ by $\sigma_{\frac{1}{2}}$. The spectrum $I_{N,3}^{(\pi)}$ pertaining to the N_2^* reactions with three pions in the final state is calculated essentially in the same manner as $J_{\pi,6}$ [Eq. (90)], except that it is the nucleon spectrum, rather than the pion spectrum from the final decay $N_1^* \rightarrow N + \pi$, which is being considered. Thus a spectrum $I_{N,3}^{(\pi,\alpha)}$ is calculated for each of the three choices of the mass $m_1^{(\alpha)}$ of the N_1^* isobar. The spectra $I_{N,3}^{(\pi,\alpha)}$ are combined in the same manner as in Eq. (90):

$$I_{N,3}^{(\pi)} = 0.25 I_{N,3}^{(\pi,1)} + 0.50 I_{N,3}^{(\pi,2)} + 0.25 I_{N,3}^{(\pi,3)}. \quad (97)$$

It should be noted that the individual spectra $I_{N,3}^{(\pi,1)}$, $I_{N,3}^{(\pi,2)}$, and $I_{N,3}^{(\pi,3)}$ have not been normalized to the same value, but are instead normalized to the quantity

$$\mathcal{N}[I_{N,3}^{(\pi,\alpha)}] = C \int \sigma_{\frac{1}{2}}(m_2) F \epsilon(m_2, m_1^{(\alpha)}) dm_2, \quad (98)$$

where C is a constant (independent of $m_1^{(\alpha)}$) and $\epsilon(m_2, m_1^{(\alpha)})$ depends on $m_1^{(\alpha)}$, as indicated. For a given mass m_2 of the isobar N_2^* , $\epsilon(m_2, m_1^{(\alpha)})$ decreases with increasing $m_1^{(\alpha)}$, as can be seen from Eqs. (82) and (84), since the phase space factor $F_d(N_2^* \rightarrow N_1^{(\alpha)*})$ decreases as $m_1^{(\alpha)}$ is increased. It is reasonable to use the normalization (98) [together with Eq. (97)], since the expression (98) is exactly what is obtained from the isobar model: The factor $\sigma_i(m_2)F$ gives the probability of formation of N_2^* , and the factor ϵ gives the probability of the subsequent decay of N_2^* into $N_1^{(\alpha)*} + \pi$. Thus, by virtue of the dependence of $\epsilon(m_2, m_1^{(\alpha)})$ on $m_1^{(\alpha)}$, the spectrum $I_{N,3}^{(\pi,1)}$ pertaining to $m_1^{(1)} = 1.15$ Bev has a somewhat greater weight than the spectrum $I_{N,3}^{(\pi,3)}$ pertaining to $m_1^{(3)} = 1.30$ Bev. This effect is important for $T_{\pi,\text{inc}} \sim 1.0$ Bev, but decreases rapidly as the incident energy is increased, so that the average $\langle m_2 \rangle$ of the mass distribution of N_2^* becomes appreciably larger than the threshold for the decay $N_2^* \rightarrow N_1^{*(3)} + \pi$, which lies at $m_{2,\min}^{(3)} = 1.30 + 0.14 = 1.44$ Bev. For $T_{\pi,\text{inc}} = 1.0$ and 1.4 Bev, the relative weights of the three spectra $I_{N,3}^{(\pi,\alpha)}$ are as follows: $R_{12} = 1.729$ and $R_{32} = 0.412$ at $T_{\pi,\text{inc}} = 1.0$ Bev; and $R_{12} = 1.407$ and $R_{32} = 0.606$ at $T_{\pi,\text{inc}} = 1.4$ Bev, where the ratio $R_{\alpha\beta}$ is defined by

$$R_{\alpha\beta} = \frac{\mathcal{N}[I_{N,3}^{(\pi,\alpha)}]}{\mathcal{N}[I_{N,3}^{(\pi,\beta)}]}. \quad (99)$$

It is seen that the ratios $R_{\alpha\beta}$ tend rather rapidly towards 1, as the incident energy $T_{\pi,\text{inc}}$ is increased above ~ 1.0 Bev.

It should be noted that the same normalization as for $I_{N,3}^{(\pi,\alpha)}$ was also used for the pion spectra $J_{\pi,5}^{(\alpha)}$ and $J_{\pi,6}^{(\alpha)}$, which enter into the expressions for $J_{\pi,5}$ and $J_{\pi,6}$, respectively, [Eqs. (87) and (90)]. This is, of course, required for the sake of consistency, since the same quantity $\sigma_i(m_2)F\epsilon(m_2, m_1^{(\alpha)})$ enters into both the pion and nucleon spectra involved in the decay $N_2^* \rightarrow N_1^{(\alpha)*} + \pi$.

In connection with the notation I and J for the nucleon and pion spectra, it may be remarked that I always denotes a c.m. energy spectrum, whereas J denotes a c.m. momentum spectrum. Thus we have

$$J_{\pi,i} = \bar{v}_\pi I_{\pi,i}, \quad (100)$$

$$J_{N,i}^{(\pi)} = \bar{v}_N I_{N,i}^{(\pi)}, \quad (101)$$

where \bar{v}_π and \bar{v}_N are the c.m. velocities of the pion and nucleon, respectively; $J_{\pi,i}$ is a pion momentum spectrum and $I_{\pi,i}$ the corresponding energy spectrum; and similarly, $J_{N,i}^{(\pi)}$ and $I_{N,i}^{(\pi)}$ are the nucleon momentum and energy spectra, respectively, of type i ($i = 1, 2, 3$).

Figures 7, 8, and 9 show the calculated recoil nucleon spectra $I_{N,i}^{(\pi)}$ for $T_{\pi,\text{inc}} = 1.0, 1.4$, and 2.0 Bev, respectively. We have also shown the energy spectrum $I_{N,3}^{(\pi)}$ obtained from the Fermi statistical theory,²²

²² E. Fermi, Progr. Theoret. Phys. (Japan) **5**, 570 (1950); Phys. Rev. **92**, 452 (1953); *ibid.* **93**, 1435 (1954).

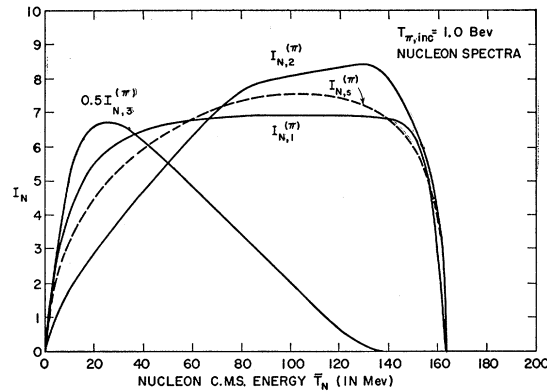


FIG. 7. Center-of-mass energy spectra of nucleons from pion-nucleon interactions at an incident pion energy $T_{\pi,\text{inc}} = 1.0$ Bev. The solid curves show the spectra obtained from the present extended isobar model. The dashed curve gives the result of the Fermi statistical theory.

which is given by the appropriate three-body phase space factor (assuming a two-pion final state).²³ We note that, in the same manner as for the pion spectra [Eq. (40)], the nucleon spectra $I_{N,i}^{(\pi)}$ are also normalized to 1. Thus:

$$\int_0^{\bar{T}_N \text{ max}} I_{N,i}^{(\pi)} d\bar{T}_N = 1, \quad (102)$$

where $\bar{T}_N \text{ max}$ is the maximum possible nucleon energy \bar{T}_N .

As was already pointed out in II, the statistical spectrum $I_{N,3}^{(\pi)}$ does not differ appreciably from the isobar model spectrum $I_{N,1}^{(\pi)}$ pertaining to the N_1^* reactions (11). Figures 7–9 also show that the spectrum $I_{N,2}^{(\pi)}$ pertaining to the N_2^* processes is quite similar in shape to $I_{N,1}^{(\pi)}$, except that $I_{N,2}^{(\pi)}$ has a broad maximum near the maximum energy $\bar{T}_N \text{ max}$, whereas $I_{N,1}^{(\pi)}$ is essentially flat in this energy region (e.g., from $\bar{T}_N \approx 60$ to 140 Mev for $T_{\pi,\text{inc}} = 1.0$ Bev). At all three incident energies, $I_{N,3}^{(\pi)}$ is generally intermediate between $I_{N,1}^{(\pi)}$ and $I_{N,2}^{(\pi)}$.

Concerning the spectrum $I_{N,3}^{(\pi)}$ for the three-pion final states, we note that the energy \bar{T}_N^M at which the maximum occurs increases very slowly with incident energy (from $\bar{T}_N^M = 25$ Mev at 1.0 Bev to $\bar{T}_N^M = 50$ Mev at 2.0 Bev). This feature is similar to the behavior of the maximum of $J_{\pi,6}$ which has been discussed above. This similarity is to be expected, since $I_{N,3}^{(\pi)}$ and $J_{\pi,6}$ pertain to the nucleon and pion originating from the same type of N_1^* decay [Eq. (9b)]. However, the nucleon spectrum $I_{N,3}^{(\pi)}$ has a long high-energy tail, and the maximum possible nucleon energy $\bar{T}_N \text{ max}$ increases somewhat faster with $T_{\pi,\text{inc}}$ than the corresponding maximum pion energy $\bar{T}_{\pi,\text{max}}$ for $J_{\pi,6}$. The increase of $\bar{T}_N \text{ max}$ with incident energy is probably caused by the increase of the average velocity of N_1^* with increasing $T_{\pi,\text{inc}}$.

²³ M. M. Block, Phys. Rev. **101**, 796 (1956).

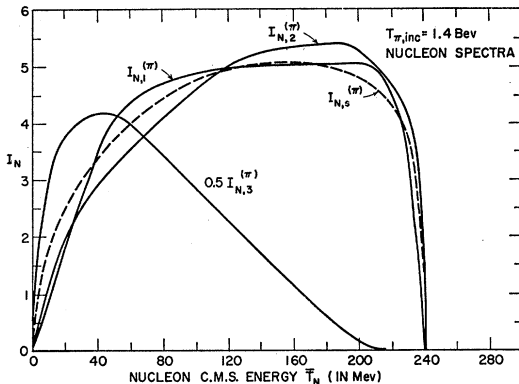


FIG. 8. Center-of-mass energy spectra of nucleons from pion-nucleon interactions at an incident pion energy $T_{\pi,\text{inc}}=1.4$ Bev. The solid curves show the spectra obtained from the present extended isobar model. The dashed curve gives the result of the Fermi statistical theory.

It may be noted that in Sec. II we have not given the expressions for the nucleon spectra from the various reactions arising from $\pi^- - p$ and $\pi^+ - p$ collisions. In terms of the spectra $I_{N,i}^{(\pi)}$, these expressions can be easily obtained.

For the single-pion production reactions (I), (II), and (III) from $\pi^- - p$ collisions, the nucleon energy spectra are given by the following equations [see Eqs. (28)–(30)]:

$$\left(\frac{d\sigma}{d\bar{T}_N}\right)^{(I)}(n) = \frac{2}{3}\sigma_{11}\left(\frac{5}{9} + \frac{26}{45}\rho_1 - \frac{7}{9}a\right)I_{N,1}^{(\pi)} + \frac{4}{9}A\sigma_{12,s}I_{N,2}^{(\pi)}, \quad (103)$$

$$\left(\frac{d\sigma}{d\bar{T}_N}\right)^{(II)}(p) = \frac{2}{3}\sigma_{11}\left(\frac{2}{9} + \frac{17}{45}\rho_1 - \frac{5}{9}a\right)I_{N,1}^{(\pi)} + \frac{2}{9}\sigma_{12,s}(A+2B)I_{N,2}^{(\pi)}, \quad (104)$$

$$\left(\frac{d\sigma}{d\bar{T}_N}\right)^{(III)}(n) = \frac{2}{3}\sigma_{11}\left(\frac{2}{9} + \frac{2}{45}\rho_1 - \frac{2}{9}a\right)I_{N,1}^{(\pi)} + \frac{2}{9}B\sigma_{12,s}I_{N,2}^{(\pi)}. \quad (105)$$

For the reactions (IV) and (V) from $\pi^+ - p$ collisions, one obtains from Eqs. (51) and (52):

$$(d\sigma/d\bar{T}_N)^{(IV)}(p) = (13/15)\sigma_{31}I_{N,1}^{(\pi)} + \frac{1}{3}\sigma_{32,s}I_{N,2}^{(\pi)}, \quad (106)$$

$$(d\sigma/d\bar{T}_N)^{(V)}(n) = (2/15)\sigma_{31}I_{N,1}^{(\pi)} + \frac{2}{3}\sigma_{32,s}I_{N,2}^{(\pi)}. \quad (107)$$

For the double-pion production reactions (A)–(D) from $\pi^- - p$ collisions, and (E)–(F) from $\pi^+ - p$ col-

lisions, the nucleon spectrum is simply proportional to $I_{N,3}^{(\pi)}$, and is given by

$$(d\sigma/d\bar{T}_N)^{(R)}(N) = \sigma^{(R)}I_{N,3}^{(\pi)}, \quad (108)$$

where $\sigma^{(R)}$ is the total cross section for the reaction (R) [$= (A), (B), \dots$ or (F)] as given by Eqs. (31)–(34) and (53)–(54).

IV. COMPARISON OF THE EXTENDED ISOBAR MODEL WITH EXPERIMENTS ON INELASTIC $\pi^- - p$ INTERACTIONS AT $T_{\pi,\text{inc}} \approx 1.0$ Bev

Recently, three experiments on $\pi^- - p$ interactions have been carried out at incident π^- energies in the region of 1.0 Bev: the experiment of Derado and Schmitz²⁴ at Göttingen with 1.0-Bev π^- , and the experiments of Alles-Borelli *et al.*²⁵ at Bologna, and of Pickup, Ayer, and Salant²⁶ at Brookhaven, both using π^- mesons of energy $T_{\pi,\text{inc}}=0.96$ Bev. These three groups have obtained fits to their data, using the calculations of our previous isobar model² involving only the N_1^* isobar. For the Bologna²⁵ and Brookhaven²⁶ experiments, reasonable agreement of the calculations with the data was obtained for both reactions (I) and (II) [Eqs. (35)–(38)]. For the Göttingen experiment,²⁴ good agreement was obtained for the π^- and π^+ spectra from reaction (I). On the other hand, there were appreciable discrepancies between the calculated and the observed spectra for the π^- mesons from reaction (II).

Aside from the single-pion production reactions $\pi^- + p \rightarrow \pi^+ + \pi^- + n$ and $\pi^- + p \rightarrow \pi^- + \pi^0 + p$, an appreciable number of double-pion production events have also been observed in the above-mentioned experi-

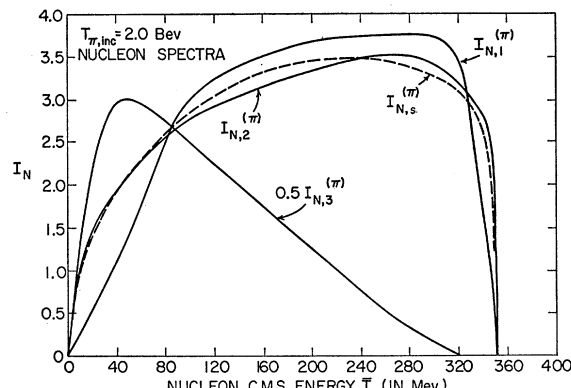


FIG. 9. Center-of-mass energy spectra of nucleons from pion-nucleon interactions at an incident pion energy $T_{\pi,\text{inc}}=2.0$ Bev. The solid curves show the spectra obtained from the present extended isobar model. The dashed curve gives the result of the Fermi statistical theory.

²⁴ I. Derado and N. Schmitz, Phys. Rev. 118, 309 (1960).

²⁵ V. Alles-Borelli, S. Bergia, E. Perez Ferreira, and P. Waloschek, Nuovo cimento 14, 211 (1959).

²⁶ E. Pickup, F. Ayer, and E. O. Salant, Phys. Rev. Letters 5, 161 (1960), and private communication. We wish to thank Dr. E. Pickup and Dr. E. O. Salant for informing us of their results in advance of publication.

ments.²⁴⁻²⁶ Thus, both the Göttingen and Bologna groups have observed a cross section of ~ 3 mb for production of two additional pions in $\pi^- + p \rightarrow \pi^- + \pi^+ + n$ collisions at ~ 1.0 Bev. In order to account for these reactions, it is necessary to have an appreciable cross section for the process $\pi^- + p \rightarrow \pi^- + N_2^*$ (along with a predominant amount of the reaction $\pi^- + p \rightarrow \pi^- + N_1^*$, which has been considered previously in II).

We have obtained an approximate fit to the combined pion momentum distributions from the three experiments, for the reactions (I) and (II). In addition, the parameters pertaining to the N_2^* processes were so adjusted as to give agreement with the total cross section $\sigma_d(\pi^- + p)$ for all types of double-pion production events, and with the observed ratio $\sigma^{(A)}/\sigma^{(C)}$ for the cross sections for reactions (A) and (C), corresponding to the final states: $p + \pi^+ + \pi^- + \pi^-$, and $n + \pi^+ + \pi^0 + \pi^-$, respectively [see Eqs. (31) and (33)].

For the three experiments,²⁴⁻²⁶ the numbers of events of type (I) and (II) were comparable, and we have weighted all of the events equally. Thus, for reaction (I), the numbers of events from the Göttingen, Bologna, and Brookhaven experiments are: $n_G^{(I)} = 235$, $n_{Bo}^{(I)} = 239$, and $n_{Br}^{(I)} = 301$, respectively. Our combined histograms for this reaction are thus normalized to 775 events (see Figs. 10 and 11). Similarly, for reaction (II), we have: $n_G^{(II)} = 118$, $n_{Bo}^{(II)} = 180$, and $n_{Br}^{(II)} = 151$, giving a total of 449 events, on which the histograms of Figs. 12 and 13 are based. The value of R from the combined experiments is: $R = 449/775 = 0.579$.

In order to determine the values of the various cross sections $\sigma_{2T,\alpha}$, we make use of the measured experimental values of the cross sections for elastic and inelastic processes. The total inelastic cross sections via N_1^* and N_2^* combined will be denoted by σ_1 and σ_3 for

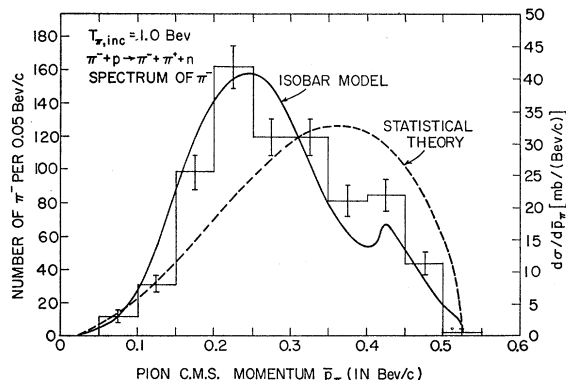


FIG. 10. Center-of-mass momentum spectrum of the π^- mesons from the reaction $\pi^- + p \rightarrow \pi^- + \pi^+ + n$ at $T_{\pi, \text{inc}} = 1.0$ Bev. The histogram represents the combined experimental data from references 24-26. The solid curve was obtained from the present extended isobar model. The right-hand ordinate scale gives the corresponding differential cross section $d\sigma/dp_\pi$ calculated from the isobar model. The dashed curve gives the result of the Fermi statistical theory.

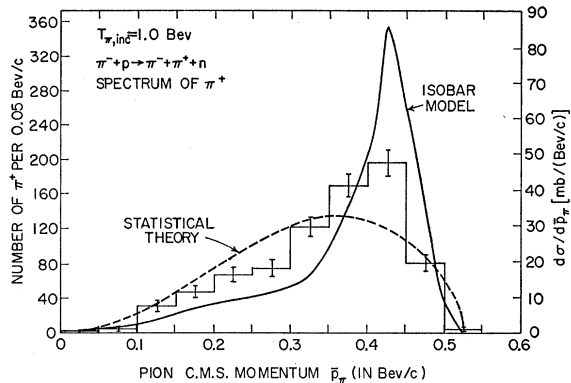


FIG. 11. Center-of-mass momentum spectrum of the π^+ mesons from the reaction $\pi^- + p \rightarrow \pi^- + \pi^+ + n$ at $T_{\pi, \text{inc}} = 1.0$ Bev. The histogram represents the combined experimental data from references 24-26. The solid curve was obtained from the present extended isobar model. The dashed curve gives the result of the Fermi statistical theory.

$T = \frac{1}{2}$ and $T = \frac{3}{2}$, respectively. Thus we have:

$$\sigma_1 = \sigma_{11} + \sigma_{12}, \quad (109)$$

$$\sigma_3 = \sigma_{31} + \sigma_{32}. \quad (110)$$

As was mentioned above, the ratios ρ_α ($\alpha = 1, 2$) are defined by

$$\rho_\alpha = \sigma_{3\alpha} / (2\sigma_{1\alpha}). \quad (111)$$

In Table I of the paper by Derado and Schmitz,²⁴ the elastic $\pi^- + p$ cross section is given as 22 mb, and the charge exchange cross section can be estimated to be ~ 3 mb, giving a total of 25 mb. On the other hand, the total $\pi^- + p$ cross section is 47 mb, so that the total inelastic cross section is:

$$\sigma_{\text{inelast}}(\pi^- + p) = 47 - 25 = 22 \text{ mb} = \frac{2}{3}\sigma_1 + \frac{1}{3}\sigma_3. \quad (112)$$

In an experiment on $\pi^+ + p$ interactions at 1.0 Bev, Erwin and Kopp²⁷ found that the inelastic $\pi^+ + p$ cross section, $\sigma_{\text{inelast}}(\pi^+ + p) = \sigma_3$, is ~ 10 mb. Upon inserting this result in Eq. (112), one obtains $\sigma_1 = 28$ mb for the $T = \frac{1}{2}$ inelastic cross section.

For the fit to the experimental data, it was assumed that the cross section for the N_2^* reactions is $\frac{3}{10}$ of the total inelastic cross section for both $T = \frac{1}{2}$ and $T = \frac{3}{2}$. A fraction of the order of $\frac{3}{10}$ is required in order to account for the observed cross section^{24,25} of ~ 3 mb for the double pion production at $T_{\pi, \text{inc}} = 1.0$ Bev. Thus we obtain:

$$\sigma_{12} = 0.3 \times 28 = 8.4 \text{ mb}; \quad \sigma_{11} = 28 - 8.4 = 19.6 \text{ mb}; \quad (113)$$

$$\sigma_{32} = 0.3 \times 10 = 3.0 \text{ mb}; \quad \sigma_{31} = 10 - 3.0 = 7.0 \text{ mb}; \quad (114)$$

$$\rho_1 = \rho_2 = 10/56 = 0.179. \quad (115)$$

In view of Eqs. (113) and (114), the part of the cross section $\sigma(\pi^- + p)$ which proceeds via N_2^* is

$$\sigma_2(\pi^- + p) = \frac{2}{3}(8.4) + \frac{1}{3}(3.0) = 6.60 \text{ mb}. \quad (116)$$

²⁷ A. Erwin and J. Kopp (private communication).

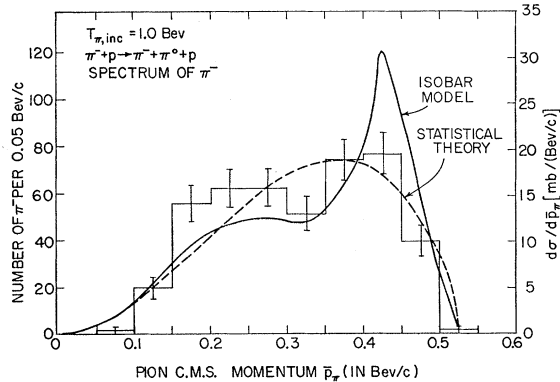


FIG. 12. Center-of-mass momentum spectrum of the π^- mesons from the reaction $\pi^- + p \rightarrow \pi^- + \pi^0 + p$ at $T_{\pi, \text{inc}} = 1.0$ Bev. The histogram represents the combined experimental data from references 24–26. The solid curve was obtained from the present extended isobar model. The dashed curve gives the result of the Fermi statistical theory.

Of this 6.60 mb, it is assumed that 3 mb goes into production of two additional pions (3-pion events), so that the probabilities P_d and P_s [Eq. (27)] have the following values:

$$P_d = 3/6.60 = 0.455; \quad P_s = 3.60/6.60 = 0.545. \quad (117)$$

The part of σ_{12} which leads to single-pion production is therefore given by

$$\sigma_{12,s} = P_s \sigma_{12} = 0.545 \times 8.4 = 4.58 \text{ mb}. \quad (118)$$

We note that the value of P_d which we must use to obtain a double-pion production cross section $\sigma_d(\pi^- - p)$ of 3 mb is appreciably larger than the value of $\langle \epsilon(m_2) \rangle = 0.111$ which would be deduced from the decay phase space factors alone [see Eqs. (82)–(85)]. This result seems to indicate that the effect of the transition matrix element and the statistical weight factors favors the decay of N_2^* to the excited state N_1^* at the expense of the direct decay $N_2^* \rightarrow N + \pi$. It should also be noted that if we had used a larger cross section for the N_2^* reactions [i.e., a larger fraction f than $\frac{3}{10}$ in Eqs. (113) and (114)], then the required P_d would have been proportionately smaller, since $\sigma_d(\pi^- - p) \propto f P_d$.

In order to obtain the values of A , B , and the phase angle φ_2 , we use the ratio of the number of 3-pion events of type (A) ($p + \pi^+ + \pi^- + \pi^-$) to number of events of type (C) ($n + \pi^+ + \pi^0 + \pi^-$), as observed by the Bologna group.²⁵ The corresponding numbers are: $n_A = 23$ and $n_C = 43$, which gives, in view of Eqs. (31) and (33):

$$\sigma^{(A)}/\sigma^{(C)} = 5A/(2A+3B) = 23/43 = 0.535. \quad (119)$$

Upon using: $A+B=1+\rho_2=1.179$ [see Eqs. (16) and (17)], one can solve (119) for A and B , with the result: $A=0.477$, $B=0.702$. Finally, from Eq. (16) or (17), one obtains $b=-0.250$, whence $\varphi_2=128.7^\circ$ from Eq. (18).

From Eqs. (113) and (117), we obtain

$$\sigma_{12,d} = P_d \sigma_{12} = 0.455 \times 8.4 = 3.82 \text{ mb}. \quad (120)$$

The resulting values of the individual cross sections, as obtained from Eqs. (31)–(34) are: $\sigma^{(A)}=0.68$ mb, $\sigma^{(B)}=0.67$ mb, $\sigma^{(C)}=1.26$ mb, and $\sigma^{(D)}=0.39$ mb. These values are in fair agreement with the experimental results of Alles-Borelli *et al.*²⁵ Thus the Bologna group has identified 23 events of type (A), 8 events of type (B), and 43 events of type (C), as compared to 240 cases of reaction (I): $\pi^- + p \rightarrow n + \pi^+ + \pi^-$. Upon using the experimental value of 10 mb for $\sigma^{(I)}$, we thus find

$$\sigma^{(A)} = (23/240) \times 10 = 0.96 \text{ mb}, \quad (121)$$

$$\sigma^{(B)} = (8/240) \times 10 = 0.33 \text{ mb}, \quad (122)$$

$$\sigma^{(C)} = (43/240) \times 10 = 1.79 \text{ mb}. \quad (123)$$

The present calculated cross sections are also in reasonable agreement with the results of Derado and Schmitz²⁴: $\sigma^{(A)}=0.6 \pm 0.3$ mb, and $\sigma^{(B)}+\sigma^{(C)}=2.5 \pm 0.7$ mb.

With the present values of A and B , the contributions of the N_2^* processes to the single-pion production reactions (I) and (II) are as follows: $\sigma_2^{(I)}=0.971$ mb, $\sigma_2^{(II)}=1.915$ mb. In view of Eqs. (28), (29), and (34a), we obtain

$$\sigma^{(I)} = 9.58 + 3.84 \cos \varphi_1, \quad (124a)$$

$$\sigma^{(II)} = 5.71 - 2.74 \cos \varphi_1, \quad (124b)$$

where the units are millibarns. From the experimental value of $R=\sigma^{(II)}/\sigma^{(I)}=0.58$ from the 3 combined experiments, one obtains by means of Eqs. (124a) and (124b): $\varphi_1=88.2^\circ$, so that (with $\rho_1=0.179$), we find $a=0.0121$. We note that the present fit to the experiments at 1.0 Bev is somewhat different from that used in reference 3. The set of parameters used here corresponds to a larger value of $\sigma_{12}/(\sigma_{11}+\sigma_{12})$ (0.3 instead

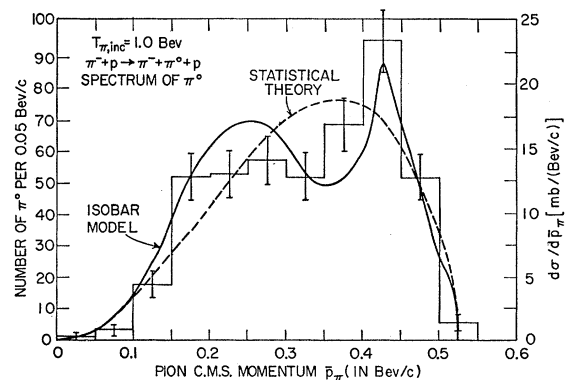


FIG. 13. Center-of-mass momentum spectrum of the π^0 mesons from the reaction $\pi^- + p \rightarrow \pi^- + \pi^0 + p$ at $T_{\pi, \text{inc}} = 1.0$ Bev. The histogram represents the combined experimental data from references 24–26. The solid curve was obtained from the present extended isobar model. The dashed curve gives the result of the Fermi statistical theory.

of 0.2), and gives better agreement with the cross sections for double-pion production $\sigma_d(\pi^- + p)$, $\sigma^{(A)}$, $\sigma^{(B)}$, and $\sigma^{(C)}$.

With the present values of a , ρ_1 , σ_{11} , and $\sigma_{12,s}$ [Eqs. (113) and (118)], Eqs. (35)–(38) give for the momentum spectra of the pions from reactions (I) and (II):

$$\left(\frac{d\sigma}{d\bar{p}_\pi} \right)^{(I)} (\pi^-) = 7.629 J_{\pi,1} + 1.107 J_{\pi,2} + 0.971 J_{\pi,3}, \quad (125)$$

$$\left(\frac{d\sigma}{d\bar{p}_\pi} \right)^{(I)} (\pi^+) = 1.107 J_{\pi,1} + 7.629 J_{\pi,2} + 0.971 J_{\pi,4}, \quad (126)$$

$$\left(\frac{d\sigma}{d\bar{p}_\pi} \right)^{(II)} (\pi^-) = 1.487 J_{\pi,1} + 2.214 J_{\pi,2} + 0.486 J_{\pi,3} + 1.429 J_{\pi,4}, \quad (127)$$

$$\left(\frac{d\sigma}{d\bar{p}_\pi} \right)^{(II)} (\pi^0) = 2.214 J_{\pi,1} + 1.487 J_{\pi,2} + 1.429 J_{\pi,3} + 0.486 J_{\pi,4}, \quad (128)$$

where the values are given in units of mb/(Bev/c). The corresponding total cross sections are: $\sigma^{(I)}=9.71$ mb, and $\sigma^{(II)}=5.62$ mb. It may be noted that the π^+ spectrum from reaction (I) and the π^0 spectrum from reaction (II) are obtained from the corresponding π^- spectra [Eqs. (125) and (127)], merely by interchanging $J_{\pi,1}$ with $J_{\pi,2}$, and $J_{\pi,3}$ with $J_{\pi,4}$. This property is exhibited explicitly in Eqs. (35)–(38) from which Eqs. (125)–(128) are derived.

The resulting c.m. momentum spectra are shown in Figs. 10–13, together with the combined histograms from the three experiments^{24–26} at $T_{\pi,\text{inc}}=1.0$ Bev. For comparison, we have also shown the momentum distribution predicted by the Fermi statistical theory.²² The two theoretical curves and the experimental histogram are normalized to the same area in each figure.

For the π^- mesons from the $\pi^- + \pi^+ + n$ reaction (Fig. 10), the isobar model curve fits the data quite well and, in particular, is able to reproduce the maximum of the histogram at $\bar{p}_\pi \approx 0.25$ Bev/c. On the other hand, the curve obtained from the statistical theory deviates considerably from the experimental histogram throughout the range of momenta.

Figure 11 shows the spectrum of π^+ mesons from the $\pi^- + \pi^+ + n$ reaction. The isobar model curve agrees reasonably well with the data. In particular, the momentum at which the peak of the isobar curve occurs ($\bar{p}_\pi=0.43$ Bev/c) is in good agreement with the position of the maximum of the experimental histogram. However, the value of the maximum of the isobar curve is somewhat too high. On the other hand, the spectrum predicted by the statistical theory is in qualitative disagreement with the data. One should note that the theoretical isobar curves of Figs. 10–13 have not been weighted by experimental resolution functions, and therefore some of the discrepancies with the data may arise from effects of finite momentum resolution.

For the π^- mesons from the $\pi^- + \pi^0 + p$ reaction (Fig. 12), the agreement of the isobar model curve with the data is comparable with that obtained by the statistical theory. As was pointed out above, the histogram represents the combined results of the three experiments of references 24–26. In this connection, we may note (as was done in reference 3), that for the Bologna and Brookhaven experiments at $T_{\pi,\text{inc}}=0.96$ for reaction (II), the average momentum of the π^- is appreciably higher than that of the π^0 mesons, whereas for the Göttingen experiment at 1.0 Bev there is a preponderance of slow π^- and fast π^0 mesons. Our previous isobar model calculations involving the isobar N_1^* only² give very good agreement with the Bologna-Brookhaven spectrum of π^- and π^0 .

We can define a fraction f of low-energy π^- mesons as the number of π^- with c.m. momenta \bar{p}_π below 300 Mev/c, divided by the total number of π^- from the $\pi^- + \pi^0 + p$ reaction. The three experiments give somewhat different values of f . Thus for the Bologna, Brookhaven, and Göttingen experiments, we have: $f_{Bo}=0.357$, $f_{Br}=0.455$, and $f_G=0.595$, respectively. If one combines all of the data, one obtains $f_{\text{exp}}=0.452$. The theoretical value of f as obtained from the isobar model curve of Fig. 12 is: $f_{\text{theor}}=0.367$. It should be noted that the experimental value of f has considerable uncertainty, since the values of f from the three experiments vary by as much as 0.24 (from 0.357 to 0.595). We also wish to point out that one may expect some effects of a possible pion-pion interaction in the $\pi^- + \pi^0 + p$ reaction, where the formation of the pion-nucleon isobar N_1^* is not as highly probable as for the π^- and neutron from the reaction leading to $\pi^- + \pi^+ + n$ [reaction (I)]. The effect of a final-state pion-pion interaction²⁸ has not been included in the present work. It has, of course, been our purpose in this work to see how far one can go in explaining the experimental results on pion production in pion-nucleon collisions, without invoking the existence of a pion-pion interaction.

For the π^0 mesons from $\pi^- + \pi^0 + p$, Fig. 13 shows that the present isobar model gives reasonable agreement with the experimental data, whereas the Fermi theory spectrum shows appreciable deviations from the histogram. The isobar model is able to predict correctly the peak of the experimental histogram in the region of \bar{p}_π between 0.40 and 0.45 Bev/c.

V. Q-VALUE DISTRIBUTIONS FOR PION-NUCLEON AND PION-PION PAIRS FROM $\pi^\pm - p$ INTERACTIONS

We have obtained the equations for the Q -value distribution functions $P(Q)$ for the various types of

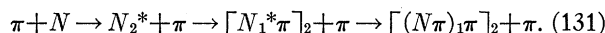
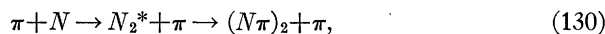
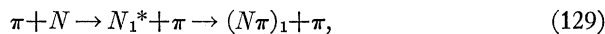
²⁸ F. Bonsignori and F. Selleri, Nuovo cimento **15**, 465 (1960); I. Derado, *ibid.* **15**, 853 (1960); L. Landovitz and L. Marshall, Phys. Rev. Letters **4**, 474 (1960); P. Carruthers and H. A. Bethe, *ibid.* **4**, 536 (1960); K. Itabashi, M. Kato, K. Nakagawa, and G. Takeda, Institute for Nuclear Studies Report No. 4, University of Tokyo, 1960 (unpublished).

TABLE I. Q -value distributions of pion-nucleon pairs arising from $\pi^- - p$ interactions.

Primary reaction	Final state	$\pi - N$ pair	Q -value distribution $P(Q)$
$\pi^- + p \rightarrow N_1^* + \pi \rightarrow N + 2\pi$	(n+-)	(n-)	$\frac{[(45+36\rho_1+90a)P_1^{(a)}+(5+16\rho_1-20a)P_1^{(b)}]}{(50+52\rho_1+70a)}$
	(p0-)	(p-)	$\frac{[(10+2\rho_1-10a)P_1^{(a)}+(10+32\rho_1-40a)P_1^{(b)}]}{(20+34\rho_1-50a)}$
	(n00)	(n0)	$\frac{1}{2}[P_1^{(a)}+P_1^{(b)}]$
$\pi^- + p \rightarrow N_2^* + \pi \rightarrow N + 2\pi$	(n+-)	(n+)	$P_2^{(a)}$
	(n+-)	(n-)	$P_2^{(b)}$
	(p0-)	(p-)	$(AP_2^{(b)}+2BP_2^{(a)})/(A+2B)$
	(p0-)	(p0)	$(AP_2^{(a)}+2BP_2^{(b)})/(A+2B)$
	(n00)	(n0)	$\frac{1}{2}[P_2^{(a)}+P_2^{(b)}]$
$\pi^- + p \rightarrow N_2^* + \pi \rightarrow N + 3\pi$	(p+-)	(p+)	$0.9\rho_1^{(a)}+0.1P^{(c)}$
	(p+-)	(p-)	$0.05\rho_1^{(a)}+0.45P^{(c)}+0.50P^{(d)}$
	(n+0-)	(n+)	$\frac{[(2A+B)\rho_1^{(a)}+(2A+9B)P^{(c)}]}{(4A+10B)}$
	(n+0-)	(n0)	$\frac{[A(\rho_1^{(a)}+P^{(c)})+5BP^{(d)}]}{(2A+5B)}$
	(n+0-)	(n-)	$\frac{[4AP^{(d)}+9B\rho_1^{(a)}+BP^{(c)}]}{(4A+10B)}$
	(p00-)	(p0)	$\frac{[4(1+\rho_2)]^{-1}[(2A+B)(\rho_1^{(a)}+P^{(c)})+2BP^{(d)}]}{(1+\rho_2)^{-1}[A\bar{P}^{(d)}+\frac{1}{2}B(\rho_1^{(a)}+P^{(c)})]}$
	(p00-)	(p-)	$\frac{1}{3}[\rho_1^{(a)}+P^{(c)}+P^{(d)}]$
	(n000)	(n0)	

pion-nucleon pairs arising from inelastic $\pi^- - p$ and $\pi^+ - p$ interactions. Here the Q value is defined as $Q \equiv \bar{E}_{\pi N^*} - (m_N + m_\pi)$, where $E_{\pi N^*}$ is the total energy of the pion and nucleon considered, in the center-of-mass system of the two particles. The functions $P(Q)$ are given in terms of certain basic functions $P_{\pi N, \alpha}^{(\eta)}(Q)$ which describe the normalized Q -value distributions for the nucleon from the decay of an isobar N_α^* and a definite pion, which may be either a recoil pion, or a decay pion originating from the same isobar N_α^* . The coefficients $c_{\alpha\eta}$ of the various $P_{\pi N, \alpha}^{(\eta)}(Q)$ will depend on the type of primary reaction (e.g., $\pi^- + p \rightarrow N_2^* + \pi$), the final state, and the pion-nucleon pair considered [e.g., $(p-\pi^-)$ from reaction (II)]. For an incident energy $T_{\pi, \text{inc}} = 1.0$ Bev, we have calculated the basic functions $P_{\pi N, \alpha}^{(\eta)}(Q)$ for $\pi - N$ pairs, which are involved for the single-pion production reactions, and the corresponding functions $P_{\pi\pi, \alpha}(Q)$ for the pion-pion pairs for single-pion production.

The notation for the functions $P_{\pi N, \alpha}^{(\eta)}(Q)$ and $P_{\pi\pi, \alpha}(Q)$ will be defined by means of the following equations which show the possible pion production reactions:



In Eqs. (129)–(131), the notations $(N\pi)_1$ and $(N\pi)_2$ represent the nucleon and pion arising from the decay of N_1^* and N_2^* , respectively. Similarly $[N_1^* \pi]_2 \rightarrow [(N\pi)_1 \pi]_2$ represents the two pions which arise from the decay of N_2^* via N_1^* .

For the reaction of Eq. (129), the Q -value distribution for the pion-pion pair is denoted by $P_{\pi\pi, 1}$. Similarly, the Q -value distribution for the pion-nucleon pair $(N\pi)_1$ which originates from the decay of N_1^* is denoted by $P_{\pi N, 1}^{(a)}$, whereas the Q value distribution pertaining to the recoil pion and the final-state nucleon is denoted by $P_{\pi N, 1}^{(b)}$.

For the reaction of Eq. (130), the notation is entirely analogous to that of Eq. (129), except that the subscript 1 is replaced by 2. Thus the pion-pion Q -value distribution for reaction (130) is denoted by $P_{\pi\pi, 2}$, and the two pion-nucleon Q distributions are written as $P_{\pi N, 2}^{(a)}$ and $P_{\pi N, 2}^{(b)}$, where $P_{\pi N, 2}^{(a)}$ pertains to the $\pi - N$ pair from $(N\pi)_2$, whereas $P_{\pi N, 2}^{(b)}$ pertains to the recoil pion and the final-state nucleon.

In connection with the double-pion production reaction of Eq. (131), we have considered only the pion-nucleon Q -value distributions in the present work (see Tables I and II). The Q distribution for the pion-nucleon pair from the decay of N_1^* [i.e., $(N\pi)_1$] is written as $\rho_{\pi N, 1}^{(a)}$. The Q distribution for the final-state nucleon and the pion which arises from the decay $N_2^* \rightarrow N_1^* + \pi$ is denoted by $P_{\pi N}^{(c)}$. Finally $P_{\pi N}^{(d)}$ denotes the Q distribution for the final-state nucleon and the recoil pion which is made together with N_2^* in the primary reaction. All of the functions $P_{\pi N, \alpha}^{(\eta)}$, $P_{\pi\pi, \alpha}$, and also $\rho_{\pi N, 1}^{(a)}$ are normalized to 1:

$$\int_0^{Q_m} P_{\pi N, \alpha}^{(\eta)}(Q)dQ = \int_0^{Q_m} P_{\pi\pi, \alpha}(Q)dQ = 1, \quad (132)$$

where Q_m is the maximum possible value of Q .

The function $P_{\pi N, 1}^{(a)}$ is essentially the same as the function \bar{P}_1 previously introduced in I (see Sec. VIII). Thus $P_{\pi N, 1}^{(a)}$ is given by

$$P_{\pi N, 1}^{(a)}(Q) = \frac{\sigma_{\frac{1}{2}}(m_I)F}{\int_{m_I, \text{min}}^{m_I, \text{max}} \sigma_{\frac{1}{2}}(m_I)F dm_I}, \quad (133)$$

where $m_I = m_N + m_\pi + Q$, $m_I, \text{min} = m_N + m_\pi = 1.078$ Bev, and $m_I, \text{max} = \bar{E} - m_\pi$ (\bar{E} = total energy in the c.m. system of the incident pion and proton). In a similar manner, the distribution $P_{\pi N, 2}^{(a)}$ pertaining to the N_2^* processes is given by

$$P_{\pi N, 2}^{(a)}(Q) = \frac{\sigma_{\frac{1}{2}}(m_I)F[1 - \epsilon(m_I)]}{\int_{m_I, \text{min}}^{m_I, \text{max}} \sigma_{\frac{1}{2}}(m_I)F[1 - \epsilon(m_I)] dm_I}. \quad (134)$$

TABLE II. Q -value distributions of pion-nucleon pairs arising from $\pi^+ - p$ interactions.

Primary reaction	Final state	$\pi - N$ pair	Q -value distribution $P(Q)$
$\pi^+ + p \rightarrow N_1^* + \pi \rightarrow N + 2\pi$	($p+0$)	($p+$)	$(9/13)P_1^{(a)} + (4/13)P_1^{(b)}$
	($p+0$)	($p0$)	$(4/13)P_1^{(a)} + (9/13)P_1^{(b)}$
	($n++$)	($n+$)	$\frac{1}{2}[P_1^{(a)} + P_1^{(b)}]$
$\pi^+ + p \rightarrow N_2^* + \pi \rightarrow N + 2\pi$	($p+0$)	($p+$)	$P_2^{(b)}$
	($p+0$)	($p0$)	$P_2^{(a)}$
	($n++$)	($n+$)	$\frac{1}{2}[P_2^{(a)} + P_2^{(b)}]$
$\pi^+ + p \rightarrow N_2^* + \pi \rightarrow N + 3\pi$	($p++-$)	($p+$)	$0.45\varphi_1^{(a)} + 0.05P^{(c)} + 0.50P^{(d)}$
	($p++-$)	($p-$)	$0.1\varphi_1^{(a)} + 0.9P^{(c)}$
	($n++0$)	($n+$)	$\frac{1}{4}\varphi_1^{(a)} + \frac{1}{4}P^{(c)} + \frac{1}{2}P^{(d)}$
	($n++0$)	($n0$)	$\frac{1}{2}[\varphi_1^{(a)} + P^{(c)}]$
	($p+00$)	($p+$)	$P^{(d)}$
	($p+00$)	($p0$)	$\frac{1}{2}[\varphi_1^{(a)} + P^{(c)}]$

Since the two-body phase space factor F , and the function $[1 - \epsilon(m_I)]$ are slowly varying functions of the isobar mass m_I , the distributions $P_{\pi N, 1}^{(a)}(Q)$ and $P_{\pi N, 2}^{(a)}(Q)$ will reflect primarily the behavior of the total cross sections $\sigma_{\frac{1}{2}}$ and $\sigma_{\frac{3}{2}}$, respectively. Figure 14 shows the functions $P_{\pi N, \alpha}^{(a)}(Q)$ for $T_{\pi, \text{inc}} = 1.0$ Bev. For $P_{\pi N, 1}^{(a)}(Q)$, the prominent peak at $Q_{\pi N} = 150$ Mev is directly due to the maximum of $\sigma_{\frac{1}{2}}$ at the $T = J = \frac{3}{2}$ resonance. For $P_{\pi N, 2}^{(a)}(Q)$, the full curve shows the result of including the low-energy $\sigma_{\frac{1}{2}}$, which results in an appreciable probability for low Q values. On the other hand, the dashed part of the curve represents the effect of disregarding the low-energy $\sigma_{\frac{1}{2}}$, i.e., taking $\sigma_{\frac{1}{2}}(m_I) \sim 0$ for $m_I < 1.23$ Bev (corresponding to incident energy $T_{\pi} < 180$ Mev). These two alternative procedures concerning the low-energy $\sigma_{\frac{1}{2}}$ have been discussed in detail in Sec. III. It should be noted that the region of small Q values which corresponds to the low-energy $\sigma_{\frac{1}{2}}$ becomes rapidly less important as the incident pion energy is raised above ~ 1 Bev. The behavior of this part of the distribution $P_{\pi N, 2}^{(a)}(Q)$ is completely analogous to the behavior of the high-energy maximum of the recoil pion spectrum $J_{\pi, 3}$ (see Sec. III), since there is a one-to-one correspondence between the recoil momentum \bar{p}_{π} and the Q value of the πN pair arising from the decay of N_2^* .

The maximum of $P_{\pi N, 2}^{(a)}$ at $Q = 350$ Mev is due to the maximum of $\sigma_{\frac{1}{2}}(m_I)$ at the first $T = \frac{1}{2}$ resonance corresponding to the state N_{2a}^* , with mass $m_I = 1.51$ Bev. This value of m_I corresponds to $Q = m_I - (m_N + m_{\pi}) = 430$ Mev. The fact that the maximum of $P_{\pi N, 2}^{(a)}$ occurs at a somewhat lower Q value (350 Mev) is due to the decrease of the two-body phase factor F with increasing m_I , i.e., decreasing momentum \bar{p}_{π} of the recoil pion. We note that at 1.0 Bev there is not enough energy in the center-of-mass system to excite the isobar N_{2b}^* (with mass $m_I = 1.68$ Bev) by the reaction (8). (We have $m_{I, \text{max}} = 1.603$ Bev at $T_{\pi, \text{inc}} = 1.0$ Bev). For this reason, the distribution $P_{\pi N, 2}^{(a)}(Q)$ has a single maximum at large Q values. For higher incident energies ($T_{\pi, \text{inc}} \gtrsim 2$ Bev), the curve of $P_{\pi N, 2}^{(a)}(Q)$ will have two maxima in this region, corresponding to the excitation of both N_{2a}^* and N_{2b}^* .

The Q -value distribution $\varphi_{\pi N, 1}^{(a)}(Q)$ which is involved for the 3-pion final states [Eq. (131)] is very similar to $P_{\pi N, 1}^{(a)}(Q)$, since both functions pertain to the pion and nucleon arising from the decay of the N_1^* isobar. However, the weighting function for $\varphi_{\pi N, 1}^{(a)}(Q)$, instead of being the two-body phase space factor F , is given by the following integral \mathcal{F} :

$$\mathcal{F}(m_1) \equiv \int_{m_1+m_{\pi}}^{\bar{E}-m_{\pi}} \sigma_{\frac{1}{2}}(m_2) F(\bar{E}, m_2) \epsilon(m_2, m_1) dm_2, \quad (135)$$

where $F(\bar{E}, m_2)$ is the two-body phase space factor for the formation of $N_2^* + \pi$ when the N_2^* isobar has mass m_2 ; $\epsilon(m_2, m_1)$ is the probability that N_2^* will decay into $N_1^* + \pi$ when N_1^* has mass m_1 [see Eq. (84)]. In terms of \mathcal{F} , $\varphi_{\pi N, 1}^{(a)}$ is given by

$$\varphi_{\pi N, 1}^{(a)}(Q) = \frac{\sigma_{\frac{1}{2}}(m_1) \mathcal{F}(m_1)}{\int_{m_{1, \text{min}}}^{m_{1, \text{max}}} \sigma_{\frac{1}{2}}(m_1) \mathcal{F}(m_1) dm_1}, \quad (136)$$

where $m_1 = Q + m_N + m_{\pi}$; $m_{1, \text{min}} = m_N + m_{\pi} = 1.078$ Bev, and $m_{1, \text{max}} = \bar{E} - 2m_{\pi}$ is the maximum mass of N_1^*

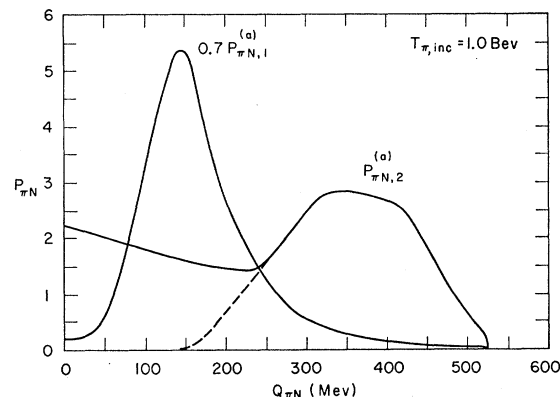


FIG. 14. Q -value distribution functions $P_{\pi N, 1}^{(a)}$ and $P_{\pi N, 2}^{(a)}$ for pion-nucleon pairs from single pion production in pion-nucleon collisions at $T_{\pi, \text{inc}} = 1.0$ Bev. The function $P_{\pi N, \alpha}^{(a)}$ ($\alpha = 1$ or 2) pertains to the nucleon and pion originating from the decay of the isobar N_{α}^* .

when two pions are produced besides N_1^* . Except for the decrease of the upper limit $m_{1,\max}$ and the replacement of F by \mathcal{F} , Eq. (136) is identical with Eq. (133) for $P_{\pi N,1}^{(a)}(Q)$.

The normalized Q -value distributions for the various πN pairs, in terms of the $P_{\pi N, \alpha}^{(\eta)}(Q)$, are given in Tables I and II for $\pi^- + p$ and $\pi^+ + p$ interactions, respectively. In these tables, in labeling the final states, we have employed the usual notation: 0 stands for a π^0 ; + and - represent π^+ and π^- , respectively. Thus $n+0-$ stands for: $n+\pi^++\pi^0+\pi^-$. For the sake of simplicity, since we are only referring to the πN pairs in these tables, we have omitted the subscript πN from $P_{\pi N, \alpha}^{(\eta)}$ and $\mathcal{P}_{\pi N, 1}^{(a)}$, which are written simply as $P_\alpha^{(\eta)}$ and $\mathcal{P}_1^{(a)}$, respectively.

Concerning the reaction $\pi^- + p \rightarrow N_1^* + \pi$ (Table I), we have not listed the Q distributions $P(n+)$ for the $n+\pi^++\pi^-$ final state, nor the distribution $P(p0)$ for the $p+\pi^0+\pi^-$ final state. These distributions can be obtained by merely interchanging $P_1^{(a)}$ and $P_1^{(b)}$ in the expressions for $P(n-)$ and $P(p-)$, respectively. The results of Tables I and II were obtained in a straightforward manner, by considering the wave functions $\Psi_{\pi^- - p}^{(\text{final})}$ and $\Psi_{\pi^+ - p}^{(\text{final})}$ which represent the various final states [see Sec. II, Eqs. (12)–(27) and (49)–(50)].

The Q value distributions $P_{\pi\pi}(Q)$ for $\pi\pi$ pairs are not included in Tables I and II. In the present isobar model, $P_{\pi\pi}(Q)$ for single-pion production is given by

$$P_{\pi\pi}(Q) = (\sigma_1 P_{\pi\pi,1} + \sigma_2 P_{\pi\pi,2})/\sigma, \quad (137)$$

where σ is the total cross section for the particular reaction considered, and σ_1, σ_2 are the parts of σ which pertain to formation of $N_1^* + \pi$ and $N_2^* + \pi$, respectively. (Thus $\sigma = \sigma_1 + \sigma_2$.)

In connection with the equations of Tables I and II, we note that the angular correlation in the c.m. system, $C_{\pi N}(\bar{\theta}_{\pi N})$, for a particular pion-nucleon pair is given by equations which are completely similar to the equations for $P_{\pi N}(Q)$, the only difference being that the functions $P_{\pi N, \alpha}^{(\eta)}(Q)$ must be replaced by basic angular correlation functions $C_{\pi N, \alpha}^{(\eta)}(\bar{\theta}_{\pi N})$ for the nucleon from the decay of N_α^* and a particular pion (decay pion from N_α^* or recoil pion). Here $\bar{\theta}_{\pi N}$ is the angle between the pion and nucleon in the c.m. system. As an example, for the π^- and proton from the reaction $\pi^- + p \rightarrow p + \pi^+ + \pi^0$ via N_1^* , the angular correlation function is given by

$$C_{\pi^- - p}(\bar{\theta}_{\pi^- - p}) = \frac{(10 + 2\rho_1 - 10a)C_{\pi N, 1}^{(a)} + (10 + 32\rho_1 - 40a)C_{\pi N, 1}^{(b)}}{20 + 34\rho_1 - 50a}. \quad (138)$$

The functions $C_{\pi N, \alpha}^{(\eta)}$ have not been calculated in the present work.

We will now describe the calculation of the Q -value

distributions $P_{\pi N, \alpha}^{(b)}$ and $P_{\pi\pi, \alpha}$ at $T_{\pi, \text{inc}} = 1.0$ Bev. We will discuss first the evaluation of the distribution $P_{\pi\pi, \alpha}(Q)$ of the Q values for $\pi\pi$ pairs. As mentioned above, $P_{\pi\pi, \alpha}$ is defined as the Q -value distribution function pertaining to the two pions made via $N_\alpha^* + \pi$. In particular, at 1.0 Bev, we expect the function $P_{\pi\pi, 1}$ to predominate in the expression for $P_{\pi\pi}(Q)$, since most of the single-pion production proceeds via the $T = \frac{3}{2}$ isobaric state N_1^* [see Eq. (137)].

For a given mass m_j of the isobar, the energy of the decay pion in the c.m. system of the incident pion and nucleon is given by

$$\bar{E}_{\pi, d} = \bar{\gamma}_j(E_\pi^* + \bar{v}_j p_\pi^* \cos\theta_\pi^*), \quad (139)$$

where \bar{v}_j is the velocity of the isobar in the c.m. system, $\bar{\gamma}_j = (1 - \bar{v}_j^2)^{-\frac{1}{2}}$, and E_π^*, p_π^* are the pion total energy and momentum in the isobar rest system; θ_π^* is the angle of emission of the pion with respect to the direction of motion of the isobar; θ_π^* is measured in the isobar rest system. The component of the c.m. momentum of the decay pion along the direction of motion of the isobar (taken as the x axis) is given by

$$\bar{p}_{\pi, d, x} = \bar{\gamma}_j(p_\pi^* \cos\theta_\pi^* + \bar{v}_j E_\pi^*). \quad (140)$$

The combined momentum of the two pions in the c.m. system is obtained from

$$\bar{p}_{\pi\pi}^2 = (\bar{p}_{\pi, d, x} - \bar{p}_{\pi, r})^2 + \bar{p}_{\pi, d, y}^2, \quad (141)$$

where $\bar{p}_{\pi, r}$ is the c.m. momentum of the recoil pion, and $\bar{p}_{\pi, d, y} = p_\pi^* \sin\theta_\pi^*$ is the transverse momentum of the decay pion. The total c.m. energy of the $\pi\pi$ system is given by

$$\bar{E}_{\pi\pi} = \bar{E}_{\pi, d} + \bar{E}_{\pi, r}, \quad (142)$$

where $\bar{E}_{\pi, r}$ is the total energy of the recoil pion.

Since the quantity $E^2 - p^2$ is invariant under a Lorentz transformation, we obtain for the total energy in the center-of-mass system of the two pions:

$$E_{\pi\pi}^* = (\bar{E}_{\pi\pi}^2 - \bar{p}_{\pi\pi}^2)^{\frac{1}{2}}, \quad (143)$$

where $\bar{p}_{\pi\pi}$ and $\bar{E}_{\pi\pi}$ are given by Eqs. (141) and (142). The Q value $Q_{\pi\pi}$ is now given by

$$Q_{\pi\pi} = E_{\pi\pi}^* - 2m_\pi, \quad (144)$$

We will assume that the isobar decays isotropically in its rest system. Similarly to the calculations of I (Sec. VIII), we have considered angles θ_π^* at intervals of 22.5° . These angles will be denoted by $\theta_{\pi, k}^*$ (i.e., $\theta_{\pi, 1}^* = 0^\circ, \theta_{\pi, 2}^* = 22.5^\circ, \dots, \theta_{\pi, 9}^* = 180^\circ$). Since the solid angle in the isobar rest system is given by $\Delta\Omega_{\pi, k}^* = \sin\theta_{\pi, k}^* \Delta\theta_{\pi, k}^*$, the Q -value distribution pertaining to the isobar mass m_j is given by

$$P_{\pi\pi}^{(j)}(Q) = M \sin\theta_{\pi, k}^* / (Q_{jk}^{(+)} - Q_{jk}^{(-)}) \quad \text{for } Q_{jk}^{(-)} < Q < Q_{jk}^{(+)}, \quad (145)$$

where $Q_{jk}^{(\pm)}$ is defined by

$$Q_{jk}^{(\pm)} \equiv \frac{1}{2}(Q_{jk} + Q_{j, k \pm 1}); \quad (146)$$

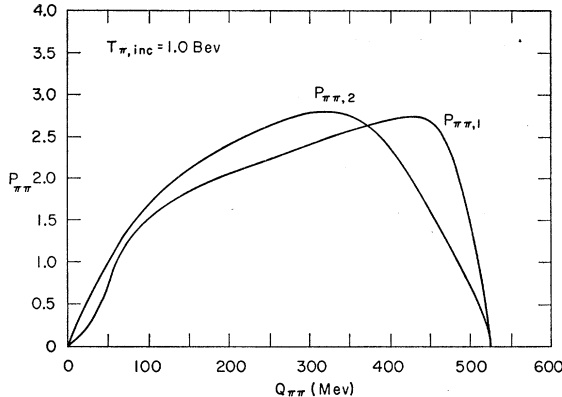


FIG. 15. Q -value distribution functions $P_{\pi\pi,1}$ and $P_{\pi\pi,2}$ for pion-pion pairs from single pion production in pion-nucleon collisions at $T_{\pi,inc}=1.0$ Bev.

Q_{jk} is the Q value of Eq. (144) pertaining to isobar mass m_j and decay angle $\theta_{\pi,k}^*$. In Eq. (145), M is a normalization factor.

Finally, the weighted distributions $P_{\pi\pi,\alpha}$ are given by the following integrals:

$$P_{\pi\pi,1}(Q)=M_1 \int P_{\pi\pi^{(j)}}(Q)\sigma_{\frac{3}{2}}(m_j)Fdm_j, \quad (147)$$

$$P_{\pi\pi,2}(Q)=M_2 \int P_{\pi\pi^{(j)}}(Q)\sigma_{\frac{1}{2}}(m_j)F[1-\epsilon(m_j)]dm_j, \quad (148)$$

where M_α is a normalization factor, $\sigma_{\frac{3}{2}}$ and $\sigma_{\frac{1}{2}}$ are the appropriate total πN cross sections in the $T=\frac{3}{2}$ and $T=\frac{1}{2}$ states, respectively, and $[1-\epsilon(m_j)]$ gives the fraction of N_2^* decays which result in single-pion production, i.e., for which $N_2^* \rightarrow N + \pi$. In Eqs. (147) and (148), F is the two-body phase space factor for the formation of $N_\alpha^* + \pi$.

The resulting $Q_{\pi\pi}$ distributions are shown in Fig. 15. It is seen that the distributions $P_{\pi\pi,1}$ and $P_{\pi\pi,2}$ are very similar, with $P_{\pi\pi,1}$ being somewhat more peaked at large Q values, near the maximum possible Q , $Q_{\max}=525$ Mev (for $T_{\pi,inc}=1.0$ Bev). The weighted distributions shown in Fig. 15 reflect the behavior of the individual distributions $P_{\pi\pi^{(j)}}(Q)$ for the various m_j . In all cases (i.e., for all m_j), these distributions increase with increasing $Q_{\pi\pi}$ to a maximum which is reached near the maximum possible Q , $Q_{\max,j}$, for the particular m_j considered. As an example, for $m_j=1.30$ Bev, $P_{\pi\pi^{(j)}}(Q)$ increases from 0 at $Q_{\min,j}=8$ Mev to 0.70 at 80 Mev, and a maximum of 1.42 at $Q=500$ Mev, then rapidly decreases to 0 at $Q_{\max,j}=525$ Mev.

If in a particular reaction (e.g., $\pi^- + p \rightarrow \pi^- + \pi^0 + p$), the pions are made via N_1^* with a probability ξ_1 , and via N_2^* with a probability $(1-\xi_1)$, then the predicted $Q_{\pi\pi}$ distribution is given by

$$P_{\pi\pi}(Q)=\xi_1 P_{\pi\pi,1}+(1-\xi_1)P_{\pi\pi,2}. \quad (149)$$

Equation (149) is equivalent to Eq. (137), in which $\sigma_1/(\sigma_1+\sigma_2)=\xi_1$.

We shall now obtain the Q -value distributions $P_{\pi N,\alpha}^{(b)}$ which pertain to the recoil pion and the nucleon arising from the decay of N_α^* . The total energy of the pion-nucleon pair in the c.m. system is given by

$$\bar{E}_{\pi N}=\bar{E}-\bar{E}_{\pi,d}, \quad (150)$$

where \bar{E} is the total energy of all particles in the c.m. system, and $\bar{E}_{\pi,d}$ is the energy of the decay pion [Eq. (139)]. The total momentum $\bar{\mathbf{p}}_{\pi N}$ of the πN system is equal to $-\bar{\mathbf{p}}_{\pi,d}$, where $\bar{\mathbf{p}}_{\pi,d}$ is the momentum of the decay pion [Eq. (140)]. Thus, in analogy to Eq. (143), the total energy in the center-of-mass system of the pion and nucleon is given by

$$E_{\pi N}^*=(\bar{E}_{\pi N}^2-\bar{p}_{\pi N,x}^2-\bar{p}_{\pi N,y}^2)^{\frac{1}{2}} \\ =[(\bar{E}-\bar{E}_{\pi,d})^2-\bar{p}_{\pi,d,x}^2-\bar{p}_{\pi,d,y}^2]^{\frac{1}{2}}. \quad (151)$$

Finally, the Q value is obtained from

$$Q_{\pi N}=E_{\pi N}^*-m_N-m_\pi. \quad (152)$$

The Q -value distribution $P_{\pi N}^{(j)}(Q)$ pertaining to a given m_j is obtained from an equation similar to (145):

$$P_{\pi N}^{(j)}(Q)=M \sin\theta_{N,k}^*/(Q_{jk}^{(+)}-Q_{jk}^{(-)}) \\ \text{for } Q_{jk}^{(-)} < Q < Q_{jk}^{(+)}, \quad (153)$$

where $Q_{jk}^{(\pm)}$ is the appropriate value of $Q_{\pi N}$ from Eq. (152), and $\theta_{N,k}^*$ is the angle of emission of the nucleon in the isobar rest system.

The weighted distributions $P_{\pi N,\alpha}^{(b)}(Q)$ are given by

$$P_{\pi N,1}^{(b)}(Q)=M_1 \int P_{\pi N}^{(j)}(Q)\sigma_{\frac{3}{2}}(m_j)Fdm_j, \quad (154)$$

$$P_{\pi N,2}^{(b)}(Q)=M_2 \int P_{\pi N}^{(j)}(Q)\sigma_{\frac{1}{2}}(m_j) \\ \times [1-\epsilon(m_j)]Fdm_j, \quad (155)$$

where M_α is a normalization factor.

The resulting distributions $P_{\pi N,1}^{(b)}(Q)$ and $P_{\pi N,2}^{(b)}(Q)$ are shown in Fig. 16. It is seen that $P_{\pi N,1}^{(b)}$ has a pronounced maximum at $Q=370$ Mev, whereas $P_{\pi N,2}^{(b)}$ has a relatively weak maximum at $Q=180$ Mev, and is essentially flat from $Q=320$ to 480 Mev. These distributions reflect the behavior of the partial distributions $P_{\pi N}^{(j)}(Q)$ pertaining to the various m_j . The $P_{\pi N}^{(j)}(Q)$ are practically constant (actually increasing slightly with increasing Q) between limits $Q_{\min,j}$ and $Q_{\max,j}$ which decrease generally with increasing m_j . Each distribution $P_{\pi N}^{(j)}(Q)$ for a given m_j is different from zero only over a limited part of the complete range of Q , which extends from 0 to 525 Mev. The region occupied by $P_{\pi N}^{(j)}(Q)$ is generally of the order of 150–200 Mev. Thus for $m_j=1.15$ Bev, $P_{\pi N}^{(j)}(Q)$ extends from $Q=368$ to 504 Mev; for $m_j=1.25$ Bev, we have $Q_{\min}=248$, $Q_{\max}=440$ Mev; for $m_j=1.40$ Bev, $Q_{\min}=106$, $Q_{\max}=308$ Mev; for $m_j=1.50$ Bev, $Q_{\min}=40$, $Q_{\max}=192$ Mev.

TABLE III. Branching ratios for pion production in $p-p$ interactions.

Reaction	$N+N_1^*$	$2N_1^*$	$N+N_2^*$	$N_1^*+N_2^*$	$2N_2^*$
$(pn+)$	5/6		2/3		
$(pp0)$	1/6		1/3		
$\bar{\sigma}$	$\sigma_1(N+N_1^*)$		$\sigma_{1,s}(N+N_2^*)$		
$(pp+-)$		1/5	5/9	1/2	0
$(pp00)$		8/45	2/9	1/18	1/9
$(pn+0)$		26/45	2/9	7/18	4/9
$(nn++)$		2/45	0	1/18	4/9
$\bar{\sigma}$		$\sigma_{1,d}(2N_1^*)$	$\sigma_{1,d}(N+N_2^*)$	$\sigma_{1,d}(N_1^*+N_2^*)$	$\sigma_{1,d}(2N_2^*)$
$(pp+0-)$				7/27	5/27
$(pp000)$				1/27	2/27
$(pn++-)$				25/54	10/27
$(pn+00)$				2/9	2/9
$(nn++0)$				1/54	4/27
$\bar{\sigma}$				$\sigma_{1,t}(N_1^*+N_2^*)$	$\sigma_{1,t}(2N_2^*)$
$(pp++--)$					25/81
$(pp+00-)$					20/81
$(pp000)$					4/81
$(pn++0-)$					20/81
$(pn+000)$					8/81
$(nn++00)$					4/81
$\bar{\sigma}$					$\sigma_{1,q}(2N_2^*)$

For $P_{\pi N,1}^{(b)}$, the maximum at $Q=370$ Mev is a direct consequence of the predominance of the distributions $P_{\pi N}^{(j)}(Q)$ for $m_j=1.20$ and 1.25 Bev, which extend from 304 to 476 Mev, and from 248 to 440 Mev, respectively. These distributions have fractional weights $f_j=0.309$ and 0.285, respectively, in the integral of Eq. (154). It should be noted that for the calculation of $P_{\pi N,\alpha}^{(b)}$ (and also $P_{\pi\pi,\alpha}$), the distributions were evaluated at intervals of 50 Mev in m_j (from $m_j=1.10$ to 1.60 Bev), and the integrals of Eqs. (147), (148), (154), and (155) were thus replaced by sums over the various $P^{(j)}$, with weighting factors determined by $\sigma_j F$ and $\sigma_j F(1-\epsilon)$.

For the distribution $P_{\pi N,2}^{(b)}$, the weighting factor has a maximum at $m_j=1.45$ Bev ($f_j=0.140$), and the maximum of $P_{\pi N,2}^{(b)}$ at $Q_{\pi N}=180$ Mev is due to the

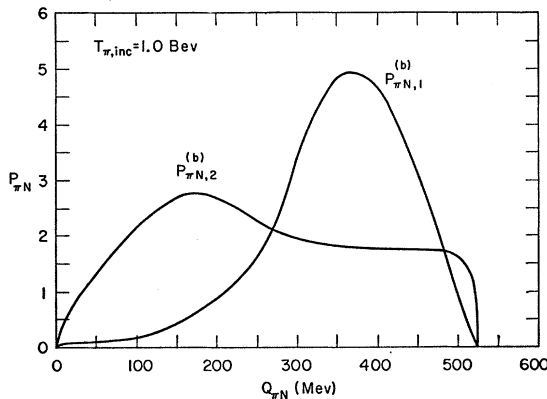


FIG. 16. Q -value distribution functions $P_{\pi N,1}^{(b)}$ and $P_{\pi N,2}^{(b)}$ for pion-nucleon pairs from single pion production in pion-nucleon collisions at $T_{\pi,inc}=1.0$ Bev. The function $P_{\pi N,\alpha}^{(b)}$ ($\alpha=1$ or 2) pertains to the recoil pion and the nucleon arising from the decay of the isobar N_α^* .

effect of the $P_{\pi N}^{(j)}$ for $m_j=1.45$ Bev, which extends from $Q=68$ to 256 Mev. However, the value of f_j at the maximum is not very large (0.140), and the other m_j values throughout the range from 1.10 to 1.60 Bev make significant contributions. This accounts for the relatively flat behavior and the large values of $P_{\pi N,2}^{(b)}$ above the maximum (i.e., from ~ 320 to ~ 480 Mev).

For a definite πN pair from a particular single-pion production reaction, the predicted Q -value distribution is given by

$$P_{\pi N} = (\sigma_1 + \sigma_2)^{-1} [\sigma_1(c_{1a}P_{\pi N,1}^{(a)} + c_{1b}P_{\pi N,1}^{(b)}) + \sigma_2(c_{2a}P_{\pi N,2}^{(a)} + c_{2b}P_{\pi N,2}^{(b)})], \quad (156)$$

where c_{aa} and c_{ab} are the coefficients of $P_{\pi N,\alpha}^{(a)}$ and $P_{\pi N,\alpha}^{(b)}$, respectively, in Table I or Table II. The cross sections σ_1 and σ_2 were defined above in connection with Eq. (137). Thus σ_1 and σ_2 are the partial cross sections for the reaction to proceed via $N_1^*+\pi$ and $N_2^*+\pi$, respectively.

As an example of the use of Eq. (156) and Table I, we will calculate the functions $P_{\pi N}(Q)$ and $P_{\pi\pi}(Q)$ for the πN and $\pi\pi$ pairs from reaction (I) at $T_{\pi,inc}=1.0$ Bev, using the values of the parameters of the present extended isobar model, which have been determined in Sec. IV. These values are as follows: $\rho_1=\rho_2=0.179$; $a=0.0121$; $A=0.477$, $B=0.702$; $\sigma_1^{(I)}=9.71$ mb, $\sigma_1^{(I)}=8.74$ mb, $\sigma_2^{(I)}=0.97$ mb, where $\sigma_\alpha^{(I)}$ is the part of $\sigma^{(I)}$ which is due to the formation of the N_α^* isobar [see Eq. (125)]. We thus obtain:

$$\xi_1 = \sigma_1^{(I)}/\sigma^{(I)} = 8.74/9.71 = 0.900. \quad (157)$$

For the $\pi^- - n$ pair from reaction (I), Table I gives $c_{1a}=0.873$, $c_{1b}=0.127$, $c_{2a}=0$, and $c_{2b}=1$, so that one

TABLE IV. Branching ratios for pion production in $n-p$ interactions.

Reaction	$N+N^*$	$2N_1^*$	$N+N_2^*$	$N_1^*+N_2^*$	$2N_2^*$
(pp^-)	$1/6$		$(1/3)C_+$		
$(pn0)$	$2/3$		$(1/3)(1+k_1)$		
$(nn+)$	$1/6$		$(1/3)C_-$		
$\bar{\sigma}$	$\frac{1}{2}\sigma_1(N+N_1^*)$		$\frac{1}{2}\sigma_{1,s}(N+N_2^*)$		
$(pp0-)$		$(1/45)+(1/9)k_0$	$(1/9)C_+$	$5/18$	$2/9$
$(pn+-)$		$(41/45)+(5/9)k_0$	$(5/9)(1+k_1)$	$2/9$	$4/9$
$(pn00)$		$(2/45)+(2/9)k_0$	$(2/9)(1+k_1)$	$2/9$	$1/9$
$(nn+0)$		$(1/45)+(1/9)k_0$	$(1/9)C_-$	$5/18$	$2/9$
$\bar{\sigma}$		$\frac{1}{2}\sigma_1(2N_1^*)$	$\frac{1}{2}\sigma_{1,d}(N+N_2^*)$	$\frac{1}{2}\sigma_{1,d}(N_1^*+N_2^*)$	$\frac{1}{2}[\sigma_{1,d}(2N_2^*)+\sigma_{0,d}(2N_2^*)]$
$(pp+- -)$				$5/54$	$5/27$
$(pp00-)$				$1/9$	$1/9$
$(pn+0-)$				$4/9$	$1/3$
$(pn000)$				$4/27$	$2/27$
$(nn++-)$				$5/54$	$5/27$
$(nn+00)$				$1/9$	$1/9$
$\bar{\sigma}$				$\frac{1}{2}\sigma_{1,t}(N_1^*+N_2^*)$	$\frac{1}{2}[\sigma_{1,t}(2N_2^*)+\sigma_{0,t}(2N_2^*)]$
$(pp+0--)$					$10/81$
$(pp000-)$					$4/81$
$(pn++- -)$					$25/81$
$(pn+00-)$					$8/27$
$(pn0000)$					$4/81$
$(nn++0-)$					$10/81$
$(nn+000)$					$4/81$
$\bar{\sigma}$					$\frac{1}{2}[\sigma_{1,q}(2N_2^*)+\sigma_{0,q}(2N_2^*)]$

obtains from Eq. (156), [with $\sigma_1/(\sigma_1+\sigma_2)=0.900$]:

$$P_{n\pi^-}(Q)=0.786P_{\pi N,1}^{(a)}+0.114P_{\pi N,1}^{(b)}+0.100P_{\pi N,2}^{(b)}. \quad (158)$$

The Q -value distribution for the $n-\pi^+$ pair is obtained from Eq. (158) by merely interchanging $P_{\pi N,\alpha}^{(a)}$ with $P_{\pi N,\alpha}^{(b)}$. Thus we find

$$P_{n\pi^+}(Q)=0.114P_{\pi N,1}^{(a)}+0.786P_{\pi N,1}^{(b)}+0.100P_{\pi N,2}^{(a)}. \quad (159)$$

For the $\pi^+-\pi^-$ pair, we obtain from Eq. (149):

$$P_{\pi^+\pi^-}(Q)=0.900P_{\pi\pi,1}+0.100P_{\pi\pi,2}. \quad (160)$$

Similarly, one obtains for the Q -value distribution of the $\pi^--\pi^0$ pair from reaction (II), with $\xi_1=0.659$:

$$P_{\pi^-\pi^0}(Q)=0.659P_{\pi\pi,1}+0.341P_{\pi\pi,2}. \quad (161)$$

Here the value $\xi_1=0.659$ is obtained from the cross sections $\sigma_1^{(II)}=3.705$ mb, $\sigma_2^{(II)}=1.915$ mb, $\sigma^{(II)}=5.62$ mb [see Eq. (127)], so that $\xi_1=3.705/5.62=0.659$. The distribution (161) is quite flat in the region of Q from ~ 200 to 500 Mev (see Fig. 15). On the other hand, if there should be a strong $\pi\pi$ interaction, with a large cross section $\sigma_{\pi\pi}$ which passes through a resonance in the region of $Q_{\pi\pi} \lesssim 500$ Mev, we would expect that the distribution $P_{\pi^-\pi^0}(Q)$ for reaction (II) will be strongly peaked near the value of Q which corresponds to the resonance of $\sigma_{\pi\pi}$. Such an effect seems to have been observed by Pickup *et al.*²⁶ in the analysis of their experiment with 0.96-Bev π^- mesons. As was pointed out above, the effect of a possible pion-pion interaction²⁸ has not been included in the present work. Of course, it

would be possible to introduce an effective pion-pion final-state interaction and to determine quantitatively how it would modify the result of Eq. (161).

VI. BRANCHING RATIOS FOR PION PRODUCTION IN NUCLEON-NUCLEON COLLISIONS

We have obtained the branching ratios for pion production in $p-p$ and $n-p$ collisions, using the following processes:

$$p+N \rightarrow N_1^*+N, \quad (a)$$

$$p+N \rightarrow 2N_1^*, \quad (b)$$

$$p+N \rightarrow N_2^*+N, \quad (c)$$

$$p+N \rightarrow N_1^*+N_2^*, \quad (d)$$

$$p+N \rightarrow 2N_2^*. \quad (e)$$

The reactions (a) and (b) have been previously investigated in I. When N_2^* is produced, we consider the possibility that it may decay into N_1^* or directly into a nucleon, i.e., we include both one-pion and two-pion decays.

The resulting branching ratios for $p-p$ interactions are given in Table III; those for $n-p$ interactions are given in Table IV. Each table is divided into four parts, corresponding to production of one, two, three, or four pions. At the end of each part, we give the expression for the cross section $\bar{\sigma}$ by which the branching ratios listed above $\bar{\sigma}$ must be multiplied in order to obtain the corresponding partial cross sections for the reactions considered. As an example, the cross section

$\sigma^{(c)}(pp+-)$ for the reaction

$$p+p \rightarrow N_2^* + N \rightarrow p+p+\pi^++\pi^-,$$

is $(5/9)\sigma_{1,d}(N+N_2^*)$. The notation used for the $\bar{\sigma}$ is as follows. Taking $\sigma_{1,d}(N+N_2^*)$ as an example, the parenthesis indicates the final state involved in the primary reaction [(a)-(e)]; the first subscript of σ gives the isotopic spin T of the system ($=1$) and the second subscript ($=d$) indicates the total number of pions produced: s for single, d =double, t =triple, q =quadruple. Thus $\sigma_{1,d}(N+N_2^*)$ is the cross section for producing $N+N_2^*$ in the state $T=1$, with subsequent decay of N_2^* into 2 pions [Eq. (9b)]. For $N+N_1^*$ and $2N_1^*$, where the number of pions is unambiguous the subscript s or d is omitted.

We note that the production of a maximum of 8 pions could be treated within the framework of the present extended isobar model. Thus we can consider the reaction: $N+N \rightarrow 2N_0^*$, with subsequent decay of each N_0^* as follows:

$$N_0^* \rightarrow N_{2b}^* + \pi \rightarrow N_{2a}^* + 2\pi \rightarrow N_1^* + 3\pi \rightarrow N + 4\pi.$$

For the $n-p$ interactions (Table IV), we have introduced the quantities k_0 , k_1 , C_+ , and C_- , which are defined as follows:

$$k_0 \equiv \sigma_0(2N_1^*)/\sigma_1(2N_1^*), \quad (162)$$

$$\begin{aligned} k_1 &\equiv \sigma_{0,s}(N_2^*+N)/\sigma_{1,s}(N_2^*+N) \\ &= \sigma_{0,d}(N_2^*+N)/\sigma_{1,d}(N_2^*+N), \end{aligned} \quad (163)$$

$$C_{\pm} \equiv 1 + k_1 \pm 2k_1^{\frac{1}{2}} \cos\varphi_0, \quad (164)$$

where φ_0 is the phase angle between the matrix elements for the reaction $N+N \rightarrow N+N_2^*$ in the $T=0$ and $T=1$ states. It may be noted that for $n-p$ interactions which lead to $N+N_1^*$ and $N_1^*+N_2^*$, the reaction can take place only in the $T=1$ state, so that the branching ratios do not involve any ratio k_i . For the pion production in $n-p$ collisions which proceeds via $2N_2^*$ [reaction (e)], all of the partial cross sections are proportional to $[\sigma_1(2N_2^*) + \sigma_0(2N_2^*)]$. We remark that the ratio k_0 was previously used in I [see Eqs. (62)-(64)]. For $n+p \rightarrow N+N_2^*$, the terms in $\cos\varphi_0$ which enter into C_+ and C_- are due to the interference between the $T=0$ and $T=1$ contributions.

The calculation of the various branching ratios is straightforward. We shall therefore give the derivation only for one case as an example, namely, the production of two pions in $n-p$ interactions, via $N+N_2^*$. The wave functions $N+N_2^*$ in the $T=1$ and $T=0$ states ($T_z=0$) are given by:

$$\Psi(T=1) = 2^{-\frac{1}{2}}(\omega_{\frac{1}{2}}\lambda_{-\frac{1}{2}} + \omega_{-\frac{1}{2}}\lambda_{\frac{1}{2}}), \quad (165)$$

$$\Psi(T=0) = 2^{-\frac{1}{2}}(\omega_{\frac{1}{2}}\lambda_{-\frac{1}{2}} - \omega_{-\frac{1}{2}}\lambda_{\frac{1}{2}}), \quad (166)$$

where ω_{Tz} is the wave function of the unexcited nucleon, and λ_{Tz} is the wave function of the N_2^* isobar. The relative probability of the various possible final states

is obtained from the following expression for $|\Psi^{(\text{final})}|^2$:

$$\begin{aligned} |\Psi^{(\text{final})}|^2 &= |\Psi(T=1) + k_1^{\frac{1}{2}} \exp(i\varphi_0) \Psi(T=0)|^2 \\ &= \frac{1}{2} C_+ \omega_{\frac{1}{2}}^2 \lambda_{-\frac{1}{2}}^2 + \frac{1}{2} C_- \omega_{-\frac{1}{2}}^2 \lambda_{\frac{1}{2}}^2. \end{aligned} \quad (167)$$

For the decay of N_2^* into $N_1^*+\pi$, $\lambda_{\frac{1}{2}}$ and $\lambda_{-\frac{1}{2}}$ are equivalent to the expressions (21) and (22) involving ψ_{Tz} (wave function of N_1^*) and ν_{Tz} (wave function of decay pion). Thus for $\lambda_{\frac{1}{2}}^2$, we may write

$$\begin{aligned} \lambda_{\frac{1}{2}}^2 &= \frac{1}{6} \psi_{-\frac{1}{2}}^2 \nu_1^2 + \frac{1}{3} \psi_{\frac{1}{2}}^2 \nu_0^2 + \frac{1}{2} \psi_{\frac{1}{2}}^2 \nu_{-1}^2 \\ &= \frac{1}{6} (\frac{2}{3} \mu_{-1}^2 \chi_{\frac{1}{2}}^2 + \frac{2}{3} \mu_1^2 \chi_{-\frac{1}{2}}^2) \nu_0^2 + \frac{1}{2} \mu_1^2 \chi_{\frac{1}{2}}^2 \nu_{-1}^2, \end{aligned} \quad (168)$$

where the last expression, in terms of μ_{Tz} and χ_{Tz} , follows from Eqs. (23)-(25). Here μ_{Tz} and χ_{Tz} represent the pion and nucleon, respectively, from the decay of N_1^* . From (168), one finds that $\lambda_{\frac{1}{2}}^2$ is equivalent to

$$\lambda_{\frac{1}{2}}^2 = (5/9)(p+-) + (2/9)(p00) + (2/9)(n+0). \quad (169)$$

By applying charge symmetry to (169), one obtains the following expression for $\lambda_{-\frac{1}{2}}^2$:

$$\lambda_{-\frac{1}{2}}^2 = (5/9)(n+-) + (2/9)(p0-) + (2/9)(n00). \quad (170)$$

Upon inserting (169) and (170) into Eq. (167), one obtains the result:

$$\begin{aligned} |\Psi^{(\text{final})}|^2 &= C_+ [(5/18)(pn+-) + \frac{1}{3}(pn00)] + C_- [(5/18)(pn+-) \\ &\quad + \frac{1}{9}(pn00) + \frac{1}{9}(nn0)]. \end{aligned} \quad (171)$$

Hence the relative probabilities of the possible two-pion final states are

$$P(pn+-) = (5/9)(1+k_1), \quad (172)$$

$$P(pn00) = (2/9)(1+k_1), \quad (173)$$

$$P(pp0-) = (1/9)C_+, \quad (174)$$

$$P(nn0+) = (1/9)C_-. \quad (175)$$

The sum of the above quantities P is

$$1+k_1 = [\sigma_{1,d}(N_2^*+N) + \sigma_{0,d}(N_2^*+N)]/\sigma_{1,d}(N_2^*+N). \quad (176)$$

Thus the branching ratios P must be multiplied by $\bar{\sigma} = \frac{1}{2}\sigma_{1,d}(N+N_2^*)$ in order to obtain the corresponding partial cross sections for pion production (see Table IV).

VII. GENERAL EQUATIONS FOR PION PRODUCTION IN NUCLEON-NUCLEON COLLISIONS

The energy spectra for the pions and nucleons from nucleon-nucleon collisions can be expressed in terms of certain basic spectra (such as $I_{\pi,s}$, $I_{\pi,d}$, $I_{\pi,i}^{(A)}$, $I_{N,i}^{(A)}$) which pertain to a pion or nucleon from a particular transition between definite isobaric states. These basic spectra are analogous to the spectra $I_{\pi,i}$ and $I_{N,i}^{(\pi)}$ pertaining to pion-nucleon interactions (Sec. II).

In this section, we will give the expressions for the

pion and nucleon energy spectra for all reactions arising from $p-p$ and $n-p$ collisions, which lead to production of one or two pions, using the processes (a), (b), (c), and (d) defined above in Sec. VI. The basic spectra are defined in the following manner. For the c.m. energy spectra from reactions (a) and (b) previously investigated in I, the notation is as follows:

$$N+N \rightarrow N(I_{N,2})+N_1^*, \quad (a1)$$

$$N_1^* \rightarrow N(I_{N,1})+\pi(I_{\pi,s}), \quad (a2)$$

$$N+N \rightarrow 2N_1^*, \quad (b1)$$

$$N_1^* \rightarrow N(I_{N,d})+\pi(I_{\pi,d}). \quad (b2)$$

Here and in the following, the expression in parentheses after N or π denotes the center-of-mass energy spectrum of the corresponding nucleon or pion. Thus $I_{N,2}$ pertains to the recoil nucleon from reaction (a), while $I_{N,1}$ and $I_{\pi,s}$ pertain to the decay nucleon and the decay pion involved in this single-pion production process. Similarly, $I_{N,d}$ and $I_{\pi,d}$ are the spectra of the decay nucleon and pion from N_1^* in the double-pion production reaction (b).

For the reaction (c), in which either one or two pions can be produced, we employ the following notation:

$$N+N \rightarrow N_2^*+N(I_{N,3}^A), \quad (c1)$$

$$N_2^* \rightarrow N(I_{N,4}^A)+\pi(I_{\pi,4}^A), \quad (c2)$$

$$N_2^* \rightarrow N_1^*+\pi(I_{\pi,5}^A), \quad (c3)$$

$$N_1^* \rightarrow N(I_{N,6}^A)+\pi(I_{\pi,6}^A). \quad (c4)$$

Thus, $I_{N,3}^A$ is the spectrum of the recoil nucleon from reaction (c). $I_{\pi,4}^A$ and $I_{N,4}^A$ pertain to the direct transition $N_2^* \rightarrow N+\pi$ which gives single-pion production. On the other hand, $I_{\pi,5}^A$, $I_{\pi,6}^A$, and $I_{N,6}^A$ correspond to the double-pion production via N_2^* . The superscript A is used here for $I_{\pi,4}^A$, $I_{\pi,5}^A$, and $I_{\pi,6}^A$, in order to distinguish these spectra from the pion spectra $I_{\pi,4}$, $I_{\pi,5}$, and $I_{\pi,6}$ previously defined in Sec. II, which pertain to pion-nucleon interactions. The same superscript A is also used for the nucleon spectra from reaction (c), for consistency of notation.

For the reaction (d), the notation is as follows:

$$N+N \rightarrow N_1^*+N_2^*, \quad (d1)$$

$$N_1^* \rightarrow N(I_{N,1}^B)+\pi(I_{\pi,1}^B), \quad (d2)$$

$$N_2^* \rightarrow N(I_{N,4}^B)+\pi(I_{\pi,4}^B), \quad (d3)$$

$$N_2^* \rightarrow N_1^*+\pi(I_{\pi,5}^B), \quad (d4)$$

$$N_1^* \rightarrow N(I_{N,6}^B)+\pi(I_{\pi,6}^B). \quad (d5)$$

$I_{N,1}^B$ and $I_{\pi,1}^B$ pertain to the decay of the isobar N_1^* which is formed in the primary reaction (d1). The other spectra: $I_{N,4}^B$, $I_{\pi,4}^B$, $I_{\pi,5}^B$, $I_{N,6}^B$, and $I_{\pi,6}^B$ are completely analogous to the corresponding spectra (with the same subscripts) from reaction (c). These five spectra pertain to the two modes of decay of the N_2^*

formed in the reaction (d). When N_2^* decays according to (d3), altogether two pions are produced, whereas the decays (d4)–(d5) correspond to production of a total of three pions in the reaction (d1).

We note that [with the exception of reaction (a2)], the same numerical subscript is used for the decay nucleon and the decay pion originating from a given isobar [e.g., $I_{N,4}^A$ and $I_{\pi,4}^A$ for reaction (c2)]. All of the pion and nucleon energy spectra I are assumed to be normalized to 1 [Cf. Eq. (102)].

For the sake of simplicity of the resulting expressions for the energy spectra, we will use the following notation, σ_i , for the various cross sections $\bar{\sigma}$ appearing in Tables III and IV:

$$\sigma_1 \equiv \sigma_1(N_1^*+N), \quad (177)$$

$$\sigma_2 \equiv \sigma_1(2N_1^*), \quad (178)$$

$$\sigma_3 \equiv \sigma_{1,s}(N_2^*+N), \quad (179)$$

$$\sigma_4 \equiv \sigma_{1,d}(N_2^*+N), \quad (180)$$

$$\sigma_5 \equiv \sigma_{1,d}(N_1^*+N_2^*), \quad (181)$$

$$\sigma_6 \equiv \sigma_{1,d}(2N_2^*). \quad (182)$$

In labeling the energy spectra $(d\sigma/d\bar{T}_N)$ and $(d\sigma/d\bar{T}_\pi)$, we will use a superscript (pj) or (nj) to denote the final state involved. Here, $(p1)$, $(p2)$, \dots $(p6)$ refer to the reactions from $p-p$ collisions, in the order in which they are listed in Table III. Thus $(p1)$ denotes the final state $(pn+)$, $(p2)$ denotes $(pp0)$, and $(p6)$ stands for $(nn++)$. Similarly, $(n1)$, $(n2)$, \dots $(n7)$ refer to the reactions from $n-p$ collisions, as given in Table IV. As an example, $(n4)$ represents the fourth reaction listed in Table IV, which gives rise to: $p+p+\pi^0+\pi^-$. This notation will be shown explicitly for each reaction below.

The derivation of the equations for the energy spectra is straightforward, and will not be given here. We note that the contribution to the final state considered from a particular basic reaction [(a), (b), (c), or (d)] is obtained from equations similar to Eqs. (167) and (168) which apply to the particular case: $n+p \rightarrow N_2^*+N \rightarrow 2N+2\pi$. In these equations, the nucleons represented by the wave functions ω_{Tz} and χ_{Tz} have energy spectra $I_{N,3}^A$ and $I_{N,6}^A$, respectively, while the pions represented by ν_{Tz} and μ_{Tz} have the spectra $I_{\pi,5}^A$ and $I_{\pi,6}^A$, respectively.

The following expressions for the spectra are normalized to $n_N\sigma$ or $n_\pi\sigma$, where σ is the total cross section for the reaction involved, and n_N , n_π are the numbers of nucleons or pions of the charge state considered which arise from the reaction. As an example, for the reaction (p3): $p+p \rightarrow p+p+\pi^++\pi^-$, the proton spectrum $(d\sigma/d\bar{T}_N)^{(p3)}(p)$ [Eq. (188)] is normalized to $2\sigma^{(p3)}$, whereas the π^+ and π^- spectra $(d\sigma/d\bar{T}_\pi)^{(p3)}(\pi^\pm)$ [Eqs. (189), (190)] are normalized to $\sigma^{(p3)}$. This normalization is the same as was used for the pion and nucleon spectra from $\pi^\pm-p$ collisions [Eqs. (35)–(48); (55)–(63)].

We will first give the results for the spectra from $p-p$ interactions. For the reaction

$$p+p \rightarrow p+n+\pi^+, \quad (p1)$$

we obtain

$$(d\sigma/d\bar{T}_N)^{(p1)}(p) = \frac{5}{6}\sigma_1(0.9I_{N,1} + 0.1I_{N,2}) + \frac{2}{3}\sigma_3I_{N,3}^A, \quad (183)$$

$$(d\sigma/d\bar{T}_N)^{(p1)}(n) = \frac{5}{6}\sigma_1(0.1I_{N,1} + 0.9I_{N,2}) + \frac{2}{3}\sigma_3I_{N,4}^A, \quad (184)$$

$$(d\sigma/d\bar{T}_\pi)^{(p1)}(\pi^+) = \frac{5}{6}\sigma_1I_{\pi,s} + \frac{2}{3}\sigma_3I_{\pi,4}^A, \quad (185)$$

where, as before (Sec. II), the parenthesis after $(d\sigma/d\bar{T})^{(p1)}$ indicates the particle considered (proton, neutron, or π^+). The cross sections σ_1 and σ_3 are defined by Eqs. (177) and (179).

For the reaction

$$p+p \rightarrow p+p+\pi^0, \quad (p2)$$

we find

$$(d\sigma/d\bar{T}_N)^{(p2)}(p) = \frac{1}{6}\sigma_1(I_{N,1} + I_{N,2}) + \frac{1}{3}\sigma_3(I_{N,3}^A + I_{N,4}^A), \quad (186)$$

$$(d\sigma/d\bar{T}_\pi)^{(p2)}(\pi^0) = \frac{1}{6}\sigma_1I_{\pi,s} + \frac{1}{3}\sigma_3I_{\pi,4}^A. \quad (187)$$

Similarly, for the reactions $p+p \rightarrow 2N+2\pi$, we obtain:

(1) For

$$p+p \rightarrow p+p+\pi^++\pi^-: \quad (p3)$$

$$(d\sigma/d\bar{T}_N)^{(p3)}(p) = \frac{2}{5}\sigma_2I_{N,d} + (5/9)\sigma_4(I_{N,3}^A + I_{N,6}^A) + \frac{1}{2}\sigma_5(I_{N,1}^B + I_{N,4}^B), \quad (188)$$

$$(d\sigma/d\bar{T}_\pi)^{(p3)}(\pi^+) = \frac{1}{5}\sigma_2I_{\pi,d} + (5/9)\sigma_4(0.1I_{\pi,5}^A + 0.9I_{\pi,6}^A) + \frac{1}{2}\sigma_5I_{\pi,1}^B, \quad (189)$$

$$(d\sigma/d\bar{T}_\pi)^{(p3)}(\pi^-) = \frac{1}{5}\sigma_2I_{\pi,d} + (5/9)\sigma_4(0.9I_{\pi,5}^A + 0.1I_{\pi,6}^A) + \frac{1}{2}\sigma_5I_{\pi,4}^B. \quad (190)$$

(2) For

$$p+p \rightarrow p+p+\pi^0+\pi^0: \quad (p4)$$

$$\left(\frac{d\sigma}{d\bar{T}_N}\right)^{(p4)}(p) = \frac{16}{45}\sigma_2I_{N,d} + \frac{2}{9}\sigma_4(I_{N,3}^A + I_{N,6}^A) + \frac{1}{18}\sigma_5(I_{N,1}^B + I_{N,4}^B), \quad (191)$$

$$\left(\frac{d\sigma}{d\bar{T}_\pi}\right)^{(p4)}(\pi^0) = \frac{16}{45}\sigma_2I_{\pi,d} + \frac{2}{9}\sigma_4(I_{\pi,5}^A + I_{\pi,6}^A) + \frac{1}{18}\sigma_5(I_{\pi,1}^B + I_{\pi,4}^B). \quad (192)$$

(3) For

$$p+p \rightarrow p+n+\pi^++\pi^0: \quad (p5)$$

$$\left(\frac{d\sigma}{d\bar{T}_N}\right)^{(p5)}(p) = \frac{26}{45}\sigma_2I_{N,d} + \frac{2}{9}\sigma_4I_{N,3}^A$$

$$+ \frac{13}{36}\sigma_5I_{N,1}^B + \frac{1}{36}\sigma_5I_{N,4}^B, \quad (193)$$

$$\left(\frac{d\sigma}{d\bar{T}_N}\right)^{(p5)}(n) = \frac{26}{45}\sigma_2I_{N,d} + \frac{2}{9}\sigma_4I_{N,6}^A$$

$$+ \frac{1}{36}\sigma_5I_{N,1}^B + \frac{13}{36}\sigma_5I_{N,4}^B, \quad (194)$$

$$\left(\frac{d\sigma}{d\bar{T}_\pi}\right)^{(p5)}(\pi^+) = \frac{26}{45}\sigma_2I_{\pi,d} + \frac{1}{9}\sigma_4(I_{\pi,5}^A + I_{\pi,6}^A)$$

$$+ \frac{5}{18}\sigma_5I_{\pi,1}^B + \frac{1}{9}\sigma_5I_{\pi,4}^B, \quad (195)$$

$$\left(\frac{d\sigma}{d\bar{T}_\pi}\right)^{(p5)}(\pi^0) = \frac{26}{45}\sigma_2I_{\pi,d} + \frac{1}{9}\sigma_4(I_{\pi,5}^A + I_{\pi,6}^A)$$

$$+ \frac{1}{9}\sigma_5I_{\pi,1}^B + \frac{5}{18}\sigma_5I_{\pi,4}^B. \quad (196)$$

(4) For

$$p+p \rightarrow n+n+\pi^++\pi^+: \quad (p6)$$

$$\left(\frac{d\sigma}{d\bar{T}_N}\right)^{(p6)}(n) = \frac{4}{45}\sigma_2I_{N,d} + \frac{1}{18}\sigma_5(I_{N,1}^B + I_{N,4}^B), \quad (197)$$

$$\left(\frac{d\sigma}{d\bar{T}_\pi}\right)^{(p6)}(\pi^+) = \frac{4}{45}\sigma_2I_{\pi,d} + \frac{1}{18}\sigma_5(I_{\pi,1}^B + I_{\pi,4}^B). \quad (198)$$

The combined proton spectrum from all $p-p$ reactions (p1-p6) is obtained by adding Eqs. (183), (186), (188), (191), and (193). The result is given by

$$\begin{aligned} \left(\frac{d\sigma}{d\bar{T}_N}\right)^{(p)}(p) = & \frac{11}{12}\sigma_1I_{N,1} + \frac{1}{4}\sigma_1I_{N,2} + \frac{4}{3}\sigma_2I_{N,d} \\ & + (\sigma_3 + \sigma_4)I_{N,3}^A + \frac{1}{3}\sigma_3I_{N,4}^A + \frac{7}{9}\sigma_4I_{N,6}^A \\ & + \frac{11}{12}\sigma_5I_{N,1}^B + \frac{7}{12}\sigma_5I_{N,4}^B. \end{aligned} \quad (199)$$

We note that the term corresponding to the recoil spectrum pertaining to the $T=\frac{1}{2}$ resonances (N_{2a}^* and N_{2b}^*) is $(\sigma_3 + \sigma_4)I_{N,3}^A$, so that the possibility of observing these resonances will depend on the value of $(\sigma_3 + \sigma_4)/\sigma_{\text{total}}^{(p)}(p)$, where $\sigma_{\text{total}}^{(p)}(p)$ is the cross section pertaining to the total outgoing proton flux,

which is given by

$$\begin{aligned}\sigma_{\text{total}}^{(p)}(p) &= \int_0^{\bar{T}_{p,m}} \left(\frac{d\sigma}{d\bar{T}_N} \right)^{(p)}(p) d\bar{T}_p \\ &= \frac{7}{6} \sigma_1 + \frac{4}{3} (\sigma_2 + \sigma_3) + \frac{16}{9} \sigma_4 + \frac{3}{2} \sigma_5.\end{aligned}\quad (200)$$

The total cross sections $\sigma^{(p,j)}$ for the reactions (p1)–(p6) will be given here for convenience. These cross sections can be obtained directly from Table III:

$$\sigma^{(p1)} = \frac{5}{6} \sigma_1 + \frac{2}{3} \sigma_3, \quad (201)$$

$$\sigma^{(p2)} = \frac{1}{6} \sigma_1 + \frac{1}{3} \sigma_3, \quad (202)$$

$$\sigma^{(p3)} = \frac{1}{5} \sigma_2 + (5/9) \sigma_4 + \frac{1}{2} \sigma_5, \quad (203)$$

$$\sigma^{(p4)} = (8/45) \sigma_2 + (2/9) \sigma_4 + (1/18) \sigma_5 + \frac{1}{9} \sigma_6, \quad (204)$$

$$\sigma^{(p5)} = (26/45) \sigma_2 + (2/9) \sigma_4 + (7/18) \sigma_5 + (4/9) \sigma_6, \quad (205)$$

$$\sigma^{(p6)} = (2/45) \sigma_2 + (1/18) \sigma_5 + (4/9) \sigma_6. \quad (206)$$

We note that the pion production via $2N_2^*$ (which is proportional to σ_6) has not been included in the expressions for the energy spectra [Eqs. (183)–(200)]. The effective threshold for the reaction $p+p \rightarrow 2N_2^*$ is $T_{p,\text{inc}} \sim 3.6$ Bev.

We will now give the corresponding expressions for the spectra from $n-p$ collisions. For the reactions $n+p \rightarrow 2N+\pi$, we obtain: (1) For the reaction

$$n+p \rightarrow p+p+\pi^-, \quad (n1)$$

the spectra of protons and π^- mesons are given by

$$\begin{aligned}(d\sigma/d\bar{T}_N)^{(n1)}(p) &= \frac{1}{12} \sigma_1 (I_{N,1} + I_{N,2}) \\ &\quad + \frac{1}{6} C_+ \sigma_3 (I_{N,3}^A + I_{N,4}^A),\end{aligned}\quad (207)$$

$$(d\sigma/d\bar{T}_\pi)^{(n1)}(\pi^-) = \frac{1}{12} \sigma_1 I_{\pi,s} + \frac{1}{6} C_+ \sigma_3 I_{\pi,4}^A, \quad (208)$$

where the constant C_+ is defined by Eq. (164). (2) For the reaction

$$n+p \rightarrow p+n+\pi^0, \quad (n2)$$

we find

$$\begin{aligned}(d\sigma/d\bar{T}_N)^{(n2)}(p) &= \frac{1}{6} \sigma_1 (I_{N,1} + I_{N,2}) \\ &\quad + \frac{1}{12} C_+ \sigma_3 I_{N,3}^A + \frac{1}{12} C_- \sigma_3 I_{N,4}^A,\end{aligned}\quad (209)$$

$$\begin{aligned}(d\sigma/d\bar{T}_N)^{(n2)}(n) &= \frac{1}{6} \sigma_1 (I_{N,1} + I_{N,2}) \\ &\quad + \frac{1}{12} C_- \sigma_3 I_{N,3}^A + \frac{1}{12} C_+ \sigma_3 I_{N,4}^A,\end{aligned}\quad (210)$$

$$(d\sigma/d\bar{T}_\pi)^{(n2)}(\pi^0) = \frac{1}{3} \sigma_1 I_{\pi,s} + \frac{1}{6} (1+k_1) \sigma_3 I_{\pi,4}^A. \quad (211)$$

(3) For

$$n+p \rightarrow n+n+\pi^+; \quad (n3)$$

$$\begin{aligned}(d\sigma/d\bar{T}_N)^{(n3)}(n) &= \frac{1}{12} \sigma_1 (I_{N,1} + I_{N,2}) \\ &\quad + \frac{1}{6} C_- \sigma_3 (I_{N,3}^A + I_{N,4}^A),\end{aligned}\quad (212)$$

$$(d\sigma/d\bar{T}_\pi)^{(n3)}(\pi^+) = \frac{1}{12} \sigma_1 I_{\pi,s} + \frac{1}{6} C_- \sigma_3 I_{\pi,4}^A. \quad (213)$$

For the reactions $n+p \rightarrow 2N+2\pi$, we find:

(1) For

$$n+p \rightarrow p+p+\pi^0+\pi^-, \quad (n4)$$

the spectra of protons, π^0 , and π^- mesons are given by

$$\left(\frac{d\sigma}{d\bar{T}_N} \right)^{(n4)}(p) = \left(\frac{1}{45} + \frac{1}{9} k_0 \right) \sigma_2 I_{N,d} + \frac{1}{18} C_+ \sigma_4 (I_{N,3}^A + I_{N,6}^A) + \frac{5}{36} \sigma_5 (I_{N,1}^B + I_{N,4}^B), \quad (214)$$

$$\left(\frac{d\sigma}{d\bar{T}_\pi} \right)^{(n4)}(\pi^0) = \left(\frac{1}{90} + \frac{1}{18} k_0 \right) \sigma_2 I_{\pi,d} + \frac{1}{36} C_+ \sigma_4 (I_{\pi,5}^A + I_{\pi,6}^A) + \frac{1}{9} \sigma_5 I_{\pi,1}^B + \frac{1}{36} \sigma_5 I_{\pi,4}^B, \quad (215)$$

$$\left(\frac{d\sigma}{d\bar{T}_\pi} \right)^{(n4)}(\pi^-) = \left(\frac{1}{90} + \frac{1}{18} k_0 \right) \sigma_2 I_{\pi,d} + \frac{1}{36} C_+ \sigma_4 (I_{\pi,5}^A + I_{\pi,6}^A) + \frac{1}{36} \sigma_5 I_{\pi,1}^B + \frac{1}{9} \sigma_5 I_{\pi,4}^B. \quad (216)$$

(2) For

$$n+p \rightarrow p+n+\pi^++\pi^-: \quad (n5)$$

$$\left(\frac{d\sigma}{d\bar{T}_N} \right)^{(n5)}(p) = \left(\frac{41}{90} + \frac{5}{18} k_0 \right) \sigma_2 I_{N,d} + \frac{5}{36} C_+ \sigma_4 I_{N,3}^A + \frac{5}{36} C_- \sigma_4 I_{N,6}^A + \frac{1}{18} \sigma_5 (I_{N,1}^B + I_{N,4}^B), \quad (217)$$

$$\left(\frac{d\sigma}{d\bar{T}_N} \right)^{(n5)}(n) = \left(\frac{41}{90} + \frac{5}{18} k_0 \right) \sigma_2 I_{N,d} + \frac{5}{36} C_- \sigma_4 I_{N,3}^A + \frac{5}{36} C_+ \sigma_4 I_{N,6}^A + \frac{1}{18} \sigma_5 (I_{N,1}^B + I_{N,4}^B), \quad (218)$$

$$\left(\frac{d\sigma}{d\bar{T}_\pi} \right)^{(n5)}(\pi^+) = \left(\frac{41}{90} + \frac{5}{18} k_0 \right) \sigma_2 I_{\pi,d} + \left(\frac{1}{8} C_+ + \frac{1}{72} C_- \right) \sigma_4 I_{\pi,5}^A + \left(\frac{1}{72} C_+ + \frac{1}{8} C_- \right) \sigma_4 I_{\pi,6}^A + \frac{1}{18} \sigma_5 (I_{\pi,1}^B + I_{\pi,4}^B), \quad (219)$$

$$\left(\frac{d\sigma}{d\bar{T}_\pi} \right)^{(n5)}(\pi^-) = \left(\frac{41}{90} + \frac{5}{18} k_0 \right) \sigma_2 I_{\pi,d} + \left(\frac{1}{72} C_+ + \frac{1}{8} C_- \right) \sigma_4 I_{\pi,5}^A + \left(\frac{1}{8} C_+ + \frac{1}{72} C_- \right) \sigma_4 I_{\pi,6}^A + \frac{1}{18} \sigma_5 (I_{\pi,1}^B + I_{\pi,4}^B). \quad (220)$$

(3) For

$$n + p \rightarrow p + n + \pi^0 + \pi^0; \quad (n6)$$

$$\left(\frac{d\sigma}{d\bar{T}_N}\right)^{(n6)}(p) = \left(\frac{1}{45} + \frac{1}{9}k_0\right)\sigma_2 I_{N,d} + \frac{1}{18}C_+ \sigma_4 I_{N,3^A} + \frac{1}{18}C_- \sigma_4 I_{N,6^A} + \frac{1}{18}\sigma_5(I_{N,1^B} + I_{N,4^B}), \quad (221)$$

$$\left(\frac{d\sigma}{d\bar{T}_N}\right)^{(n6)}(n) = \left(\frac{1}{45} + \frac{1}{9}k_0\right)\sigma_2 I_{N,d} + \frac{1}{18}C_- \sigma_4 I_{N,3^A} + \frac{1}{18}C_+ \sigma_4 I_{N,6^A} + \frac{1}{18}\sigma_5(I_{N,1^B} + I_{N,4^B}), \quad (222)$$

$$\left(\frac{d\sigma}{d\bar{T}_\pi}\right)^{(n6)}(\pi^0) = \left(\frac{2}{45} + \frac{2}{9}k_0\right)\sigma_2 I_{\pi,d} + \frac{1}{9}(1+k_1)\sigma_4(I_{\pi,5^A} + I_{\pi,6^A}) + \frac{1}{9}\sigma_5(I_{\pi,1^B} + I_{\pi,4^B}). \quad (223)$$

(4) For

$$n + p \rightarrow n + n + \pi^+ + \pi^0; \quad (n7)$$

$$\left(\frac{d\sigma}{d\bar{T}_N}\right)^{(n7)}(n) = \left(\frac{1}{45} + \frac{1}{9}k_0\right)\sigma_2 I_{N,d} + \frac{1}{18}C_- \sigma_4(I_{N,3^A} + I_{N,6^A}) + \frac{5}{36}\sigma_5(I_{N,1^B} + I_{N,4^B}), \quad (224)$$

$$\left(\frac{d\sigma}{d\bar{T}_\pi}\right)^{(n7)}(\pi^+) = \left(\frac{1}{90} + \frac{1}{18}k_0\right)\sigma_2 I_{\pi,d} + \frac{1}{36}C_- \sigma_4(I_{\pi,5^A} + I_{\pi,6^A}) + \frac{1}{36}\sigma_5(I_{\pi,1^B} + \frac{1}{9}\sigma_5 I_{\pi,4^B}), \quad (225)$$

$$\left(\frac{d\sigma}{d\bar{T}_\pi}\right)^{(n7)}(\pi^0) = \left(\frac{1}{90} + \frac{1}{18}k_0\right)\sigma_2 I_{\pi,d} + \frac{1}{36}C_- \sigma_4(I_{\pi,5^A} + I_{\pi,6^A}) + \frac{1}{9}\sigma_5(I_{\pi,1^B} + \frac{1}{36}\sigma_5 I_{\pi,4^B}). \quad (226)$$

From Eqs. (207), (209), (214), (217), and (221), one obtains for the combined proton spectrum from all $n-p$ reactions (n1-n7):

$$\begin{aligned} \left(\frac{d\sigma}{d\bar{T}_N}\right)^{(n)}(p) = & \frac{1}{4}\sigma_1(I_{N,1} + I_{N,2}) + \frac{1}{2}(1+k_0)\sigma_2 I_{N,d} + \frac{1}{4}C_+(\sigma_3 + \sigma_4)I_{N,3^A} + \left(\frac{1}{6}C_+ + \frac{1}{12}C_-\right)\sigma_3 I_{N,4^A} \\ & + \left(\frac{1}{18}C_+ + \frac{7}{36}C_-\right)\sigma_4 I_{N,6^A} + \frac{1}{4}\sigma_5(I_{N,1^B} + I_{N,4^B}). \end{aligned} \quad (227)$$

The partial cross section for the recoil spectrum pertaining to the $T=\frac{1}{2}$ resonances is $\frac{1}{4}C_+(\sigma_3 + \sigma_4)$. This result can be compared with the effective cross section $\sigma_{\text{total}}^{(n)}(p)$ pertaining to the total outgoing proton flux, which is given by

$$\sigma_{\text{total}}^{(n)}(p) = \frac{1}{2}\sigma_1 + \frac{1}{2}(1+k_0)\sigma_2 + \left(\frac{5}{12}C_+ + \frac{1}{12}C_-\right)\sigma_3 + \left(\frac{11}{36}C_+ + \frac{7}{36}C_-\right)\sigma_4 + \frac{1}{2}\sigma_5. \quad (228)$$

The total cross sections $\sigma^{(n)}$ for the reactions (n1)-(n7) are as follows (see Table IV):

$$\sigma^{(n1)} = \frac{1}{12}\sigma_1 + \frac{1}{6}C_+\sigma_3, \quad (229)$$

$$\sigma^{(n2)} = \frac{1}{3}\sigma_1 + \frac{1}{6}(1+k_1)\sigma_3, \quad (230)$$

$$\sigma^{(n3)} = \frac{1}{12}\sigma_1 + \frac{1}{6}C_-\sigma_3, \quad (231)$$

$$\begin{aligned} \sigma^{(n4)} = & \left(\frac{1}{90} + \frac{1}{18}k_0\right)\sigma_2 + \frac{1}{18}C_+\sigma_4 + \frac{5}{36} \\ & + \frac{1}{9}\sigma_6(1+k_2), \end{aligned} \quad (232)$$

$$\begin{aligned} \sigma^{(n5)} = & \left(\frac{41}{90} + \frac{5}{18}k_0\right)\sigma_2 + \frac{5}{18}(1+k_1)\sigma_4 \\ & + \frac{1}{9}\sigma_5 + \frac{2}{9}\sigma_6(1+k_2), \end{aligned} \quad (233)$$

$$\sigma^{(n6)} = \left(\frac{1}{45} + \frac{1}{9}k_0\right)\sigma_2 + \frac{1}{9}(1+k_1)\sigma_4$$

$$+ \frac{1}{9}\sigma_5 + \frac{1}{18}\sigma_6(1+k_2), \quad (234)$$

$$\sigma^{(n7)} = \left(\frac{1}{90} + \frac{1}{18}k_0\right)\sigma_2 + \frac{1}{18}C_-\sigma_4$$

$$+ \frac{5}{36}\sigma_5 + \frac{1}{9}\sigma_6(1+k_2), \quad (235)$$

where k_2 is defined by

$$k_2 \equiv \sigma_{0,d}(2N_2^*)/\sigma_{1,d}(2N_2^*). \quad (236)$$

VIII. CALCULATION OF THE PION AND NUCLEON SPECTRA FROM NUCLEON-NUCLEON INTERACTIONS

The center-of-mass energy spectra of the pions and nucleons from reactions (a) and (b) (see Sec. VI) have been previously obtained in I for incident nucleon energies $T_{N,\text{inc}}=0.8, 1.5, 2.3$, and 3.0 Bev . The effective threshold for reaction (c) is $\sim 1.6 \text{ Bev}$, while that for reaction (d) is $\sim 2.6 \text{ Bev}$. As explained in Sec. I, these threshold values were obtained by using isobar masses $m(N_1^*)=1.3 \text{ Bev}$ and $m(N_2^*)=1.6 \text{ Bev}$, which exceed by a small amount ($\sim 80 \text{ Mev}$) the masses pertaining to the maxima of the corresponding cross sections $\sigma_{\frac{1}{2}}$ and $\sigma_{\frac{3}{2}}$. In the present work, we have obtained the energy spectra for reaction (c) at $T_{N,\text{inc}}=2.3$ and 3.0 Bev , and for reaction (d) at 3.0 Bev .

We will first discuss the calculations for the reaction (c). The spectrum $I_{N,3}^A$ is obtained in the same manner as the spectrum $J_{\pi,3}$ for $\pi-N$ interactions [Eqs. (75)–(78)]. In fact, the equation for $I_{N,3}^A$ is completely similar to Eq. (75) for $J_{\pi,3}$. We have

$$I_{N,3}^A(\bar{T}_N) = K_3^A \sigma_{\frac{3}{2}}(m_2) (dm_2/d\bar{T}_N) F, \quad (237)$$

where K_3^A is a normalization factor, and F is the two-body phase space factor for N_2^*+N , for the total energy \bar{E} in the center-of-mass system. As compared to Eq. (75), a factor \bar{v}_N is missing, corresponding to the fact that $I_{N,3}^A$ gives the nucleon energy spectrum, while $J_{\pi,3}$ gives the momentum distribution of the recoil pions [see Eqs. (100), (101)].

In view of Eq. (237), the spectrum $I_{N,3}^A$ will essentially reproduce the $T=\frac{1}{2}$ cross section $\sigma_{\frac{3}{2}}(m_2)$ with the two maxima at $m_2=1.51$ and 1.68 Bev , provided that the incident energy is high enough so that both the N_{2a}^* and N_{2b}^* isobaric states can be excited. This is the case for $T_{N,\text{inc}} \gtrsim 2 \text{ Bev}$. Figures 17 and 18 show the various spectra at $T_{N,\text{inc}}=2.3$ and 3.0 Bev , respectively. The maxima of $I_{N,3}^A$ at $\bar{T}_N=120$ and 210 Mev for $T_{N,\text{inc}}=2.3 \text{ Bev}$, and at 260 and 340 Mev for $T_{N,\text{inc}}=3.0 \text{ Bev}$ correspond directly to the N_{2a}^* and N_{2b}^* isobars. It would obviously be of great interest to verify experimentally the presence of the two peaks in the spectrum $I_{N,3}^A$. However, the question as to whether the two maxima will be distinguishable from the background due to the other components ($I_{N,1}, I_{N,2}, I_{N,d}, I_{N,4}^A, I_{N,6}^A$) will depend on the value of the cross section $\sigma_1(N_2^*+N)$ in relation to $\sigma_1(N_1^*+N)$, $\sigma_1(2N_1^*)$, and $\sigma_1(N_1^*+N_2^*)$ for the case of $p-p$ collisions. Here, $\sigma_1(N_2^*+N)$ is the sum of $\sigma_{1,s}(N_2^*+N)$ and $\sigma_{1,d}(N_2^*+N)$ as used in Table III. [In the notation of Eqs. (177)–(182), we have: $\sigma_1(N_2^*+N)=\sigma_3+\sigma_4$.] In the case that all recoil protons are observed (as in a counter experiment), the spectrum is given by Eq. (199), and the relevant quantity which measures the relative strength of $I_{N,3}^A$ is the ratio $\sigma_1(N_2^*+N)/\sigma_{\text{total}}^{(p)}(p)$, where $\sigma_{\text{total}}^{(p)}(p)$ is given by Eq. (200).

In Figs. 17 and 18, it may be noted that near the

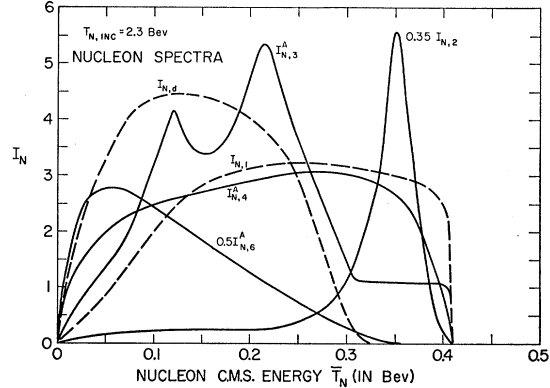


FIG. 17. Center-of-mass energy spectra of nucleons from nucleon-nucleon interactions at an incident nucleon energy $T_{N,\text{inc}}=2.3 \text{ Bev}$.

maximum nucleon energy $\bar{T}_{N,\text{max}}$, the spectrum $I_{N,3}^A$ is almost constant with energy (for $\bar{T}_N \approx 0.32$ – 0.41 Bev at $T_{N,\text{inc}}=2.3 \text{ Bev}$, and for $\bar{T}_N \approx 0.45$ – 0.53 Bev at 3.0 Bev). This part of the energy distribution $I_{N,3}^A$ corresponds to the formation of isobars N_2^* with low mass values m_I in the range from 1.08 to $\sim 1.30 \text{ Bev}$, which pertain to the low-energy $T=\frac{1}{2}$ cross section $\sigma_{\frac{3}{2}}$. As has been extensively discussed in Sec. III, the low-energy $\sigma_{\frac{3}{2}}$ is approximately energy-independent ($\sim 7 \text{ mb}$), which accounts for the fact that $I_{N,3}^A$ is nearly constant at the high-energy end of the spectrum. We note that the phase space factor F which also enters into Eq. (237) increases only very slightly with increasing nucleon energy \bar{T}_N in this region. The high-energy part of $I_{N,3}^A$ is essentially analogous to the high-energy maximum of the recoil pion spectrum $J_{\pi,3}$ for $\pi-N$ interactions (see Figs. 2–4). From Figs. 17 and 18, it is seen that the high-energy region of constant $I_{N,3}^A$ becomes relatively less important with increasing incident energy $T_{N,\text{inc}}$, in similarity to the corresponding behavior of the maxima of $J_{\pi,3}$.

The spectrum $I_{N,3}^A$ can be compared with $I_{N,2}$,

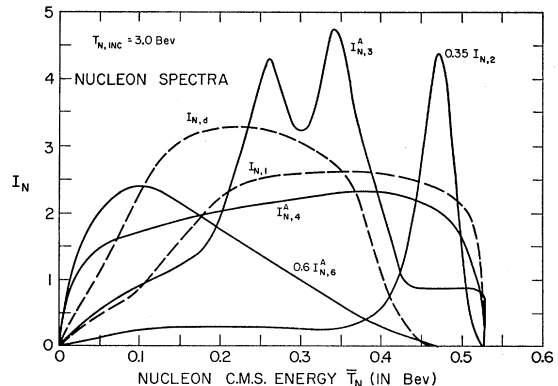


FIG. 18. Center-of-mass energy spectra of nucleons from nucleon-nucleon interactions at an incident nucleon energy $T_{N,\text{inc}}=3.0 \text{ Bev}$.

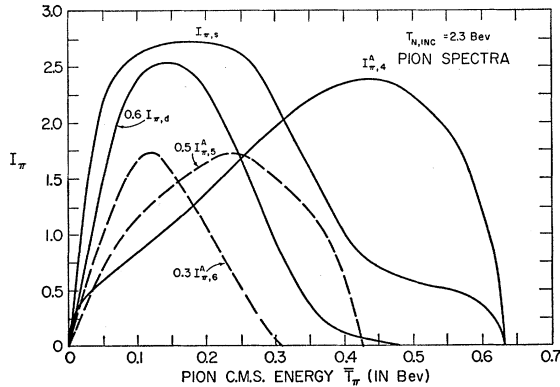


FIG. 19. Center-of-mass energy spectra of pions from nucleon-nucleon interactions at an incident nucleon energy $T_{N,\text{inc}}=2.3$ Bev.

which pertains to the recoil nucleons from reaction (a). Figures 17 and 18 show the spectra $I_{N,2}$ for $T_{N,\text{inc}}=2.3$ and 3.0 Bev. The maximum of $I_{N,2}$ is at $\bar{T}_N=350$ Mev for 2.3 Bev, and 470 Mev for 3.0 Bev. These maxima are at higher energies than those of $I_{N,3}^A$, corresponding to the lower mass of the N_1^* isobar ($m_I=1.23$ Bev).

The nuclear spectra $I_{N,1}$ and $I_{N,2}$ have been previously obtained in I. However, these nucleon spectra, and also the pion spectrum $I_{\pi,s}$, were recalculated in the present work for each energy (2.3 and 3.0 Bev), using a slightly different procedure than that employed in I. The modification consists in including all kinematically possible isobar mass values m_I up to the maximum, $m_{I,\text{max}}=\bar{E}-m_N$, instead of using a cutoff at $M_b=m_N+m_\pi+0.5$ Bev=1.578 Bev for the maximum isobar mass, as was done in I. The present procedure concerning $m_{I,\text{max}}$ for $I_{N,1}$, $I_{N,2}$, and $I_{\pi,s}$ is the same as was used in the present work for the pion spectra $J_{\pi,1}$ and $J_{\pi,2}$ from $\pi-N$ interactions [see the discussion after Eq. (90)]. We note that the present spectrum $I_{N,2}$ extends to zero energy, $\bar{T}_N=0$, (see Figs. 17 and 18), whereas in the calculation of I, $I_{N,2}$ was zero below $\bar{T}_N \sim 175$ Mev for $T_{N,\text{inc}}=2.3$ Bev, as a result of the use of the cutoff M_b (see Fig. 8 of I). However, as is shown by Fig. 17, the present revised $I_{N,2}$ is quite small below ~ 200 Mev, as a result of the smallness of the $\pi^+ + p$ cross section $\sigma_{\frac{1}{2}}$ in the appropriate energy range ($T_\pi=700-1200$ Mev), relative to its maximum at 180 Mev.

We note that the nucleon spectra $I_{N,d}$ and the pion spectra $I_{\pi,d}$ from reaction (b) were not recalculated with the higher value of $m_{I,\text{max}}=\bar{E}-m_N-m_\pi$. It is believed that since these spectra pertain to the formation of two isobars: $N+N \rightarrow 2N_1^*$, the region of isobar masses between $M_b=1.58$ Bev and the kinematic maximum $m_{I,\text{max}}$ will be less important. This value of $m_{I,\text{max}}$ is smaller by one pion mass (m_π) than the value of $m_{I,\text{max}}$ for $N+N \rightarrow N_1^*+N$. Thus $m_{I,\text{max}}$ for $N+N \rightarrow 2N_1^*$ equals 1.721 Bev for $T_{N,\text{inc}}=2.3$ Bev, and 1.946 Bev for $T_{N,\text{inc}}=3.0$ Bev.

The spectrum $I_{N,4}^A$ of the decay nucleons from $N_2^* \rightarrow N+\pi$ is obtained in the same manner as the spectrum $I_{\pi,4}$ for $\pi-N$ collisions [see Eqs. (79)-(81)]. As is expected from the large mass difference of N_2^* and N , the maximum of $I_{N,4}^A$ occurs at relatively high c.m. energies ($\bar{T}_N^M=270$ Mev at 2.3 Bev, $\bar{T}_N^M=375$ Mev at 3.0 Bev).

The spectrum $I_{N,6}^A$ pertains to the nucleon from the double transition, Eq. (9b). The corresponding spectra for the two emitted pions are denoted by $I_{\pi,5}^A$ and $I_{\pi,6}^A$. In order to simplify the calculation of these spectra, we have assumed that the N_1^* is produced with a single mass, $m_I=1.225$ Bev, corresponding to the center of the $T=\frac{3}{2}$ resonance ($T_\pi=180$ Mev). It is expected that no appreciable error is introduced by this procedure, since the maximum isobar mass $m_{I,\text{max}}$ is 1.861 Bev at $T_{N,\text{inc}}=2.3$ Bev, and 2.086 Bev at 3.0 Bev, so that we are considerably above threshold for the two-pion decay of N_2^* at both energies. The situation is thus similar to that for 2.0-Bev incident pions ($m_{I,\text{max}}=2.077$ Bev), where we have also used a single mass m_I for N_1^* (see discussion of Fig. 4 in Sec. III). As expected because of the small mass difference $m_I-(m_N+m_\pi)=147$ Mev, the maximum of the $I_{N,6}^A$ distributions occurs at a low c.m. energy ($\bar{T}_N^M=60$ Mev at 2.3 Bev, and 100 Mev at 3.0 Bev). However, these spectra have a long high-energy tail (extending up to $\bar{T}_N=470$ Mev for $T_{N,\text{inc}}=3.0$ Bev), presumably because of the effect of the relatively large maximum kinetic energy of N_1^* in the c.m. system. In connection with the two-pion decay of N_2^* , we note that the average of the probability $\epsilon(m_2)$ as obtained from Eq. (85) is: $\langle \epsilon(m_2) \rangle=0.239$ at $T_{N,\text{inc}}=2.3$ Bev, and 0.273 at 3.0 Bev.

The pion spectra from nucleon-nucleon collisions are shown in Figs. 19 and 20 for $T_{N,\text{inc}}=2.3$ and 3.0 Bev, respectively. The spectra $I_{\pi,s}$ and $I_{\pi,d}$ pertain to the N_1^* processes (a) and (b), and have been previously obtained in I. As mentioned above, the spectrum $I_{\pi,s}$ (pions from the decay $N_1^* \rightarrow N+\pi$) has been recalculated in the present work, using the kinematic upper limit $m_{I,\text{max}}=\bar{E}-m_N$ for the range of isobar masses m_I , instead of the cutoff $M_b=1.578$ Bev employed in I. Figures 19 and 20 show that the resulting spectra $I_{\pi,s}$ have an appreciable high-energy tail, especially at 3.0 Bev, which was not present in the previous work (see Fig. 3). This tail arises directly from the decay of isobars with large mass values m_I between ~ 1.5 Bev and $m_{I,\text{max}}$ ($m_{I,\text{max}}=1.861$ Bev at 2.3 Bev, and 2.086 Bev at 3.0 Bev). It would be of interest to verify experimentally whether this high-energy tail for the single-pion production via N_1^* is indeed present. However, an experimental check is made difficult by the probable presence of the reaction $p+p \rightarrow N_2^*+N$, which tends to give predominantly high-energy pions (spectrum $I_{\pi,4}^A$). Perhaps use could be made of the somewhat different branching ratios in order to establish the relative magnitude of $\sigma_1(N_1^*+N)$ and $\sigma_{1,s}(N_2^*+N)$. Thus the ratio of the ($p+n$) to ($p+p$) final states in

$p-p$ collisions is 5/1 for the reaction via N_1^*+N and 2/1 for N_2^*+N (see Table III).

The spectrum $I_{\pi,4}^A$ pertains to the decay $N_2^* \rightarrow N+\pi$. This spectrum is obtained in the same manner as $I_{N,4}^A$ (for $N-N$ collisions) or $J_{\pi,4}$ for $\pi-N$ interactions [Eqs. (79)-(81)]. As expected from the large mass difference of N_2^* and N , the maximum of $I_{\pi,4}^A$ occurs at a relatively large energy in the c.m. system ($\bar{T}_\pi^M = 440$ Mev at 2.3 Bev, $\bar{T}_\pi^M = 520$ Mev at 3.0 Bev).

Concerning the spectra $I_{\pi,5}^A$ and $I_{\pi,6}^A$ pertaining to the two-pion decay of N_2^* , we note that in order to simplify the calculations, the assumption was made (as for $I_{N,6}^A$) that the N_1^* has a single mass $m_1=1.225$ Bev, corresponding to the center of the $T=\frac{3}{2}$ resonance. This assumption does not introduce any significant inaccuracies for $I_{\pi,5}^A$, but for $I_{\pi,6}^A$ (decay pions from $N_1^* \rightarrow N+\pi$), it was found that the spectrum would be zero for $\bar{T}_\pi \lesssim 30$ Mev, which is directly attributable to the use of a single mass value m_1 for N_1^* . Actually the pions of very small energies ($0 < \bar{T}_\pi \lesssim 50$ Mev) will arise mainly from N_1^* isobars having low mass values, in the range $1.078 < m_1 \lesssim 1.15$ Bev, where 1.078 Bev = m_N+m_π . Since these isobars are produced in the actual decay of N_2^* (although with relatively small probability), we have modified the spectrum $I_{\pi,6}^A$ between $\bar{T}_\pi=0$ and the energy of the maximum of $I_{\pi,6}^A$ ($\bar{T}_\pi^M=120$ Mev), so as to obtain a non-zero intensity in this region. This modification amounts to only 5–10% of the total area under the $I_{\pi,6}^A$ spectrum. For the other spectra from the two-pion decay of N_2^* , $I_{\pi,5}^A$ and $I_{N,6}^A$, no modification was made. As expected because of the small difference $m_1 - (m_N+m_\pi) = 147$ Mev, the maximum of $I_{\pi,6}^A$ occurs at a low c.m. energy ($\bar{T}_\pi^M \sim 120$ Mev). The maximum pion energy $\bar{T}_{\pi,m}$ is 310 Mev for $T_{N,\text{inc}}=2.3$ Bev, and 370 Mev for 3.0 Bev. The spectrum $I_{\pi,5}^A$ occupies an intermediate energy region between $I_{\pi,4}^A$ and $I_{\pi,6}^A$.

In order to obtain the spectra pertaining to reaction (d) at 3.0 Bev: $N+N \rightarrow N_1^*+N_2^*$, we have again made the simplifying assumption of replacing the mass distribution of N_1^* by a single mass value $m_1=1.225$ Bev. This assumption is made, in particular, for the isobar N_1^* produced in the primary reaction (d1). The resulting spectra will necessarily be somewhat less accurate than those obtained above for reactions (a)–(c), but it is believed that at least the qualitative features will be obtained correctly. Since the wide mass distribution of N_2^* was correctly taken into account, and in view of the smearing-out effect of the motion of the decay nucleon and pion in the N_1^* and N_2^* rest systems, it is believed that no large errors are introduced by the use of a single mass value for N_1^* , both in the primary reaction and for the N_1^* involved in the two-pion decay of N_2^* .

The calculation of the decay spectra $I_{N,1}^B$ and $I_{\pi,1}^B$ is similar to that of $I_{N,4}^A$ and $I_{\pi,4}^A$ for $N-N$ collisions, or $J_{\pi,4}$ for $\pi-N$ collisions. Thus, for each mass m_2 of the N_2^* isobar, there is a single velocity \bar{v}_1 of N_1^* , and

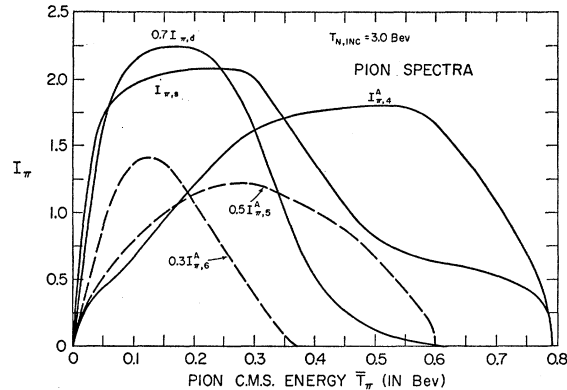


FIG. 20. Center-of-mass energy spectra of pions from nucleon-nucleon interactions at an incident nucleon energy $T_{N,\text{inc}}=3.0$ Bev.

hence a step-function distribution for the energy spectrum of either the decay nucleon or the decay pion from N_1^* . The complete spectrum $I_{N,1}^B$ or $I_{\pi,1}^B$ is obtained by adding all such step functions pertaining to different m_{2j} with the appropriate weighting factors $\sigma_{\frac{1}{2}}(m_{2j})F_j$. The calculation of the spectra $I_{N,4}^B$, $I_{\pi,4}^B$, $I_{\pi,5}^B$, $I_{N,6}^B$, and $I_{\pi,6}^B$ is completely analogous to that of the corresponding spectra $I_{N,4}^A$, $I_{\pi,4}^A$, ..., $I_{\pi,6}^A$ for reaction (c), except that in the kinematics the mass of the recoil nucleon is replaced by the mass of the N_1^* isobar, $m_1=1.225$ Bev.

The resulting spectra for reaction (d) at 3.0 Bev are quite similar to those for reaction (c) at 2.3 Bev. The spectra for reaction (d) are not shown in this paper, but we will give the following characteristics. For each spectrum, we list the energy \bar{T}_π^M or \bar{T}_N^M at which the distribution has its maximum intensity, and also the maximum energy of the pion or nucleon, $\bar{T}_{\pi,m}$ or $\bar{T}_{N,m}$ (above which $I=0$). For the pion spectra, one finds: for $I_{\pi,1}^B$: $\bar{T}_\pi^M=125$ Mev; $\bar{T}_{\pi,m}=370$ Mev; for $I_{\pi,4}^B$: 420 and 600 Mev; for $I_{\pi,5}^B$: 230 and 380 Mev; for $I_{\pi,6}^B$: 125 and 310 Mev. For the nucleon spectra, one obtains: for $I_{N,1}^B$: $\bar{T}_N^M=100$ Mev, $\bar{T}_{N,m}=470$ Mev; for $I_{N,4}^B$: 270 and 410 Mev; for $I_{N,6}^B$: 65 and 345 Mev.

By comparing these results with Figs. 17 and 19, it may be noted that with the exception of $I_{\pi,1}^B$ and $I_{N,1}^B$ which have no equivalent for reaction (c), the other (d) reaction spectra have closely the same characteristics (\bar{T}_π^M , $\bar{T}_{\pi,m}$, \bar{T}_N^M , $\bar{T}_{N,m}$) as the corresponding spectra for reaction (c) at 2.3 Bev; e.g., for $I_{\pi,4}^A$ at 2.3 Bev: $\bar{T}_\pi^M=440$ Mev, $\bar{T}_{\pi,m}=630$ Mev, as compared to 420 and 600 Mev for $I_{\pi,4}^B$ at 3.0 Bev. Presumably, the extra energy ΔE in the center-of-mass system which results from the increase of $T_{N,\text{inc}}$ from 2.3 to 3.0 Bev ($\Delta E=225$ Mev) is essentially used in producing the N_1^* isobar (as compared to a recoil nucleon), so that the spectra resulting from the decay of N_2^* are generally similar for reaction (c) at 2.3 Bev and reaction (d) at 3.0 Bev.

IX. PION PRODUCTION IN ANTINUCLEON-NUCLEON INTERACTIONS

For the processes of pion production in antinucleon-nucleon collisions which do not result in annihilation, we may assume that one or two anti-isobars \bar{N}_α^* ($\alpha=1$ or 2) are formed, with subsequent decay of \bar{N}_α^* into an antinucleon \bar{N} and one or several pions. \bar{N}_α^* is defined as the antiparticle of the isobar N_α^* . From charge conjugation invariance, the basic energy spectra, Q -value distributions, and angular correlations will be the same as for pion production in nucleon-nucleon collisions (for the same incident energy). The exact prescription for treating these interactions can be obtained from the formulas developed in I and in the present paper. One should note here that the fact that the isobar model seems to work rather well for nucleon-nucleon meson-producing interactions does not necessarily imply that it will work equally well for antinucleon-nucleon nonannihilation meson-producing interactions. These interactions are basically very different in one important respect.

Since the isobar lifetime is not much larger than the range of interaction, there are possible corrections in the nucleon-nucleon case due to the interaction between the various final-state particles including the nucleon-nucleon pair. However, the agreement of the experiments with the basic predictions of the model in the nucleon-nucleon case implies that these corrections are not very important.

However, in the antinucleon-nucleon case, the strong annihilation interaction may have a more important effect. Furthermore, the availability of the 1.88-Bev annihilation energy may enhance virtual off-the-energy shell processes which are neglected in the present isobar model.

Nevertheless, one can hope that the present model will still describe the dominant features, since the non-annihilation meson-producing interactions are probably due to peripheral collisions for which the $\bar{N}-N$ interaction is expected to be considerably less strong than for close collisions.

We will first consider $\bar{p}-p$ interactions, and we will assume that the incident antiproton energy is sufficiently low ($T_{\bar{p}} \lesssim 1.5$ Bev), so that only the isobaric states N_1^* and \bar{N}_1^* need to be considered. According to the present model, two single-pion production reactions are possible:

$$\bar{p} + p \rightarrow N_1^* + \bar{N}, \quad (238)$$

$$\bar{p} + p \rightarrow \bar{N}_1^* + N. \quad (239)$$

These two reactions have equal cross sections, from charge conjugation invariance. We note that although the initial state $\bar{p}+p$ consists of an equal mixture of $T=1$ and $T=0$ states, only the $T=1$ part contributes to the reactions (238) and (239), as a result of the isotopic spin $T=\frac{3}{2}$ of N_1^* and \bar{N}_1^* .

The final state wave function $\Psi_{\bar{p}-p}^{(1)}$ can be written

as follows:

$$\Psi_{\bar{p}-p}^{(1)} = -\frac{1}{2}\psi_{-\frac{1}{2}}\bar{\eta}_{\frac{1}{2}} + \frac{1}{2}\psi_{\frac{1}{2}}\bar{\eta}_{-\frac{1}{2}} - \frac{1}{2}\bar{\psi}_{-\frac{1}{2}}\eta_{\frac{1}{2}} + \frac{1}{2}\bar{\psi}_{\frac{1}{2}}\eta_{-\frac{1}{2}}, \quad (240)$$

where ψ_{Tz} and $\bar{\eta}_{Tz}$ are the wave functions of N_1^* and \bar{N} , respectively, from (238), while $\bar{\psi}_{Tz}$ and η_{Tz} are the wave functions of \bar{N}_1^* and N , respectively, from (239).

From Eqs. (24) and (25), it is seen that the states $\psi_{\frac{1}{2}}$ and $\psi_{-\frac{1}{2}}$ are equivalent to

$$\psi_{\frac{1}{2}} = \frac{2}{3}(p0) + \frac{1}{3}(n+), \quad (241)$$

$$\psi_{-\frac{1}{2}} = \frac{1}{3}(p-) + \frac{2}{3}(n0). \quad (242)$$

Similarly, $\bar{\psi}_{\frac{1}{2}}$ and $\bar{\psi}_{-\frac{1}{2}}$ lead to

$$\bar{\psi}_{\frac{1}{2}} = \frac{2}{3}(\bar{n}0) + \frac{1}{3}(\bar{p}+), \quad (243)$$

$$\bar{\psi}_{-\frac{1}{2}} = \frac{1}{3}(\bar{n}-) + \frac{2}{3}(\bar{p}0). \quad (244)$$

From Eqs. (240)–(244), the probability density $|\Psi_{\bar{p}-p}^{(1)}|^2$ is given by

$$|\Psi_{\bar{p}-p}^{(1)}|^2 = \frac{1}{12}(\bar{n}_r p_d -) + \frac{1}{6}(\bar{n}_r n_d 0) + \frac{1}{6}(\bar{p}_r p_d 0) + \frac{1}{12}(\bar{p}_r n_d +) + \frac{1}{12}(\bar{n}_d p_r -) + \frac{1}{6}(\bar{p}_d p_r 0) + \frac{1}{6}(\bar{n}_d n_r 0) + \frac{1}{12}(\bar{p}_d n_r +), \quad (245)$$

where the subscript d or r indicates whether the N (or \bar{N}) arises from the decay of N_1^* (or \bar{N}_1^*), or whether it is a recoil particle.

In view of Eq. (245), the relative intensities of the four possible final states are as follows:

$$I(\bar{p}p0) = \frac{1}{6}(\bar{p}_r p_d 0) + \frac{1}{6}(\bar{p}_d p_r 0), \quad (246)$$

$$I(\bar{n}n0) = \frac{1}{6}(\bar{n}_r n_d 0) + \frac{1}{6}(\bar{n}_d n_r 0), \quad (247)$$

$$I(\bar{n}p-) = \frac{1}{12}(\bar{n}_r p_d -) + \frac{1}{12}(\bar{n}_d p_r -), \quad (248)$$

$$I(\bar{p}n+) = \frac{1}{12}(\bar{p}_r n_d +) + \frac{1}{12}(\bar{p}_d n_r +). \quad (249)$$

The branching ratios for the various final states are as follows: $P(\bar{p}p0) = P(\bar{n}n0) = \frac{1}{3}$; $P(\bar{n}p-) = P(\bar{p}n+) = \frac{1}{6}$. The corresponding total cross sections for the four reactions are given by: $\sigma_1(\bar{N}_1^* + N)P$, where $\sigma_1(\bar{N}_1^* + N)$ is the cross section for the reaction $\bar{N} + N \rightarrow \bar{N}_1^* + N$ in the isotopic spin $T=1$ state. We note that this result includes two compensating factors of $\frac{1}{2}$ and 2: the factor $\frac{1}{2}$ arises from the probability $\frac{1}{2}$ that the initial $\bar{p}+p$ system be in the $T=1$ state; the factor 2 takes into account the equal contribution of the reaction $\bar{N} + N \rightarrow N_1^* + \bar{N}$ [see Eqs. (238) and (239)]. As an example, for the reaction $\bar{p}+p \rightarrow \bar{p}+p+\pi^0$, we have $\sigma = \frac{1}{3}\sigma_1(\bar{N}_1^* + N)$.

We note that the branching ratios P lead to the following relations between the cross sections for the 4 possible final states:

$$\sigma(\bar{p}p0) : \sigma(\bar{n}n0) : \sigma(\bar{n}p-) : \sigma(\bar{p}n+) = 2:2:1:1. \quad (250)$$

The final state $(\bar{n}n0)$ would be very difficult to identify. However, the other three reactions are probably measurable with reasonable accuracy. It would thus be possible to check experimentally the predictions of Eq. (250). We note that the basic cross section $\sigma_1(\bar{N}_1^* + N)$

can be obtained from the observed value of any one of the 4 cross sections of Eq. (250).

Equations (246)–(249) show that for each final state, both N and \bar{N} have equal probabilities of being the decay or the recoil particle. Thus, in terms of the functions $I_{N,1}$ and $I_{N,2}$ of I, the normalized center-of-mass energy spectrum is given by

$$I(N) = I(\bar{N}) = \frac{1}{2}(I_{N,1} + I_{N,2}). \quad (251)$$

$I_{N,1}$ pertains to the decay nucleon from the N_1^* isobar, while $I_{N,2}$ is the recoil spectrum. The pion spectrum is given by $I_{\pi,s}$ (see Fig. 3 of I).

The Q -value distribution for (π, N) and (π, \bar{N}) pairs is given by

$$P[Q(\pi, N)] = P[Q(\pi, \bar{N})] = \frac{1}{2}(\bar{P}_1 + \bar{P}_2), \quad (252)$$

where \bar{P}_1 is the Q -value distribution for the decay pion and the decay nucleon (or \bar{N}) originating from the same isobar N_1^* (or \bar{N}_1^*); \bar{P}_2 is the Q -value distribution for the recoil nucleon (or \bar{N}) and the pion from the decay of N_1^* or \bar{N}_1^* . The distributions \bar{P}_1 and \bar{P}_2 have been previously calculated in I [Eqs. (95) and (98)].

The distribution of the c.m. angles between π and N , or between π and \bar{N} , is given by

$$C(\pi, N) = C(\pi, \bar{N}) = \frac{1}{2}(\bar{C}_1 + \bar{C}_2), \quad (253)$$

where \bar{C}_1 and \bar{C}_2 are the angular correlation functions for the pion-nucleon pairs pertaining to \bar{P}_1 and \bar{P}_2 , respectively. \bar{C}_1 and \bar{C}_2 have been previously obtained in I (Sec. VII).

We have calculated the normalized nucleon spectra $I_{N,1}$ and $I_{N,2}$ for $T_{N,\text{inc}}=1.0$ Bev. These spectra are shown in Fig. 21, together with the spectrum $\frac{1}{2}(I_{N,1}+I_{N,2})$ of Eq. (251). We have also obtained the Q -value distributions \bar{P}_1 and \bar{P}_2 for $T_{N,\text{inc}}=1.0$ Bev. The functions \bar{P}_1 and \bar{P}_2 , together with $\frac{1}{2}(\bar{P}_1+\bar{P}_2)$ are shown in Fig. 22. We note that the spectra $I_{N,1}$ and $I_{N,2}$ (but not \bar{P}_1 and \bar{P}_2) have been previously obtained in I for $T_{N,\text{inc}}=1.0$ Bev (see Fig. 7 of I). We have neverthe-

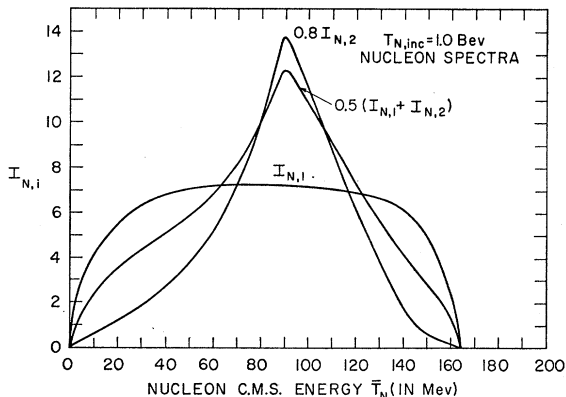


FIG. 21. Center-of-mass energy spectra of nucleons from nucleon-nucleon interactions at an incident nucleon energy $T_{N,\text{inc}}=1.0$ Bev.

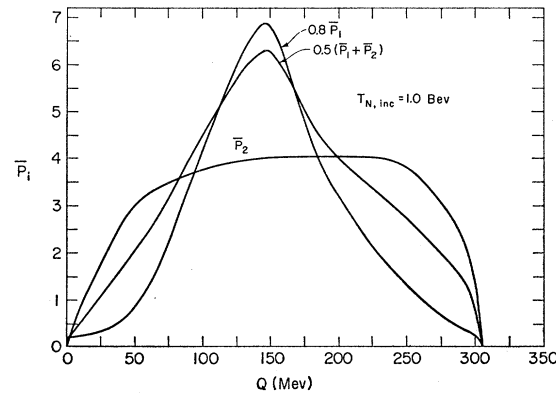


FIG. 22. Q value distribution functions \bar{P}_1 and \bar{P}_2 for pion-nucleon pairs from single pion production in nucleon-nucleon collisions at $T_{N,\text{inc}}=1.0$ Bev.

less included these spectra in Fig. 21, since we wanted also to show the function $\frac{1}{2}(I_{N,1}+I_{N,2})$, which is the predicted energy distribution $I(N)$ or $I(\bar{N})$ for all of the single-pion production reactions from $\bar{p}-p$ collisions. The pion spectrum $I_{\pi,s}$ for $T_{N,\text{inc}}=1.0$ Bev is shown in Fig. 3 of I. The functions $I_{N,i}$ and \bar{P}_i of Figs. 21 and 22 are normalized to 1, if \bar{T}_N and Q are in Bev.

It would obviously be of interest to verify experimentally the present results for the nucleon, antinucleon, and pion spectra, as well as for the Q -value distributions and angular correlations for $\pi-N$ and $\pi-\bar{N}$ pairs. We note that Eqs. (250)–(253) contain no adjustable constants. This result follows from the fact that only one isotopic spin state ($T=1$) is involved for the single-pion production reactions for $\bar{p}-p$ collisions.

We will now discuss the production of two pions by the reaction

$$\bar{p}+p \rightarrow N_1^* + \bar{N}_1^* \rightarrow \bar{N} + N + 2\pi. \quad (254)$$

For this case, both the $T=1$ and $T=0$ states contribute, in the same manner as for $n-p$ interactions. The final state wave functions for $T=1$ and $T=0$ are given by [see Eqs. (60) and (61) of I]:

$$\Psi_{\bar{p}-p}^{(2)}(T=1) = (9/20)^{\frac{1}{2}}\psi_{\frac{1}{2}}\bar{\psi}_{-\frac{1}{2}} - (1/20)^{\frac{1}{2}}\psi_{\frac{1}{2}}\bar{\psi}_{-\frac{1}{2}} - (1/20)^{\frac{1}{2}}\psi_{-\frac{1}{2}}\bar{\psi}_{\frac{1}{2}} + (9/20)^{\frac{1}{2}}\psi_{-\frac{1}{2}}\bar{\psi}_{\frac{1}{2}}, \quad (255)$$

$$\Psi_{\bar{p}-p}^{(2)}(T=0) = -\frac{1}{2}\psi_{\frac{1}{2}}\bar{\psi}_{-\frac{1}{2}} + \frac{1}{2}\psi_{\frac{1}{2}}\bar{\psi}_{-\frac{1}{2}} - \frac{1}{2}\psi_{-\frac{1}{2}}\bar{\psi}_{\frac{1}{2}} + \frac{1}{2}\psi_{-\frac{1}{2}}\bar{\psi}_{\frac{1}{2}}. \quad (256)$$

The probabilities of the various final states are obtained from the expression for $|\Psi_{\bar{p}-p}^{(\text{final})}|^2$:

$$|\Psi_{\bar{p}-p}^{(\text{final})}|^2 = |\Psi_{\bar{p}-p}^{(2)}(T=1) + \rho^{\frac{1}{2}}e^{i\varphi}\Psi_{\bar{p}-p}^{(2)}(T=0)|^2, \quad (257)$$

where ρ is defined by

$$\rho \equiv \sigma_0(N_1^* + \bar{N}_1^*)/\sigma_1(N_1^* + \bar{N}_1^*). \quad (258)$$

Here $\sigma_0(N_1^* + \bar{N}_1^*)$ and $\sigma_1(N_1^* + \bar{N}_1^*)$ are the cross sections for the reaction $\bar{N} + N \rightarrow N_1^* + \bar{N}_1^*$ in the states with total isotopic spin $T=0$ and $T=1$, respec-

tively; φ is the phase angle between the matrix elements for the $T=0$ and $T=1$ states. One obtains

$$|\Psi_{\bar{p}-p}^{(\text{final})}|^2 = a_1 \psi_{\frac{1}{2}}^2 \bar{\psi}_{-\frac{1}{2}}^2 + a_2 \psi_{\frac{1}{2}}^2 \bar{\psi}_{\frac{1}{2}}^2 + a_3 \psi_{-\frac{1}{2}}^2 \bar{\psi}_{\frac{1}{2}}^2 + a_4 \psi_{-\frac{1}{2}}^2 \bar{\psi}_{-\frac{1}{2}}^2, \quad (259)$$

where the coefficients a_i are given by

$$a_1 = (9/20) + \frac{1}{4}\rho - 3\xi, \quad (260)$$

$$a_2 = (1/20) + \frac{1}{4}\rho - \xi, \quad (261)$$

$$a_3 = (1/20) + \frac{1}{4}\rho + \xi, \quad (262)$$

$$a_4 = (9/20) + \frac{1}{4}\rho + 3\xi, \quad (263)$$

and ξ is defined by

$$\xi \equiv (\rho/20)^{\frac{1}{2}} \cos \varphi. \quad (264)$$

In order to illustrate the evaluation of (259), we will consider the term $\psi_{\frac{1}{2}}^2 \bar{\psi}_{-\frac{1}{2}}^2$ as an example. From (241) and (244), one finds

$$\begin{aligned} \psi_{\frac{1}{2}}^2 \bar{\psi}_{-\frac{1}{2}}^2 &= [\frac{2}{3}(\bar{p}0) + \frac{1}{3}(n+)] [\frac{1}{3}(\bar{n}-) + \frac{2}{3}(\bar{p}0)] \\ &= (4/9)(\bar{p}p00) + (2/9)(\bar{p}n+0) \\ &\quad + (2/9)(\bar{n}p0-) + \frac{1}{9}(\bar{n}n+-). \end{aligned} \quad (265)$$

The probabilities of the various possible reactions, as obtained from (259), are as follows:

$$P(\bar{p}p- -) = (1+\rho)^{-1}[a_1 + (1/9)a_3] = (1+\rho)^{-1}[(41/90) + (5/18)\rho - (26/9)\xi], \quad (266)$$

$$P(\bar{n}n+-) = (1+\rho)^{-1}[a_4 + (1/9)a_2] = (1+\rho)^{-1}[(41/90) + (5/18)\rho + (26/9)\xi], \quad (267)$$

$$P(\bar{n}p0-) = P(\bar{p}n+0) = (2/9)(1+\rho)^{-1}(a_2 + a_3) = (1+\rho)^{-1}[(1/45) + (1/9)\rho], \quad (268)$$

$$P(\bar{p}p00) = (4/9)(1+\rho)^{-1}a_2 = (1+\rho)^{-1}[(1/45) + (1/9)\rho - (4/9)\xi], \quad (269)$$

$$P(\bar{n}n00) = (4/9)(1+\rho)^{-1}a_3 = (1+\rho)^{-1}[(1/45) + (1/9)\rho + (4/9)\xi]. \quad (270)$$

The corresponding total cross sections are given by $\frac{1}{2}\sigma_1(N_1^* + \bar{N}_1^*)(1+\rho)P$. The pion spectra are given by $I_{\pi,a}$ (Fig. 4 of I); the spectra of N and \bar{N} are given by $I_{N,d}$ (Fig. 8 of I).

We note that we have one final state with four prongs, $(\bar{p}p- -)$, and four possible final states with two prongs and two neutral particles: $(\bar{n}n+-)$, $(\bar{n}p0-)$, $(\bar{p}n+0)$, and $(\bar{p}p00)$. One can use any three of these five cross sections to determine the three parameters, $\sigma_1(N_1^* + \bar{N}_1^*)$, ρ , and ξ . From the values of ρ and ξ , the phase angle φ can be obtained by means of Eq. (264). If all of the five cross sections pertaining to formation of 4 or 2 prongs can be determined experimentally, then two of the relations of Eqs. (266)–(269) can be used as a check on the validity of the present isobar model. It would also be of interest to compare the experimental spectra for pions, nucleons, and antinucleons with the functions $I_{\pi,d}$ and $I_{N,d}$ of the isobar model.

We will now obtain the branching ratios and energy spectra for single-pion production in $\bar{p}-n$ interactions. We will again have two reactions of the type (238) and (239), with equal cross sections. We note that the total isotopic spin of the system is $T=1$. The final-state wave function is given by

$$\Psi_{\bar{p}-n}^{(1)} = (1/2\sqrt{2})(-\bar{\psi}_{-\frac{1}{2}} \eta_{-\frac{1}{2}} + \sqrt{3}\bar{\psi}_{-\frac{1}{2}} \eta_{\frac{1}{2}} - \bar{\psi}_{\frac{1}{2}} \bar{\eta}_{-\frac{1}{2}} + \sqrt{3}\bar{\psi}_{\frac{1}{2}} \bar{\eta}_{\frac{1}{2}}). \quad (271)$$

One thus obtains:

$$\begin{aligned} |\Psi_{\bar{p}-n}^{(1)}|^2 &= \frac{1}{8}\bar{\psi}_{-\frac{1}{2}}^2 \eta_{-\frac{1}{2}}^2 + \frac{3}{8}\bar{\psi}_{-\frac{1}{2}}^2 \eta_{\frac{1}{2}}^2 + \frac{1}{8}\bar{\psi}_{\frac{1}{2}}^2 \bar{\eta}_{-\frac{1}{2}}^2 \\ &\quad + \frac{3}{8}\bar{\psi}_{\frac{1}{2}}^2 \bar{\eta}_{\frac{1}{2}}^2 \\ &= (1/24)(\bar{n}d n_r -) + \frac{1}{12}(\bar{p}_d n_r 0) \\ &\quad + \frac{3}{8}(\bar{p}_a p_r -) + (1/24)(\bar{p}_r p_d -) \\ &\quad + \frac{1}{12}(\bar{p}_r n_d 0) + \frac{3}{8}(\bar{n}_r n_d -). \end{aligned} \quad (272)$$

The intensities of the three possible final states can be written as follows:

$$I(\bar{n}n-) = \frac{3}{8}(\bar{n}_r n_d -) + (1/24)(\bar{n}_d n_r -), \quad (273)$$

$$I(\bar{p}p-) = (1/24)(\bar{p}_r p_d -) + \frac{3}{8}(\bar{p}_d p_r -), \quad (274)$$

$$I(\bar{p}n0) = \frac{1}{12}(\bar{p}_r n_d 0) + \frac{1}{12}(\bar{p}_d n_r 0). \quad (275)$$

The corresponding branching ratios are: $P(\bar{n}n-) = P(\bar{p}p-) = 5/12$; $P(\bar{p}n0) = \frac{1}{6}$. The total cross sections for the three reactions are given by $2\sigma_1(\bar{N}_1^* + N)P$; e.g., for $\bar{p}+n \rightarrow \bar{n}+n+\pi^-$, we have $\sigma = \frac{5}{6}\sigma_1(\bar{N}_1^* + N)$. For $(\bar{p}p-)$, the antiproton is predominantly a decay particle, while for $(\bar{n}n-)$, the antineutron is predominantly the recoil particle. For $(\bar{p}n0)$, \bar{p} and n have the same spectrum.

The branching ratios P lead to the following relations between the cross sections for the three possible final states:

$$\sigma(\bar{p}p-):\sigma(\bar{n}n-):\sigma(\bar{p}n0) = 2.5:2.5:1. \quad (276)$$

The final state $(\bar{p}p-)$ is probably much easier to identify than the other two, since it leads to the formation of 3 prongs, whereas $(\bar{n}n-)$ and $(\bar{p}n0)$ are 1-prong states. Nevertheless, it may be possible to obtain a reliable experimental result for the sum: $[\sigma(\bar{n}n-) + \sigma(\bar{p}n0)]$, in which case one can attempt to verify the prediction that the ratio $\sigma(\bar{p}p-)/[\sigma(\bar{n}n-) + \sigma(\bar{p}n0)]$ should equal $2.5/3.5 = 0.71$.

For $(\bar{p}p-)$, the normalized \bar{p} and p spectra are as follows:

$$I(\bar{p}) = 0.9I_{N,1} + 0.1I_{N,2}, \quad (277)$$

$$I(p) = 0.1I_{N,1} + 0.9I_{N,2}. \quad (278)$$

The corresponding Q -value distributions are given by

$$P[Q(\bar{p},\pi^-)] = 0.9\bar{P}_1 + 0.1\bar{P}_2, \quad (279)$$

$$P[Q(p,\pi^-)] = 0.1\bar{P}_1 + 0.9\bar{P}_2. \quad (280)$$

Similarly, the angular correlation functions C are given by

$$C(\bar{p},\pi^-) = 0.9\bar{C}_1 + 0.1\bar{C}_2, \quad (281)$$

$$C(p,\pi^-) = 0.1\bar{C}_1 + 0.9\bar{C}_2. \quad (282)$$

For the final state considered here, $(\bar{p}p-)$, it should be relatively simple to measure the spectra of \bar{p} and p . According to Eqs. (277) and (278), the energy distributions of \bar{p} and p should be quite different, especially at the higher incident energies, $T_{\bar{p},\text{inc}} \gtrsim 1$ Bev, where the spectra $I_{N,1}$ and $I_{N,2}$ are considerably different from each other. The energy distribution of the protons should thus show a sharp peak corresponding to the resonance maximum of the $T = \frac{3}{2}$ cross section $\sigma_{\frac{3}{2}}$ which enters into $I_{N,2}$.

For $(\bar{n}n-)$, the \bar{n} and n spectra are as follows:

$$I(\bar{n}) = 0.1I_{N,1} + 0.9I_{N,2}, \quad (283)$$

$$I(n) = 0.9I_{N,1} + 0.1I_{N,2}. \quad (284)$$

For $(\bar{p}n0)$, we have

$$I(\bar{p}) = I(n) = \frac{1}{2}(I_{N,1} + I_{N,2}). \quad (285)$$

For the double-pion production via $N_1^* + \bar{N}_1^*$, the final-state wave function is given by

$$\Psi_{\bar{p}-n}^{(2)} = -(3/10)\psi_{-\frac{1}{2}}\bar{\psi}_{\frac{1}{2}} + (4/10)\psi_{-\frac{1}{2}}\bar{\psi}_{-\frac{1}{2}} - (3/10)\psi_{\frac{1}{2}}\bar{\psi}_{-\frac{1}{2}}. \quad (286)$$

From the resulting expression for $|\Psi_{\bar{p}n}^{(2)}|^2$,

$$|\Psi_{\bar{p}-n}^{(2)}|^2 = (3/10)\psi_{-\frac{1}{2}}^2\bar{\psi}_{\frac{1}{2}}^2 + (4/10)\psi_{-\frac{1}{2}}^2\bar{\psi}_{-\frac{1}{2}}^2 + (3/10)\psi_{\frac{1}{2}}^2\bar{\psi}_{-\frac{1}{2}}^2, \quad (287)$$

one obtains the following branching ratios:

$$P(\bar{p}p0-) = P(\bar{n}n0-) = 13/45, \quad (288)$$

$$P(\bar{p}n+-) = 1/5, \quad (289)$$

$$P(\bar{p}n00) = 8/45, \quad (290)$$

$$P(\bar{n}p--) = 2/45. \quad (291)$$

The corresponding cross sections for the various reactions are given by $\sigma_1(N_1^* + \bar{N}_1^*)P$.

We may consider, in particular, the final states giving rise to three prongs and one neutral particle, namely $(\bar{p}p0-)$, $(\bar{p}n+-)$, and $(\bar{n}p--)$. The branching ratios of Eqs. (288), (289), and (291) lead to the following relations for the corresponding reaction cross sections:

$$\sigma(\bar{p}p0-)/\sigma(\bar{p}n+-)/\sigma(\bar{n}p--) = 6.5:4.5:1. \quad (292)$$

We note that from any one of these three $\bar{p}-n$ reactions, we can obtain a value for the basic cross section $\sigma_1(\bar{N}_1^* + N_1^*)$, which can be compared with the corresponding value of $\sigma_1(\bar{N}_1^* + N_1^*)$ as deduced from the $\bar{p}-p$ interactions at the same incident energy [Eqs. (266)–(270)].

We note that the results of the present isobar model for pion production in $\bar{n}-p$ interactions can be obtained by simply applying charge conjugation to the preceding equations pertaining to $\bar{p}-n$ interactions [Eqs. (271)–(292)]. Thus for single-pion production in $\bar{n}-p$ collisions, the intensities of the three possible final states are given [see Eqs. (273)–(275)] by

$$I(\bar{n}n+) = \frac{3}{8}(\bar{n}_d n_r+) + (1/24)(\bar{n}_r n_d+), \quad (293)$$

$$I(\bar{p}p+) = (1/24)(\bar{p}_d p_r+) + \frac{3}{8}(\bar{p}_r p_d+), \quad (294)$$

$$I(\bar{n}p0) = \frac{1}{12}(\bar{n}_d p_r0) + \frac{1}{12}(\bar{n}_r p_d0). \quad (295)$$

The corresponding branching ratios are

$$P(\bar{n}n+) = P(\bar{p}p+) = 5/12; \quad P(\bar{n}p0) = 1/6.$$

Equation (294) shows that for $(\bar{p}p+)$, the antiproton is predominantly the recoil particle. The normalized \bar{p} and p spectra for $(\bar{p}p+)$ are given by

$$I(\bar{p}) = 0.1I_{N,1} + 0.9I_{N,2}, \quad (296)$$

$$I(p) = 0.9I_{N,1} + 0.1I_{N,2}. \quad (297)$$

By comparing with (277) and (278), it is seen that the spectrum of the antiprotons from the reaction $\bar{n}+p \rightarrow \bar{p}+p+\pi^+$ is identical with the proton spectrum from the reaction $\bar{p}+n \rightarrow \bar{p}+p+\pi^-$. This result is, of course, a direct consequence of charge conjugation invariance.

The Q -value distributions for $(\bar{p}p+)$ are given by

$$P[Q(\bar{p},\pi^+)] = 0.1\bar{P}_1 + 0.9\bar{P}_2, \quad (298)$$

$$P[Q(p,\pi^+)] = 0.9\bar{P}_1 + 0.1\bar{P}_2. \quad (299)$$

For the double-pion production in $\bar{n}-p$ interactions, we obtain the following branching ratios [See Eqs. (288)–(291)]:

$$P(\bar{p}p+0) = P(\bar{n}n+0) = 13/45, \quad (300)$$

$$P(\bar{n}p+-) = 1/5, \quad (301)$$

$$P(\bar{n}p00) = 8/45, \quad (302)$$

$$P(\bar{p}n++) = 2/45. \quad (303)$$

Recently, measurements on pion production in $\bar{p}-p$ collisions have been carried out at the Berkeley Bevatron, with antiprotons of momentum 1.61 Bev/c (energy = 925 Mev), using the 72-in. hydrogen bubble chamber.²⁹ This experiment gave the following results for two of the four possible single-pion production reactions:

$$\sigma(\bar{p}+p \rightarrow \bar{p}+p+\pi^0) = 1.5 \pm 0.4 \text{ mb};$$

$$\sigma(\bar{p}+p \rightarrow \bar{p}+n+\pi^+) = 1.1 \pm 0.3 \text{ mb}.$$

The ratio of these two cross sections is 1.4 ± 0.5 , which is somewhat smaller than the value of 2 predicted by the present model [Eq. (250)]. However, there is

²⁹ F. Solmitz, *Proceedings of the 1960 Annual International Conference on High-Energy Physics at Rochester* (Interscience Publishers, New York, 1960), p. 164.

probably no real disagreement with the theory, in view of the experimental uncertainties due to the limited statistics [22 cases of $(\bar{p}p0)$, 17 cases of $(\bar{p}n+)$].

From the above results for the two partial cross sections, Solmitz²⁹ has deduced a value of 5.1 ± 1 mb for the total cross section for single-pion production (for all four reactions) by 925-Mev antiprotons. (Double-pion production is negligible at this energy.) In view of the discussion following Eq. (249), we thus obtain: $\sigma_1(\bar{N}_1^* + N) = 5 \pm 1$ mb at $T_{\bar{N},\text{inc}} = 925$ Mev.

By a more indirect method, Chamberlain³⁰ has deduced that the total pion production cross section for $\bar{n}-p$ collisions (without annihilation) is 20 ± 9 mb at $T_{\bar{n},\text{inc}} = 900$ Mev. According to the discussion following Eq. (275), this cross section should equal $2\sigma_1(\bar{N}_1^* + N)$, from which one would obtain: $\sigma_1(\bar{N}_1^* + N) = 10 \pm 4.5$ mb at $T_{\bar{N},\text{inc}} = 900$ Mev. In view of the large experimental uncertainties, this result is probably not inconsistent with the value 5 ± 1 mb deduced from the direct measurements on $\bar{p}-p$ interactions. It should be noted that the value of 20 ± 9 mb for $\bar{n}-p$ interactions was obtained³⁰ by a subtraction of the annihilation cross section of 44 ± 6 mb from the complete inelastic cross section of 64 ± 6 mb. The fact that $\sigma(\bar{n}+p \rightarrow \bar{N}+N+\pi)$ is considerably larger than $\sigma(\bar{p}+p \rightarrow \bar{N}+N+\pi)$ seems to confirm the basic assumptions of the present isobar model, according to which single-pion production does not take place in the isotopic spin $T=0$ part of the $\bar{p}+p$ system, since the final state $\bar{N}_1^* + N$ or $N_1^* + \bar{N}$ cannot have $T=0$.

X. DETERMINATION OF THE BASIC CROSS SECTIONS $\sigma_{2T,\alpha}$ AND THE PHASE ANGLES φ_α FOR PION PRODUCTION IN $\pi^\pm-p$ INTERACTIONS

In connection with the general equations for pion production in pion-nucleon collisions, which have been given in Sec. II, we will describe a possible procedure for obtaining the basic cross sections $\sigma_{2T,\alpha}$, the phase angles φ_α ($\alpha=1$ or 2), and the probabilities P_s and P_d pertaining to the decay of the N_2^* isobar. The principal idea which underlies this procedure is to obtain the aforementioned quantities from the measured cross sections for various single- and double-pion production reactions. After the basic parameters have thus been determined, they can be inserted into the expressions for the energy distributions of the final-state pions and nucleon, and for the Q -value distributions of pion-nucleon and pion-pion pairs. The resulting calculated energy spectra and Q -value distributions can then be compared with the corresponding experimental results, so as to obtain a direct test of the validity of the present extended isobar model.

A comparison of this type has been carried out in Sec. IV for the momentum distributions of the pions from single-pion production at $T_{\pi,\text{inc}} = 1.0$ Bev, which

were compared with the combined results from three experiments on $\pi^- - p$ interactions in this energy region. However, it should be noted that we had to make a simplifying assumption in order to obtain the $\sigma_{2T,\alpha}$ and φ_α , since there was not enough information available on the cross sections for the various possible reactions. In particular, no detailed measurements have as yet been carried out for the pion production reactions arising from $\pi^+ - p$ collisions [reactions (IV), (V), and (E)-(G)]. For this reason, we have made the assumption that: $\sigma_{12}/(\sigma_{11} + \sigma_{12}) = \sigma_{31}/(\sigma_{31} + \sigma_{32}) = 0.3$, in obtaining the fit to the data (Figs. 10-13).

We will now outline the type of procedure which can be used when the cross sections for the pion production reactions from $\pi^+ - p$ collisions will have been measured. If the cross sections $\sigma^{(IV)}$ and $\sigma^{(V)}$ for the two single-pion production reactions from $\pi^+ - p$ collisions are known experimentally, then Eqs. (51) and (52) for $\sigma^{(IV)}$ and $\sigma^{(V)}$ can be solved for σ_{31} and $\sigma_{32,s}$. If, in addition, the cross sections $\sigma^{(E)}$, $\sigma^{(F)}$, and $\sigma^{(G)}$ pertaining to the three-pion final states from $\pi^+ - p$ interactions are known, one of these cross sections can be used to determine $\sigma_{32,d}$ from (53) or (54). Then the other two relations of Eqs. (53) and (54), including the equality $\sigma^{(F)} = \sigma^{(G)}$, can be used to test the validity of the present model. Since $\sigma^{(E)}$ pertains to 4-prong events ($\pi^+ + p \rightarrow p + \pi^+ + \pi^+ + \pi^-$), whereas $\sigma^{(F)}$ and $\sigma^{(G)}$ correspond to 2-prong events (with 2 neutral particles), it is likely that $\sigma^{(E)}$ can be measured more accurately than $\sigma^{(F)}$ and $\sigma^{(G)}$. Thus it would seem advantageous to determine $\sigma_{32,d}$ from $\sigma^{(E)}$, by means of Eq. (53), and then to calculate $\sigma^{(F)}$ and $\sigma^{(G)}$ from Eq. (54), and compare the resulting values with the experimental cross sections for the reactions (F) and (G).

With the values of σ_{31} , $\sigma_{32,s}$, and $\sigma_{32,d}$ thus determined, one can calculate the pion spectra of Eqs. (55)-(63), and the nucleon spectra of Eqs. (106)-(108), using the basic spectra $J_{\pi,i}$ and $I_{N,i}^{(\pi)}$ of Figs. 2-4 and 7-9. If experimental data for these spectra are available for the various reactions, the calculated spectra can be compared with them, thus providing an important test of the present isobar model.

Concerning the $\pi^- - p$ interactions [see Eqs. (28)-(34)], we must determine four parameters: σ_{11} , σ_{12} , φ_1 , and φ_2 . We consider first the single-pion production reactions. We will assume that $\sigma^{(I)}$ and $\sigma^{(II)}$ (pertaining to $\pi^- + \pi^+ + n$ and $\pi^- + \pi^0 + p$) can be measured accurately, but that $\sigma^{(III)}$ (pertaining to the reaction $\pi^- + p \rightarrow n + \pi^0 + \pi^0$) cannot be obtained reliably with the present experimental techniques, since there are no outgoing prongs, and it seems impossible in general to distinguish this final state from $n + \pi^0$ (charge exchange) or $n + 3\pi^0$. For the same reason, we assume that $\sigma^{(D)}$ (pertaining to $\pi^- + p \rightarrow n + 3\pi^0$) cannot be reliably obtained with the present techniques.

We assume that the cross sections $\sigma^{(A)}$, $\sigma^{(B)}$, and $\sigma^{(C)}$ for double-pion production can be measured with reasonable accuracy. These cross sections are given by

²⁹ O. Chamberlain, reference 29, p. 653.

Eqs. (31)–(33). For the purpose of the present discussion, we rewrite Eqs. (32) and (33) for $\sigma^{(B)}$ and $\sigma^{(C)}$, as follows:

$$\sigma^{(B)} = (4/27)\sigma_{12,d} + (2/27)\sigma_{32,d}, \quad (304)$$

$$\sigma^{(C)} = (2/27)\sigma_{12,d}(5 - 3A) + (5/27)\sigma_{32,d}, \quad (305)$$

where we have made use of the relations

$$\rho_2 = \sigma_{32,d}/(2\sigma_{12,d}), \quad (306)$$

and $B = 1 + \rho_2 - A$.

Since $\sigma_{32,d}$ has been obtained from the $\pi^+ - p$ inelastic cross sections, we have only two unknown quantities in Eqs. (31), (304) and (305), namely $\sigma_{12,d}$ and A . Two of these equations can therefore be used to determine $\sigma_{12,d}$ and A , while the third equation can serve as a check on the validity of the present model.

It may be noted that an accurate measurement of $\sigma^{(A)}$ should be relatively easy, since the final state ($p + \pi^+ + 2\pi^-$) gives rise to four prongs. The experimental values of $\sigma^{(B)}$ and $\sigma^{(C)}$ will probably have somewhat larger uncertainties, since the corresponding final states give rise to two prongs, with two neutral particles emerging from the reactions. In some cases, it may be possible to eliminate some of the uncertainties connected with reactions (B) and (C) by combining the events from both reactions, so as to obtain the value of $[\sigma^{(B)} + \sigma^{(C)}]$. The equations for $\sigma^{(A)}$ and $[\sigma^{(B)} + \sigma^{(C)}]$ [as derived from (304) and (305)] can then be solved for $\sigma_{12,d}$ and A .

Upon inserting the resulting value of $\sigma_{12,d}$ into (306), one obtains ρ_2 . The cross section $\sigma_{12,s}$ is then given by

$$\sigma_{12,s} = \sigma_{32,s}/(2\rho_2), \quad (307)$$

where $\sigma_{32,s}$ has been obtained previously from the $\pi^+ - p$ inelastic cross sections.

We can now use the experimental values of the cross sections $\sigma^{(I)}$ and $\sigma^{(II)}$ pertaining to the single-pion production reactions (I) and (II), in order to determine the two remaining quantities, σ_{11} and a . For this purpose, we rewrite Eqs. (28) and (29) as follows:

$$\sigma^{(I)} = \frac{2}{3}\sigma_{11}\left(\frac{5}{9} + \frac{7}{9}a\right) + \frac{26}{135}\sigma_{31} + \frac{4}{9}A\sigma_{12,s}, \quad (308)$$

$$\sigma^{(II)} = \frac{2}{3}\sigma_{11}\left(\frac{2}{9} + \frac{5}{9}a\right) + \frac{17}{135}\sigma_{31} + \frac{2}{9}\sigma_{12,s}(2 + 2\rho_2 - A), \quad (309)$$

where we have used the definition of ρ_1 [$\equiv \sigma_{31}/(2\sigma_{11})$]. We note that the parameters $\sigma_{12,s}$, σ_{31} , A , and ρ_2 have been previously determined, so that Eqs. (308) and (309) can be solved for σ_{11} and a . In view of Eq. (34a),

$\cos\varphi_1$ is given by

$$\cos\varphi_1 = (5/2)^{\frac{1}{2}}(\sigma_{11}/\sigma_{31})^{\frac{1}{2}}a. \quad (310)$$

Finally, φ_2 can be obtained using the values of A and ρ_2 . From Eqs. (16) and (18), one finds

$$\cos\varphi_2 = (3/2\sqrt{2})\rho_2^{-\frac{1}{2}}(A - \frac{2}{3} - \frac{1}{3}\rho_2). \quad (311)$$

In order to summarize the preceding discussion, we note that there are seven independent parameters which characterize the pion production in $\pi - N$ interactions: σ_{11} , σ_{12} , σ_{31} , σ_{32} , φ_1 , φ_2 , and $P_s = \sigma_{12,s}/\sigma_{12} = \sigma_{32,s}/\sigma_{32}$. P_s is the probability that the isobar N_2^* decays into $N + \pi$, giving rise to single-pion production. In order to determine these seven constants, the cross sections for three inelastic $\pi^+ - p$ reactions and four $\pi^- - p$ reactions were used. The three $\pi^+ - p$ reactions, namely (IV), (V), and one of the double-pion production reactions (E), (F), and (G), enable us to obtain the values of σ_{31} , σ_{32} ($= \sigma_{32,s} + \sigma_{32,d}$), and $P_s = \sigma_{32,s}/\sigma_{32}$. The four $\pi^- - p$ reactions, namely (I), (II), and two of the reactions (A), (B), and (C), lead to the determination of σ_{11} , σ_{12} , φ_1 , and φ_2 .

Upon using the values of σ_{11} , $\sigma_{12,s}$, ρ_1 , a , A , and B , one can calculate the pion and nucleon spectra for single-pion production from Eqs. (35)–(39) and (103)–(105). The calculated spectra can be compared with experiment in the same manner as was done in Sec. IV.

For the double-pion production reactions, we need only the values of $\sigma_{12,d}$, A , and B , in order to obtain the pion and nucleon spectra from Eqs. (41)–(48) and Eq. (108). A comparison with experiment is again possible for the reactions (A)–(C), if the appropriate pion and nucleon momentum distributions have been measured with adequate statistics.

The constants ρ_1 , ρ_2 , a , A , and B can also be used to calculate the various coefficients of Table I for the Q -value distributions of pion-nucleon pairs from $\pi^- - p$ interactions. For the case of single-pion production, these coefficients have been denoted by c_{1a} , c_{1b} , c_{2a} , and c_{2b} in the discussion of Sec. V, and their values can be used to obtain the $Q(\pi, N)$ distribution by means of Eq. (156). The basic Q -value distributions $P_{\pi N, \alpha}^{(a)}$ and $P_{\pi N, \alpha}^{(b)}$ which enter into Eq. (156) are given in Figs. 14 and 16 for $T_{\pi, \text{inc}} = 1.0$ Bev. We note that Eq. (156) also involves the cross sections σ_1 and σ_2 for the particular reaction considered to proceed via $N_1^* + \pi$ and $N_2^* + \pi$, respectively. These partial cross sections are given by the appropriate parts of the right-hand sides of Eqs. (28)–(30); e.g., for reaction (II), we have: $\sigma_2 = (2/9)\sigma_{12,s}(A + 2B)$.

XI. DETERMINATION OF THE BASIC CROSS SECTIONS σ_1 – σ_6 AND THE PARAMETERS k_i AND φ_0 FOR PION PRODUCTION IN $p - p$ AND $n - p$ INTERACTIONS

In the same manner as for $\pi^\pm - p$ interactions (Sec. X), we can also use experimental values of the cross

sections for pion production reactions in $p-p$ and $n-p$ collisions in order to determine the corresponding basic cross sections σ of Tables III and IV, which have been denoted by $\sigma_1, \sigma_2, \dots, \sigma_6$ in Eqs. (177)–(182). In fact, these six cross sections can be obtained from the cross sections for inelastic $p-p$ interactions alone, without having recourse to $n-p$ interactions. On the other hand, the parameters k_0, k_1, k_2 , and φ_0 which pertain to the nucleon-nucleon system in the $T=0$ state can be obtained from four suitably chosen single- or double-pion production cross sections for $n-p$ collisions.

We will first discuss the determination of the six independent cross sections $\sigma_1-\sigma_6$ from the inelastic $p-p$ cross sections. Referring to the two single-pion production reactions (p1) and (p2), corresponding to the final states $(pn+)$ and $(pp0)$, we note that Eqs. (201) and (202) for $\sigma^{(p1)}$ and $\sigma^{(p2)}$ can be solved directly for $\sigma_1 [= \sigma_1(N_1^* + N)]$ and $\sigma_3 [= \sigma_{1,s}(N_2^* + N)]$.

The four double-pion production reactions (p3)–(p6) can be similarly used to determine the values of the four basic cross sections $\sigma_2, \sigma_4, \sigma_5$, and σ_6 by means of Eqs. (203)–(206). However, we note that for incident proton energies below ~ 3.6 Bev, the cross section σ_6 which pertains to $N+N \rightarrow 2N_2^*$ [reaction (e)] is expected to be very small compared to the other cross sections involved (including σ_5 which pertains to $N+N \rightarrow N_1^* + N_2^*$). This result follows from the fact that the effective threshold for reaction (e) is $T_{p,\text{inc}} \sim 3.6$ Bev. If we set $\sigma_6=0$, then only three out of the four possible double-pion reactions have to be used to determine the basic cross sections involved (σ_2, σ_4 , and σ_5). In this connection, we note that $\sigma^{(p3)}$ can probably be measured more accurately than $\sigma^{(p4)}, \sigma^{(p5)}$, or $\sigma^{(p6)}$, since reaction (p3) leads to the formation of 4 prongs, whereas (p4), (p5), and (p6) give rise to 2 prongs, with 2 neutral particles emerging from the reactions.

If the relevant experimental data on the total cross sections are available, then $\sigma_1-\sigma_5$ can be determined by the procedure given above. Upon inserting these values of $\sigma_1-\sigma_5$ into Eqs. (183)–(199), one then obtains the theoretical energy spectra of the pions and nucleons from the various reactions for $p-p$ collisions, which can be compared with experiment. The basic nucleon and pion spectra (e.g., $I_{N,i}^A$ and $I_{\pi,i}^A$) which also enter into Eqs. (183)–(199) are given in Figs. 17–20 for incident proton energies $T_{p,\text{inc}} = 2.3$ and 3.0 Bev.

As was mentioned above, the parameters k_0, k_1, k_2 , and φ_0 can be determined from the pion production reaction cross sections for $n-p$ collisions. There are three single-pion production reactions, (n1)–(n3), whose total cross sections are given by Eqs. (229)–(231). We assume that σ_1 and σ_3 are known from the $p-p$ inelastic cross sections. Then we can use the cross sections for any two of the three single-pion reactions to determine the two constants, k_1 and φ_0 . We note that φ_0 enters into Eqs. (229) and (231) through the parameters C_+ and C_- [see Eq. (164)]. It may be remarked that $\sigma^{(n1)}$,

which pertains to the 3-prong final state $(pp-)$, can probably be measured more accurately than $\sigma^{(n2)}$ and $\sigma^{(n3)}$, which pertain to the 1-prong final states $(pn0)$ and $(nn+)$. However, the sum $[\sigma^{(n2)} + \sigma^{(n3)}]$ can probably be determined with greater accuracy than either $\sigma^{(n2)}$ or $\sigma^{(n3)}$ separately, because of possible ambiguities for events which can be classified as either $(pn0)$ or $(nn+)$. It may therefore be advantageous to use the equation for the sum:

$$\sigma^{(n2)} + \sigma^{(n3)} = (5/12)\sigma_1 + \frac{1}{6}(1+k_1+C_-)\sigma_3, \quad (312)$$

along with Eq. (229) for $\sigma^{(n1)}$, in order to determine k_1 and φ_0 .

We have four double-pion production reactions, (n4)–(n7), two of which lead to three prongs with only one neutral particle [(n4)= $(pp0-)$ and (n5)= $(pn+-)$]. The other two reactions [(n6)= $(pn00)$ and (n7)= $(nn0+)$] lead to only one prong (and three neutral particles), and are therefore very difficult to identify reliably, especially since they may be confused with the one-prong single-pion production reactions, (n2) and (n3). The remaining constants, which have not yet been determined, are k_0 and k_2 . Upon choosing Eqs. (232) and (233) for the 3-prong cross sections pertaining to $(pp0-)$ and $(pn+-)$, we have two equations which can be solved for the two parameters k_0 and k_2 . If we assume that $\sigma_6=0$ (as was discussed above for the case of $p-p$ collisions), then one of the two equations can be used as a check, to give an independent determination of k_0, k_1 , or φ_0 . Of course, if either or both of the one-prong reactions (n6) and (n7) should be measurable, then Eqs. (234) and (235) could serve as an additional test of the validity of the present model.

With the constants k_0, k_1 , and φ_0 thus determined, and with $\sigma_1-\sigma_6$ as obtained from the $p-p$ reactions, one can now calculate the various pion and nucleon spectra from $n-p$ interactions, using Eqs. (207)–(227). The resulting theoretical energy distributions can be compared with experiment, if these distributions have been measured with adequate statistics.

XII. SUMMARY AND CONCLUSIONS

In this paper, we have presented an extension of the isobaric nucleon model of pion production^{1,2} and we have given the results of calculations on pion production in πN , NN , and $\bar{N}N$ interactions. In contrast to our previous publications,^{1,2} the present calculations include the effect of the two-higher resonances of the pion-nucleon system in the isotopic spin $T=\frac{1}{2}$ state, in addition to the well-known low-energy $T=J=\frac{3}{2}$ resonance, which has been considered in our previous work. The higher $T=\frac{1}{2}$ resonances occur at incident pion energies $T_\pi=600$ and 880 Mev, corresponding to isobar masses $m_I=1.51$ and 1.68 Bev, respectively, as compared to $m_I=1.23$ Bev ($T_\pi=180$ Mev) for the

$T=J=\frac{3}{2}$ resonance. We note that our previous work^{1,2} on the isobar model quite generally stated the possible existence of several isobaric nucleon levels or intermediate states in pion production.

By including the $T=\frac{1}{2}$ isobaric states, which are denoted by N_{2a}^* and N_{2b}^* , we are able to give a theory of the production of two additional pions in pion-nucleon collisions, corresponding to a total of three pions in the final state.³¹ For each type of possible reaction, i.e., $\pi+N \rightarrow N_1^*+\pi$ and $\pi+N \rightarrow N_2^*+\pi$ (where N_1^* denotes the $T=\frac{3}{2}$ isobar), we have taken into account the interference between the matrix elements for production in the states of isotopic spin $T=\frac{1}{2}$ and $T=\frac{3}{2}$ of the pion-nucleon system. By adjusting the phase angles φ_1 and φ_2 between the corresponding $T=\frac{1}{2}$ and $T=\frac{3}{2}$ matrix elements for the two types of processes (involving $N_1^*+\pi$ and $N_2^*+\pi$), we have obtained agreement with the branching ratios for the different possible final states for π^-+p interactions. In particular, φ_1 is determined primarily by the ratio

$$R = \sigma(\pi^-+p \rightarrow \pi^-+\pi^0+p)/\sigma(\pi^-+p \rightarrow \pi^-+\pi^++n),$$

while φ_2 can be obtained from the experimental value of the ratio:

$$\sigma(\pi^-+p \rightarrow p+\pi^++\pi^-+\pi^-)/\sigma(\pi^-+p \rightarrow n+\pi^++\pi^0+\pi^-).$$

We have thus obtained $\varphi_1=88^\circ$ and $\varphi_2=129^\circ$ for an incident pion energy $T_{\pi,\text{inc}}=1.0$ Bev. The experimental branching ratios at this energy were derived from the results of three experiments²⁴⁻²⁶ which have been recently carried out at $T_{\pi,\text{inc}}=0.96$ and 1.0 Bev.³² For the single-pion production reactions, the pion momentum spectra calculated from the isobar model are in reasonable agreement with the combined pion momentum distributions from the three experiments (see Figs. 10-13). It should be noted that for these single-pion production reactions, i.e., $\pi^-+p \rightarrow \pi^-+\pi^++n$, and $\pi^-+p \rightarrow \pi^-+\pi^0+p$, the predominant contribution comes from the process $\pi^-+p \rightarrow N_1^*+\pi$ which has been considered in II, so that these reactions constitute primarily a test of our previous work on the isobar model, in which only the lowest isobaric state N_1^* (with $T=J=\frac{3}{2}$) was included. On the other hand, if the model is applied to the double-pion production reactions for πN collisions, this process necessarily involves the production of the higher isobars N_{2a}^* or N_{2b}^* .

Concerning the present calculations for pion-nucleon

³¹ As was discussed in Sec. II, we can now treat up to four-pion final states in $\pi-N$ interactions. However, in the present treatment, the small contribution of the transition $N_{2a}^* \rightarrow N_{2a}^*+\pi$ has been neglected, so that only two- and three-pion final states are considered.

³² See also E. Pickup, D. K. Robinson, and E. O. Salant, reference 29, p. 72; J. G. Rushbrooke and D. Radojicic, Phys. Rev. Letters 5, 567 (1960).

interactions, we have given expressions for the center-of-mass energy spectra of the final-state pions and nucleons, for both π^-+p and π^+-p collisions, in terms of certain basic spectra denoted by $J_{\pi,1}, J_{\pi,2}, \dots, J_{\pi,6}$ for the pions and by $I_{N,1}^{(\pi)}, I_{N,2}^{(\pi)}$, and $I_{N,3}^{(\pi)}$ for the nucleons. These spectra $J_{\pi,i}$ and $I_{N,i}^{(\pi)}$ have been calculated for incident pion energies $T_{\pi,\text{inc}}=1.0, 1.4$, and 2.0 Bev (see Figs. 2-9).

In connection with the single-pion production in pion-nucleon collisions, we have obtained the Q -value distributions for pion-nucleon and pion-pion pairs for incident energy $T_{\pi,\text{inc}}=1.0$ Bev, for both the reactions $\pi+N \rightarrow N_1^*+\pi$ and $\pi+N \rightarrow N_2^*+\pi$ (see Figs. 14-16). Expressions have also been obtained for the Q -value distribution functions $P(Q)$ for all pion-nucleon pairs arising in the various possible single- and double-pion production reactions in π^-+p and π^+-p collisions. The functions $P(Q)$ are expressed in terms of certain basic Q -value distribution functions, such as $P_{\pi N, \alpha}^{(a)}$ and $P_{\pi N, \alpha}^{(b)}$ (see Tables I and II).

In the calculations for nucleon-nucleon interactions, we have considered the production of the isobar N_2^* by means of the reactions: $N+N \rightarrow N_2^*+N$ and $N+N \rightarrow N_1^*+N_2^*$. In the former reaction, either one or two pions are produced, while the latter reaction corresponds to the production of two or three pions in the final state. For both the cases of $p-p$ and $n-p$ collisions, we have obtained the branching ratios for the various possible pion production reactions corresponding to production of one, two, three, or four pions (see Tables III and IV). In obtaining these branching ratios, we have also included the reactions $N+N \rightarrow N_1^*+N$ and $N+N \rightarrow 2N_1^*$, which have been previously considered, as well as $N+N \rightarrow 2N_2^*$, which can lead to the production of two, three, or four pions.³³ For $n-p$ collisions, the pion production will in some cases proceed in both the isotopic spin $T=0$ and $T=1$ states of the nucleon-nucleon system. In particular, for the reaction $n+p \rightarrow N_2^*+N$, there are interference terms between the contributions of the $T=0$ and $T=1$ states, which involve the phase angle φ_0 between the matrix elements pertaining to $T=0$ and $T=1$. Thus, from the measured branching ratios, one can derive the value of φ_0 . φ_0 can be deduced, in principle, from a measurement of the cross sections $\sigma(n+p \rightarrow p+p+\pi^-)$, $\sigma(n+p \rightarrow p+n+\pi^0)$, and $\sigma(n+p \rightarrow n+n+\pi^+)$, provided that the part of these cross sections which arises from the reaction $n+p \rightarrow N_1^*+N$ (in the $T=1$ state) has been determined from a separate measurement of the single-pion production cross sections for $p-p$ collisions, i.e., $\sigma(p+p \rightarrow p+n+\pi^+)$ and $\sigma(p+p \rightarrow p+p+\pi^0)$. Such a measurement of the $p-p$ interactions will also give information on the cross section for the reaction $n+p \rightarrow N_2^*+N$ to occur in the $T=1$

³³ As previously mentioned, up to eight-pion final states in $N-N$ interactions could be treated by the present extension of the isobar model.

state of the NN system, which enters into the determination of φ_0 .

In analogy with the basic spectra $J_{\pi,i}$ and $I_{N,i}^{(\pi)}$ for pion-nucleon interactions, we have also defined and calculated the basic spectra for pion production in nucleon-nucleon interactions, which are denoted by $I_{\pi,s}$, $I_{\pi,i}^{(A)}$, $I_{\pi,i}^{(B)}$ for the final-state pions, and $I_{N,1}$, $I_{N,2}$, $I_{N,i}^{(A)}$, and $I_{N,i}^{(B)}$ for the final-state nucleons. Here the superscripts (A) and (B) indicate that the spectra pertain to the reactions (A): $N+N \rightarrow N_2^*+N$, and (B): $N+N \rightarrow N_1^*+N_2^*$, respectively. The nucleon spectra $I_{N,1}$ and $I_{N,2}$ pertain to the reaction $N+N \rightarrow N_1^*+N$, and have been previously introduced in I. The corresponding pion spectrum (which pertains to single-pion production) is denoted by $I_{\pi,s}$. In the present work, calculations have been carried out for incident nucleon energies $T_{N,\text{inc}}=2.3$ and 3.0 Bev. The resulting basic pion and nucleon spectra are shown in Figs. 17-20. For all of the reactions which lead to single- and double-pion production, both in $p-p$ and $n-p$ collisions, expressions have been obtained for the center-of-mass energy spectra of the final-state nucleons and pions, in terms of the basic energy spectra discussed above. For the case of $p-p$ and $n-p$ interactions, no new comparisons with experiments have been carried out in the present paper. However, we may note that extensive comparisons which we have previously made in reference 1, for the experiments carried out before 1956, showed that essential agreement was obtained with the previous work on the isobar model, which involves only the reactions $N+N \rightarrow N_1^*+N$ and $N+N \rightarrow 2N_1^*$. The more recent experiments of Batson *et al.*⁹ and Chadwick *et al.*¹⁰ also provide good confirmation of most of the essential features of our previous calculations which involve only the isobaric state N_1^* corresponding to the $T=J=\frac{3}{2}$ resonance. In order to detect the formation of the $T=\frac{1}{2}$ isobaric states N_{2a}^* and N_{2b}^* , additional experiments in the range of $T_{N,\text{inc}}$ from ~ 2 to ~ 3 Bev will probably be required. One possibility seems to be the measurement of the branching ratios for the production of two and three pions in $p-p$ collisions. As can be seen from Table III, the ratio

$$\sigma(p+p \rightarrow p+n+\pi^++\pi^0)/\sigma(p+p \rightarrow p+p+\pi^++\pi^-)$$

should equal $26/9=2.89$ if the reactions proceed exclusively via $p+p \rightarrow 2N_1^*$, while it should be $2/5=0.40$ for the process $p+p \rightarrow N_2^*+N$. If the double-pion production involves a mixture of the two basic reactions $p+p \rightarrow 2N_1^*$ and $p+p \rightarrow N_2^*+N$, one expects, of course, that the ratio of the cross sections discussed above will have a value intermediate between the extreme values of 0.40 and 2.89. Similarly, for the production of three pions at $T_{p,\text{inc}} \sim 3$ Bev, the most likely possibility according to the present isobar model is the reaction $p+p \rightarrow N_1^*+N_2^*$, in which case, for

example, the ratio

$$\begin{aligned} \sigma(p+p \rightarrow p+n+\pi^++\pi^++\pi^-)/ \\ \sigma(p+p \rightarrow p+p+\pi^++\pi^0+\pi^-) \end{aligned}$$

should have the value $25/14=1.79$.

Concerning the measurement of the energy spectrum of the final-state protons from proton interactions in a liquid hydrogen target¹⁰ (irrespective of the number or type of pions produced), we can draw the following conclusions from Eq. (199) and Figs. 17 and 18. The coefficient $(\sigma_3+\sigma_4)$ of the recoil spectrum $I_{N,3}^A$ pertaining to the formation of the N_2^* isobar is likely to be smaller than the coefficient $\frac{1}{4}\sigma_1$ of the recoil spectrum $I_{N,2}$ pertaining to N_1^* , unless the incident nucleon energy is sufficiently high (possibly $T_{N,\text{inc}} \gtrsim 3$ Bev). Here σ_1 is the cross section for the reaction $N+N \rightarrow N_1^*+N$ in the $T=1$ state of the NN system, while $\sigma_3+\sigma_4$ represents the corresponding cross section for $N+N \rightarrow N_2^*+N$ in the $T=1$ state [see Eqs. (177), (179), and (180)]. Moreover, as is shown by Figs. 17 and 18, the maxima of $I_{N,3}^A$ which arise from the presence of the isobars N_{2a}^* and N_{2b}^* are considerably less prominent than the maximum of $I_{N,2}$ due to the N_1^* isobar. This difference is mainly a consequence of the fact that the maxima of σ_1 at $T_\pi=600$ and 880 Mev have an amplitude of only ~ 20 mb, superposed on a rather large and approximately constant background of ~ 40 mb, as compared to the considerably larger maximum of the $T=\frac{3}{2}$ resonance ($\sigma_{\frac{3}{2},\text{max}}=200$ mb), which involves essentially no nonresonant background. (The $T=\frac{3}{2}$ cross section $\sigma_{\frac{3}{2}}$ is ~ 4 mb at very low energies, $T_\pi \lesssim 20$ Mev, and above the 180-Mev resonance, it decreases to a minimum of 16 mb at $T_\pi=650$ Mev.) Thus it is expected that the maxima of the combined proton spectrum $(d\sigma/dT_N)^{(p)}(p)$ [Eq. (199)] due to the recoil from the N_{2a}^* and N_{2b}^* isobars will be much less prominent than the maximum which arises from the presence of N_1^* .

Taft and co-workers³⁴ have studied single-pion production in $p-p$ collisions at an incident proton energy of 2.85 Bev. Their results for the momentum spectra of the outgoing pions and nucleons, and for the pion-nucleon Q values, agree quite well with the predictions of the isobar model. The important feature of these results is the observation that in single-pion production the nucleons are strongly peaked forward and backward in the center-of-mass system. Previous evidence⁴ has indicated that for double-pion production, this may not be the case. This difference in the angular distribution of the isobar for the single- and double-pion production may be responsible for some of the discrepancies between the predictions of the isobar model and the experimental results of reference 10.

³⁴ H. Taft, Bull. Am. Phys. Soc. 6, 17 (1961).

Detailed predictions for the angular distribution of the isobar production and of the decay products in the isobar rest system have not been made in the present phenomenological treatment, but we have previously considered¹ two likely cases, which, especially in combination, seemed reasonable to assume: (a) isotropic isobar production; (b) forward and backward peaked isobar production, followed by isotropic decay (i.e., isotropic distribution of the decay products in the isobar rest system) [see Fig. 5 of I]. The present evidence on angular distributions in $p-p$ pion production interactions in the incident energy region of 2 to 3 Bev appears to be consistent with the assumption of sharply forward and backward isobar production in single-pion production, and more or less isotropic isobar production in double-pion production.

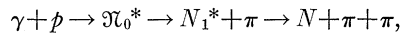
Calculations on single-pion production in $\pi-N$ and $N-N$ interactions at lower energies using the isobar model have been carried out by Bergia, Bonsignori, and Selleri²¹ and by Mandelstam.³⁵ Selove³⁶ has considered possible effects on the angular distribution of single-pion production in nucleon-nucleon collisions. Ito, Minami, and Tanaka³⁷ have also done related work on pion production.

In Sec. IX, we have given a discussion of single- and double-pion production in antinucleon-nucleon interactions which do not lead to annihilation. The pion production is assumed to involve the production of anti-isobars \bar{N}_1^* and \bar{N}_2^* , which are defined to be the antiparticles of N_1^* and N_2^* , respectively. Specific predictions have been obtained for the branching ratios and the energy spectra of nucleons, antinucleons, and pions for single- and double-pion production in $\bar{p}-p$, $\bar{p}-n$, and $\bar{n}-p$ interactions. These predictions have been compared with preliminary results of experiments with 925-Mev antiprotons, using the 72-in. hydrogen bubble chamber at the Berkeley Bevatron.^{29,30} As an example of the theoretical results, we note that for the four possible single-pion final states which arise from $\bar{p}-p$ interactions, namely: $\bar{p}+p+\pi^0$, $\bar{n}+n+\pi^0$, $\bar{n}+p+\pi^-$, and $\bar{p}+n+\pi^+$, the energy spectrum for any of the final-state nucleons or antinucleons is predicted to be $\frac{1}{2}(I_{N,1}+I_{N,2})$, while the Q -value distribution function for any of the πN or $\pi \bar{N}$ pairs is given by $\frac{1}{2}(\bar{P}_1+\bar{P}_2)$, where \bar{P}_1 and \bar{P}_2 are basic Q -value distribution functions which have been introduced in I. The functions $\frac{1}{2}(I_{N,1}+I_{N,2})$ and $\frac{1}{2}(\bar{P}_1+\bar{P}_2)$ for incident energy $T_{N,\text{inc}}=1.0$ Bev are shown in Figs. 21 and 22.

The pion production in $\pi^\pm-p$, $p-p$, and $n-p$ interactions involves certain basic cross sections $\sigma_{2T,\alpha}$ and σ_i according to the present isobar model. In Secs. X and

XI, we have given a possible procedure for determining these cross sections, together with the phase angles φ_i , from experimental data on the total cross sections for various pion production reactions. After the basic cross sections and the phase angles have thus been determined, the theoretical energy spectra of the pions and nucleons from the various possible reactions can be calculated and compared with experiment, in order to obtain a test of the validity of the isobar model.

It may be noted that the process of isobar formation is also expected to occur in the production of pion pairs by incident γ rays. As an example, the double-pion photoproduction could proceed as follows:



where one of the final-state pions is the recoil pion, while the other pion arises from the decay of the isobar N_1^* . Several investigations of pion photoproduction have been carried out using the present concept of isobar formation.³⁸ The resulting basic spectra of the final-state pions and nucleon are similar to the spectra $J_{\pi,1}$, $J_{\pi,2}$, and $I_{N,1}^{(\pi)}$ pertaining to pion production in πN collisions (for the same total energy \bar{E} in the center-of-mass system).

Finally, we note that the recent discovery of the Y^* isobar and the K' particle³⁹ seems to indicate that the process of isobar formation is not restricted to nucleons, but that on the contrary, for the three cases of the nucleon, the Λ particle, and the K meson, if an additional pion is produced in the original reaction, it will have a strong tendency to resonate with the nucleon, Λ , or K , so as to produce an isobar, which can be considered as a real particle existing in intermediate states. In all three cases, one can make the assumption that the isobar (N^* , Y^* , or K') lives long enough ($\tau \gtrsim 10^{-23}$ sec), and its mass distribution is sufficiently narrow, so that the other particle produced in the original reaction (π or N) will have a characteristic recoil spectrum, with a narrow peak which corresponds to the formation of the isobar with the most probable mass value.

In a sense, one can now formulate a generalization of the isobaric levels, which can also be described as intermediate-state particle levels. In addition to the pion-nucleon and pion-pion particle levels, there exist also levels with strangeness $S=-1$ (e.g., Y^*) and $S=+1$ (K' particle). The levels with $S \neq 0$ are obviously important in considering the production of strange particles accompanied by pions in $\pi-N$, $N-\bar{N}$, and $\bar{N}-N$ interactions. If one knows the characteristics of these

³⁵ S. Mandelstam, Proc. Roy. Soc. (London) A244, 491 (1958).
³⁶ W. Selove, Phys. Rev. Letters 5, 163 (1960).
³⁷ D. Ito, S. Minami, and K. Tanaka, Nuovo cimento 8, 135 (1958); *ibid.* 9, 208 (1958).

³⁸ H. H. Bingham and A. B. Clegg, Phys. Rev. 112, 2053 (1958); M. Bloch and M. Sands, *ibid.* 113, 305 (1959); R. F. Peierls, *ibid.* 118, 325 (1960).
³⁹ M. Alston, L. W. Alvarez, P. Eberhard, M. L. Good, W. Graziano, H. K. Ticho, and S. G. Wojcicki, Phys. Rev. Letters 5, 520 (1960); and M. L. Good (private communication).

$S=+1$ and $S=-1$ isobaric states, a phenomenological treatment similar to the present work can be developed for them.

Finally, we should note that we are well aware that a number of simplifying assumptions have been made in our work, notably the assumption that the isobar lifetime can be considered long enough so that interference effects due to its decay are negligible. Never-

theless, in view of the agreement which has been obtained so far with experiments on inelastic $N-N$ and $\pi-N$ interactions, one can hope that most of the important features of the future related experiments will be described within the framework of the present model or, at the very least, that the discrepancies which will certainly appear will perhaps be somewhat better understood.